Thyrotropin receptor signalling links skin and thyroid disease

Candidate

Ibtessam Mustafa El-Mansori

Supervisors

Dr Rebecca M Porter
Prof Marian Ludgate

Submitted to in partial fulfillment of the requirements for the degree of Doctor of Medicine

Department of Dermatology

School of Medicine

Cardiff University

November 2012

DECLARATION

This work has not previously been accepted in substance for any degree and is not concurrently submitted in candidature for any degree.

Signed …… (candidate) Date ……

STATEMENT 1

This thesis is being submitted in partial fulfillment of the requirements for the degree of Doctor of Medicine (**MD**)

Signed …… (candidate) Date ……

STATEMENT 2

This thesis is the result of my own independent work/investigation, except where otherwise stated.
Other sources are acknowledged by explicit references.

Signed …… (candidate) Date ……

STATEMENT 3

I hereby give consent for my thesis, if accepted, to be available for photocopying and for inter-library loan, and for the title and summary to be made available to outside organisations.

Signed …… (candidate) Date ……

STATEMENT 4: PREVIOUSLY APPROVED BAR ON ACCESS

I hereby give consent for my thesis, if accepted, to be available for photocopying and for inter-library loans **after expiry of a bar on access previously approved by the Graduate Development Committee.**

Signed …… (candidate) Date ……

Abstract

Thyrotropin signalling links skin and thyroid disease

Thyroid dysfunction is frequently associated with skin and hair diseases; however, the underlying pathogenic mechanisms are poorly understood. Pathological activation of the thyroid stimulating hormone receptor (TSHR) is the key feature of both hyper- and hypo-thyrodism. Expression of the (TSHR) has been reported in several extra-thyroidal locations including adipose tissue, bone and skin fibroblasts. TSHR expression may explain the association between the thyroid and skin disease. The TSHR can also be activated by a newly discovered glycoprotein hormone, known as thyrostimulin. This hormone is composed of a dimer of unique α 2 and β 5 subunits. Although thyrostimulin has not been detected in the circulation. However, both subunits have been shown to be expressed in different tissues including the skin. The aim of this study is to examine the expression of the TSHR and thyrostimulin in the skin. In addition, to investigate the expression of a variant form of the TSHR in human and mouse skin and, other mouse tissues. RT-PCR using primers specific for the full length receptor and the truncated variant revealed that although the variant was widely expressed in mouse tissues including skin, it was not found in human skin. The full length receptor and thyrostimulin were found to be co-expressed in eye, testis and skin. Immunohistochemistry of frozen skin and thyroid sections using commercially available antibodies against the extracellular (A9) and transmembrane domains (A7) of TSHR demonstrates that TSHR is not expressed in the epidermis but expressed in dermal fibroblasts and in myoepithelium around sweat glands. A new β5 antibody was characterised by western blotting and immunohistochemistry for future investigation of β5 expression in the skin. These data suggest a functional role for TSHR signalling possibly via thyrostimulin in the skin and that the variant form, although potentially present in some tissues, is unlikely to be important in human skin.

Acknowledgments

The first thing to start with is to thank Almighty God for giving me the strength to carry on with joy

I would like to express my sincere gratitude and thanks to my supervisors Dr Rebecca M Porter and Prof Marian Ludgate for their wholehearted guidance, unfailing patience, encouragement and support throughout the project, especially for the faith and confidence they have shown in me which helped me to accomplish this work. I am also grateful for Rebecca's IT abilities which helped with many of the thesis illustrations.

I gratefully acknowledge the Libyan Government for funding the project. Many thanks for giving me this scholarship to accomplish my post-graduate studies in the UK

I wish to sincere thank all my friends and colleagues in the Department of Dermatology for their support, encouragement and advice, especially at the start of the project. Special thanks go to Tammy Ester, Fiona Ruge in particular for their technical help, support and friendship during my MD project.

I would like to express my sincere appreciation and thanks to colleagues in Centre of Endocrine and Diabetes Science Dr Fiona Grennan-Jones, Dr Lei Zhang for their invaluable technical support and help in tissue culture. A special thank goes to Mr Ameen Bakhsh for his invaluable help and technical support especially with finishing some of the experiment in their laboratory.

I would like to acknowledge the PGR Office team; Mrs Amina Latif, Ms Sarah Williams and Ms Frances Murphy for their endless advice, help and support.

Big thank you to my friends Hanan, Rasha, Dena, for making my life in Cardiff more enjoyable and more colourful.

Last but not the least; I would like to express my deepest gratitude to my husband, and my family in Libya without whose encouragement, support it would have been difficult to work during my study period. I cannot thank my mother enough for supporting me in every endeavour. Thank you to my special sister and my beloved brother whose constant support and encouragement have known no bounds.

List of abbreviations

Abbreviation	Full name
AA	Alopecia areata
aa	Amino acids
ABC	Avidin-biotin
APM	Arrector pili muscle
ACTH	Adrenocorticotropic hormone
ATPase	Adenosine triphosphatase
BM	Basement membrane
BSA	Bovine serum albumin
BPB	Bromophenol Blue
cAMP	Cyclic adenosine monophosphate
cDNA	Complementary DNA
CTS	Connective tissue sheath
CGH	Chorionic gonadotropin
CKGF	Cysteine-knot growth factors
DNA	Deoxyribonucleic acid
DEJ	Dermal-epidermal junction
dNTP	Mix of deoxyribonucleotides (ATP, CTP, GTP, TTP)
DP	Dermal papilla
DLE	Discoid lupus erythematosus
DIT	Diiodotyrosine
DMEM	Dulbecco's modified Eagle's medium
DAB	Diaminobenzidine
DTT	Dithiothreitol
ECD	Extracellular Domain
FITC	Fluorescein Isothiocyanate
FLG	Filaggrin
FGF	Fibroblast growth factor;
FSH	Follitropin (follicular stimulating hormone)
FCS	Fetal calf serum
FSH-R	Follicular stimulating hormone receptor
GH	Growth hormone
GD	Graves' disease
GPHα1	Glycoprotein hormone α1 subunit
GPHβ	Glycoprotein hormone β subunit
GPCR	G-protein coupled receptor
Gs α	Stimulatory G protein alpha subunit
HS	Hair shaft,
HGF	Hepatocytes growth factor;
HA	Hyaluronic acid

HRP	Horse radish peroxidase
IRS	Inner root sheath
I	Iodine
ICD	Intra cellular domain
IHC	Immunohistochemistry
K	Keratin
KOH	Potassium hydroxide
kb	kilobases
kDa	Kilo Dalton
KGM	Keratinocyte Growth Medium
LH	Lutropin (Luteinizing hormone)
LH-R	Luteinizing hormone receptor
LRRs	Leucine-rich repeats
M	Matrix
MIT	Monoiodotyrosine
MNG	Multi-nodular goiter
mRNA	Messenger Ribonucleic acid
TMG	Trans membrane domain
$MgCl_2$	Magnesium chloride
NaOAc	Sodium Acetate
NT	Neurotrophin
NIS	Sodium iodide symporter
ORS	Outer root sheath
Pax8	Paired box protein
PAS	Periodic acid-Schiff
PRL	Prolactin
PCR	Polymerase chain reaction
PBS	Phosphate buffered saline
PBMC	Peripheral blood mononuclear cells
PVDF	polyvinylidene difluoride
RNA	Ribonucleic acid
RT-PCR	Reverse transcription polymerase chain reaction
SG	Sebaceous gland
Stat	Signal transducer and activator of transcription
shh	Sonic hedgehog.
SDS	Sodium Dodecyl Sulphate
SDS-PAGE	Sodium dodecyl sulfate polyacrylamide gel electrophoresis
TBPA	Thyroxine-binding pre-albumin
TGF	Transforming growth factor
TGF-β/ BMP	Transforming growth factor β/ bone morphogenic protein
TG	Thyroglobulin
THr	Thyroid hormone receptors
TTF1	Thyroid transcription factor 1

TTF2	Thyroid transcription factor 2
T3	Triiodothryonine
T4	Thyroxine
TSH	Thyrotropin (thyroid stimulating hormone)
TRH	Thyrotropin releasing hormone
TTR	Transthyretin
Tyr	Tyrosine
TSHR	Thyrotropin receptor (thyroid stimulating hormone receptor)
TPO	Thyroid peroxidase
TBG	Thyroxine binding globulin
TSAbs	Thyroid stimulating antibodies
TSHRV	Thyroid stimulating hormone receptor variant
TEMED	N,N,N,N tetramethyl ethylene diamine

List of figures

List of tables

List of contents

To my father

Chapter One

General Introduction

1. Chapter One

1.1 Skin Biology

1.1.1 Skin structure

An insight into normal skin structure and differentiation is crucial for understanding the molecular biology of skin. The skin makes up approximately 15% of the total body weight and covers a surface area of about two square meters. Skin has several vital functions. Its most important functions are to form an effective barrier between the inside and the outside of the body, thermoregulation through sweating and protection against harmful UV rays via melanin synthesis (melanocytes)[1]. It also has an antimicrobial function and a major role in immunity (Langerhans and T-Cells). Morphologically, the skin is composed of two layers, the outer epidermis and the inner dermis, underneath the dermis (but not part of skin) is the hypodermis or the subcutaneous layer. The epidermis and dermis are separated by a basement membrane. The skin has a number of appendages including pilosebaceous gland (hair follicles & sebaceous glands), nails, apocrine and eccrine sweat glands[2].

The epidermis is a stratified squamous epithelium and the dermis is a connective tissue consisting of fibroblasts and structural proteins such as collagens and fibronectin[3]. The dermal epidermal junction is undulating where ridges of the epidermis, known as rete ridges, project into the dermis. The basement membrane lies at this junction and provides mechanical support for the epidermis and acts as a partial barrier against exchange of cells and large molecules. Underneath the dermis is a fatty layer, the panniculus adipose tissue,

usually designated as 'subcutaneous' tissue [3]. There are two main types of human skin. Glabrous skin (non hairy skin), found on the lips, palms and soles, is grooved on its surface and characterized by; thick epidermis, the presence of encapsulated sense organs within the dermis and, the lack of hair follicles and sebaceous glands. On the other hand, hair-bearing skin has both hair follicles and sebaceous glands but lacks the encapsulated sense organs[3].

1.1.1.1The epidermis

The epidermis consists largely of differentiated stratified squamous epithelium. The main cell component of the epidermis is the keratinocyte. However, there are several other cell populations namely melanocytes which donate pigment to keratinocytes, Langerhans cells, which have immunological functions and Merkel cells are also present but in small numbers[1,3]. The main function of melanocytes is the production of pigment secreted in melanosomes and transferred to the keratinocytes, forming a supranuclear cap to protect nuclear DNA from UV radiation. Langerhans cells are important for immune surveillance and Merkel cells are transducers of fine touch stimuli[1,3].

In normal epidermis, the keratinocyte regenerate continuously by division and give rise to several layers as they move upwards, a process known as epidermal differentiation[3,4]. Cell division occurs primarily in the basal layer where cells are attached to the basement membrane. Due to a poorly understood trigger, certain basal cells released from the basement membrane, lose their mitotic activity, stop dividing and begin to differentiate, stratify and change morphologically and biochemically. These triggered cells begin to synthesize a new set of structural proteins and enzymes that are characteristic of differentiation[1,4]. Histologically, the epidermis is divided into four layers; stratum basale

(basal layer), stratum spinosum (spinous layer), stratum granulosum (granular layer) and stratum corneum (horny layer) (**figure 1.1**)[5].

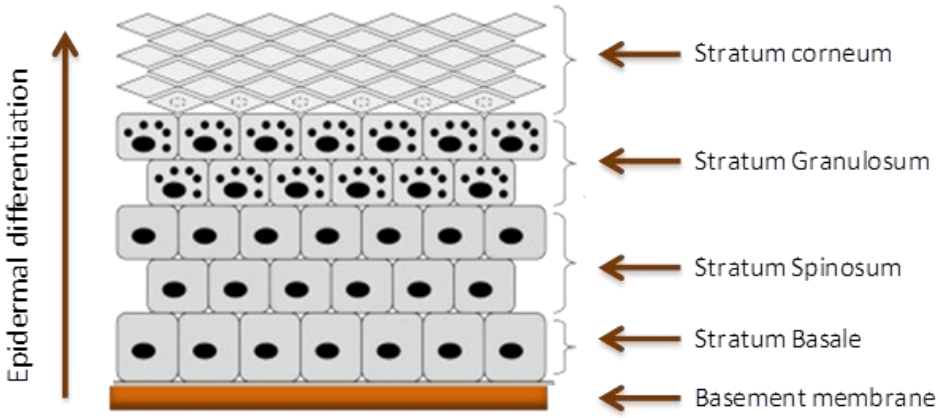

Figure 1.1: Skin cartoon showing cellular component of epidermis (adapted from Champion, R,1998)[5]

The stratum basale is the lower most cell layer and contains the germinative cells and is attached to the basement membrane (basal lamina) which separates the dermal layer from the epidermis[4]. The small columnar or cuboidal cells are attached to the basement membrane at hemidesmosomes and to the surrounding cells by desmosomes[1,6,7]. Keratin 5 (K5) and keratin 14 (K14) are expressed in these mitotically active basal layer cells, and their expression is down-regulated as cells differentiate. The rate of basal cell proliferation is under the control of a variety of intrinsic and extrinsic factors[1,4]. The stratum spinosum is located immediately above the stratum basale layer and is named for the spine-like appearance of the cell border which is due to the presence of numerous desmosomes joining adjacent cells[3]. Morphologically the cells are more cuboidal than the basal cells with a rounded nucleus. The spinous cells are metabolically active. Here, the cells dedicate most of their protein synthesis to synthesize new keratins K1 and K10 which replace the pre-existing K5 and K14[1,3]. Involucrin is another important protein in terms of epidermal

differentiation which is expressed by the spinous cells and forms the initial scaffold adjacent to the inner aspect of the plasma membrane for cell envelope formation[2,4]. Furthermore, the lamellar granules are made at this stage, they are found in the upper spinous and granular layers adjacent to the cell membrane which will subsequently fuse with the plasma membrane and release lipids into the intercellular space of the granular layer and the stratum corneum[4].

The granular layer lies just above the spinous layer, so named due to the presence of keratohyalin granules. The keratohyalin granules are composed mainly of Profilaggrin which is a high molecular mass precursor of the protein filaggrin (FLG) an important structural protein essential for the formation of a functional environmental barrier[3,4]. At this stage the cells stop generating keratin and envelope proteins, and start their final tailoring in protein synthesis, including production of filaggrin which aggregates the keratin filaments into tight bundles[4]. Moreover, loricrin which is major structural protein component of the cornified envelope is also synthesized here at a later stage[8].

Additionally, lipid-filled lamellar granules or lamellar bodies are found in the upper spinous and granular layers adjacent to the cell membrane. The intercellular skin lipids are synthesised and stored in these lamellar granules, which fuse with the plasma membrane and release their lipid contents into the extracellular space in the upper granular layer during keratinisation[1]. Complex changes in lipid composition occur after the extrusion of the contents of the lamellar granules by enzymatic action of a group of acid hydrolases, which are also secreted into the extracellular space forming an important barrier to permeability[9,10]. Skin lipids play important roles in barrier function which help to avoid trans-epidermal water loss and intercellular cohesion within the stratum corneum[4,11].

The stratum corneum or the cornified layer is the outermost layer of the epidermis and is composed of terminally differentiated keratinocytes sealed together by lipids[4]. During the transition from the granular to cornified layer, the keratinocyte (now named corneocytes) loses its nuclei and cytoplasmic organelles. The cells become flattened and the keratin filaments align into disulphide cross-linked macrofibers, under the influence of filaggrin. This promotes the collapse of the cells into a flattened shape which is characteristic of corneocytes. The corneocytes also contain remnants of organelles, melanin pigment, and membrane profiles[1]. Together, keratins and filaggrin constitute 80-90% of the protein mass of mammalian epidermis and the series of changes whereby keratin filaments aggregates into bundles through the action of filaggrin is known as keratinisation (squame biogenesis)[12].

1.1.1.2 The basement membrane zone (BMZ)

The basement membrane zone (BMZ) is a highly specialized structure located at the interface between the epidermis and the dermis[13]; it forms the junction between the lower epidermis and upper dermis and for that reason it is known as the dermal-epidermal junction (DEJ)[7,13]. The DEJ provides epidermal-dermal adherence, a mechanical support for the epidermis, and a barrier to the exchange of cells and of some large molecules across the junction, thus governing the overall structural integrity of the skin[1,13]. This zone contains supporting structures, which are critical for the integrity of the stable association between epidermis and dermis[14]. These structures are known as anchoring complexes, the anchoring complex consists of hemidesmosomes, anchoring filaments and anchoring fibrils[14].

1.1.1.3 The dermis

The dermis is an integrated fibrous, filamentous structure located underneath the epidermis and consisting of cellular connective tissue that accommodates the nerve and vascular networks and the epidermally derived appendages. In addition, it contains many resident cell types including fibroblasts, macrophages, mast cells and the transient circulating cells of the immune system[1,3]. The function of the dermis is to provide pliability, elasticity, and tensile strength to the skin; it also supports the epidermis above and the appendages within it. Furthermore, it protects the body from the mechanical injury, binds water within the body and accommodates sensory receptors[3]. In addition, the dermis is a vascular layer which is necessary for thermoregulation and the supply of nutrients to the epidermis which has no blood supply[1]. The dermis sits on a cushion of subcutaneous adipose and a thin layer of muscle[3].

The dermis is divided into two regions, the upper papillary dermis and the reticular dermis. The upper papillary dermis undulates and forms rete ridges, which increases the surface area with the epidermis to provide better adhesion and allowing a greater exchange of nutrients by diffusion. The lower regions of the dermis are reticular and form the major portion[3]. The interlacing (reticular) structure of collagen and elastin fibres within the dermis provides resilience and elasticity to the skin. The dermis consists mainly of a supporting matrix or ground substances in which polysaccharides and proteins coexist and interact. The bulk of the dermis is composed of type I and type III collagen[3]. In addition, fibroblast, macrophage, and mast cells are considered the main cellular components of the dermis. These cells are usually located in the papillary dermis surrounding the subpapillary plexus (dermal vascular network). However, they may present in the reticular dermis mainly between collagen fibre bundles[1].

The fibroblasts are the most predominant cells found in the loose connective tissue; they have a mesenchymal origin and have a spindle shape appearance. These cells exist in different phenotypes even within the same tissue[1]. These cells migrate through the tissues and are responsible for synthesis of all the dermal connective tissue elements or their precursors[15]. In addition, fibroblasts play a crucial role in wound healing and scaring by increasing their proliferative and synthetic activity[1].

There is a wide regional variation between different body sites. For example the scalp with its large hair follicles may be contrasted with the forehead which has only small vellus hair-producing follicles, although associated with large sebaceous glands. The axilla is distinguished because it has apocrine glands in addition to the eccrine sweat glands which are found throughout the body[3].

1.1.2 Skin appendages

Skin appendages include sebaceous glands, sweat glands, hair follicles and nails.

1.1.2.1 Sebaceous glands

The sebaceous gland is a unilobular or multilobular structure that is usually associated with the hair follicle. The sebaceous gland and the associated hair follicle are known as the pilosebaceous unit[5,16]. This gland produces sebum, an oily liquid released by holocrine secretion, through a duct into the upper follicle, which lubricates the hair shaft and epidermis[16]. It is largest and most numerous on the face, scalp, trunk, in the external auditory canal (ceruminous glands) and on the anogenital surfaces, but not normally present on the palms or soles, and only sparsely on the dorsal surface of the hands and feet[3]. It is regulated by androgens and retinoids. However, other factors are also

involved[16]. Histologically, it consists of acini connected to a common excretory duct composed of stratified epithelium; the glands are composed of highly mitotic cuboidal or columnar sebocytes and of keratinocytes that line the sebaceous duct, the cells progress towards the middle of the duct and accumulate lipid droplets as they terminally differentiate [16]. When fully differentiated the sebocytes are full of lipids and lack all other cellular organelles. The sebaceous gland is surrounded by a connective tissue capsule composed of collagen fibres which provide physical protection to the gland[16].

1.1.2.2 Sweat Glands

Two types of sweat glands had been recognised in humans, namely eccrine and apocrine sweat glands[3]. The eccrine sweat glands are smaller in size than the apocrine sweat glands and are distributed all over the body except the lips, external ear canal, clitoris or labia minora. Eccrine sweat gland secret hypotonic sweat consisting mostly of water and electrolytes, their main function is to control body temperature during exposure to hot environment or during physical exercise, failure to regulate body temperature under either of these conditions leads to hyperthermia and/or heat stroke. Sweat lowers body temperature by dissipation of heat by evaporation. The average density of eccrine sweat gland varies according to race and anatomical site[17]. Histologically, it is a simple tubular epithelium consisting of a secretary portion and a ductal portion[18]. The coiled portion of the sweat gland is made up of the secretary coil and the proximal duct. The secretory coil is composed of three distinct cell types; clear (secretory), dark (mucoid), and myoepithelial[18]. The dark cells are located near the apical or the luminal surface of the secretory tubules whereas, the clear cells are located either directly on the basement membrane or on the myoepithelial cells (Sato, 2001)[18]. When two or more clear cells lies adjacent to each other they form an intercellular canalculi. The canaliculi merge

immediately above the basement membrane or the myoepithelial cells and open directly into the lumen of the gland. Furthermore, the spindle shape myoepithelial cells are located adjacent to the clear cells, together with masses of myofilaments which lie on the basement membrane. The distal duct is relatively straight and connects the coil with the epidermis. Furthermore, the duct forms a spiral in the epidermis and the stratum corneum (forming the acrosyringium or intraepidermal sweat duct unit), and it opens directly onto the skin surface[17,18]. The clear cells are most likely responsible for making the sweat secretion, while the function of the dark cells is unknown. The myoepithelial cells are contractile cells with abundant filament and have a smooth muscle-like function[17,18]

Apocrine sweat glands are different from eccrine sweat glands in structure and function[17] Apocrine sweat glands are larger in size than the eccrine ones and distributed on the axillae, areola and genital areas, they become active at puberty and secret proteinaceous viscous sweat which has unique odour[17] . The apocrine sweat glands are composed of three segments: the secretory portion, the intradermal duct, and the intraepithelial duct. Ducts of apocrine sweat glands open to the hair follicle whereas ducts of eccrine sweat glands open to the surface of the skin through the epidermis. Furthermore, ducts of apocrine sweat glands enter pilosebaceous follicle in the infundibulum above the entrance of sebaceous duct. The ductal portion of apocrine sweat glands is composed of two layers of ductal cells while the secretory portion of apocrine sweat glands consists of a single layer of columnar secretory cells and a single layer of surrounding myoepithelial cells[1,17].

1.1.2.3 The hair follicle

The hair follicle is one of the most complex mini organs of the human body. They vary considerably in size and shape, depending on their location, but they all have the same

basic structure. The hair follicles are sloped in the dermis, and the longer follicles extend into the subcutaneous layer[3]. An oblique muscle, the arrector pili muscle, runs from the mid region of the follicle wall to a point in the papillary dermis close to DEJ[19]. Above the muscle lies one or more sebaceous glands, and in some regions of the body an apocrine gland also, opens into the follicle[19]. Together, these structures form the so called pilosebaceous unit[3]. It is believed that the hair follicle has ectodermal-mesodermal origin[19,20]. The epithelial components of hair follicle including the sebaceous gland and the apocrine gland are derived from the ectodermal hair follicle stem cells; while, the follicular dermal papilla and connective tissue sheath are originated from mesoderm derived cells. In addition the hair follicle pigmentary unit is derived from neural crest derived melanocyte[21,22].

The hair follicle is divided into a 'permanent' upper part, which does not cycle visibly, and a lower part, which is continuously remodeled in each hair cycle. The upper part of the hair follicle consists of the infundibulum, and the isthmus. The lower part of the hair follicle consists of suprabulbar and bulbar area **(figure 1.2 A)**[23]. The sebaceous gland duct joins the hair shaft at the lower end of the infundibulum, whereas, the arrector pili muscle is inserted at the proximal end of the infundibulum (**figure 1.2 A**)[23].

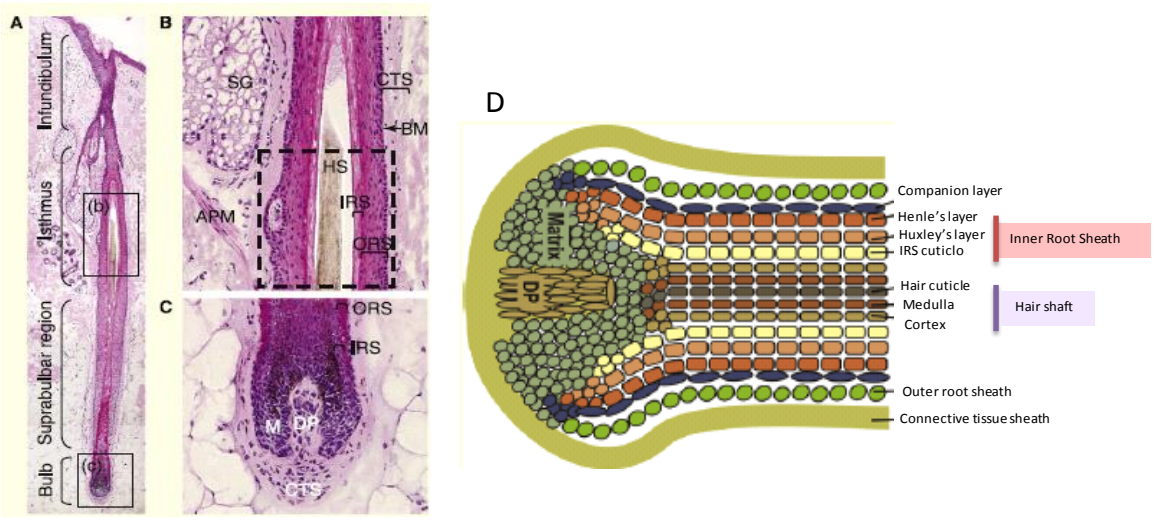

Figure 1.2: Histomorphology of the hair follicle & hair bulb (adapted fromSchmidt-Ullrich, 2005[19,24]. **A)** Longitudinal section through a human scalp hair follicle (anagen VI) showing the main components of the hair follicle; the (infundibulum, isthmus), the suprabulbar and the bulbar region **(B)** High magnification image of the isthmus. The bulge region is shown in the dashed square. **(C)** High magnification image of the bulb. **(D)** Schematic drawing illustrating the concentric layers of the outer root sheath (ORS), inner root sheath (IRS) and shaft at the level of the bulb. The inner root sheath is composed of four layers: Companion layer (CL), Henle's layer, Huxley's layer, and the inner root sheath cuticle. (BM = basal membrane; APM=arrector pili muscle; CTS= connective tissue sheath; DP= dermal papilla; M= matrix; HS= hair shaft, IRS= inner root sheath; ORS= outer root sheath; SG=sebaceous gland) [24].

In cross-section the hair follicle epithelium forms a cylinder with at least nine different concentric layers, each one expressing a distinct pattern of keratins [23]. Starting from the outermost to innermost, these layers include the connective tissue sheath (CTS), the outer root sheath (ORS), the inner root sheath (IRS), the hair shaft cortex, hair shaft medulla, the hair cuticle, the each layer is characterized by the expression of hair follicle specific keratins. Furthermore, the IRS is made of three concentric rings of epithelia: the outermost Henle's layer, the central Huxley's layer and the inner most is the inner root cuticle. The companion layer is a single layer of tiny cells derived from the matrix. It is in close cell-cell contact with Henle's layer, it provides a slippage plain between ORS and IRS[25]**(figure 1.2.D).**

In adult humans, there are two major hair types: the terminal hairs which are heavily pigmented, found on the scalp, and other sites e.g. beard. The vellus hairs, are non-pigmented and most abundant e.g. in facial and truncal skin. The follicles grow deep into subcutaneous layer in terminal scalp hairs and only penetrate the dermis in the case of vellus hair producing follicles[1].

1.1.2.4 The nail & the nail bed

The finger nail is made up of the nail plate which is the horny dead product, and four specialized epithelia; the proximal nail fold, the nail matrix, the nail bed, and the hyponychium[26]. The nail plate is a semi-transparent horny structure lying on the dorsal surface of the terminal phalanx and surrounded proximally and laterally by a fold of skin (nail folds)[27]. The proximal nail fold is a skin fold that has two surfaces, dorsal and ventral; at the junction of the two, the cuticle projects distally onto the nail surface[26]. The nail matrix is a specialized epithelial region underneath the proximal nail and above the mid portion of the distal phalanx. It produces the major part of the normal nail plate, and is subdivided into dorsal (ventral aspect of the proximal nail fold), intermediate (germinal matrix) and ventral (nail bed) sections[28]. The lunula or "half moon" is white in colour and represents the most distal region of the matrix[27]. The nail bed extends from the distal margin of the lunula to the onychodermal band and it is completely visible through the nail plate[26]. The hyponychium is the anatomical area that lies between the nail bed and the distal groove, where the nail plate attaches with the dorsal digit[15].

1.1.3 Hair follicle Biology

1.1.3.1 Hair cycle

The hair follicle is a dynamic structure. It undergoes continuous cycles of growth, involution and rest throughout the life of a mammal. It is strongly believed that the mouse is an excellent model system for studying the hair cycle for the following reasons; firstly, the mouse has a short hair cycle, about three weeks compared to humans; the time for each stage is a lot shorter making it easy to study. Secondly, the mouse hair cycle is synchronised whereas in human each hair follicle cycles independently of each other. Thirdly, the stages of hair cycle have been well characterized in the mouse[29]. Moreover, there is no evidence to suggest that the mouse hair cycle differs structurally in any way from that of the human. Finally, because, cycling hair follicles cannot be maintained for any length of time in culture [30], most of the knowledge about the hair follicle cycle is obtained from the studies of spontaneous or genetically engineered mouse hair loss mutants[31]. The main stages of the hair cycle are anagen (growth phase) and catagen (regression phase) and telogen (resting phase) (**figure 1.3)**[31].

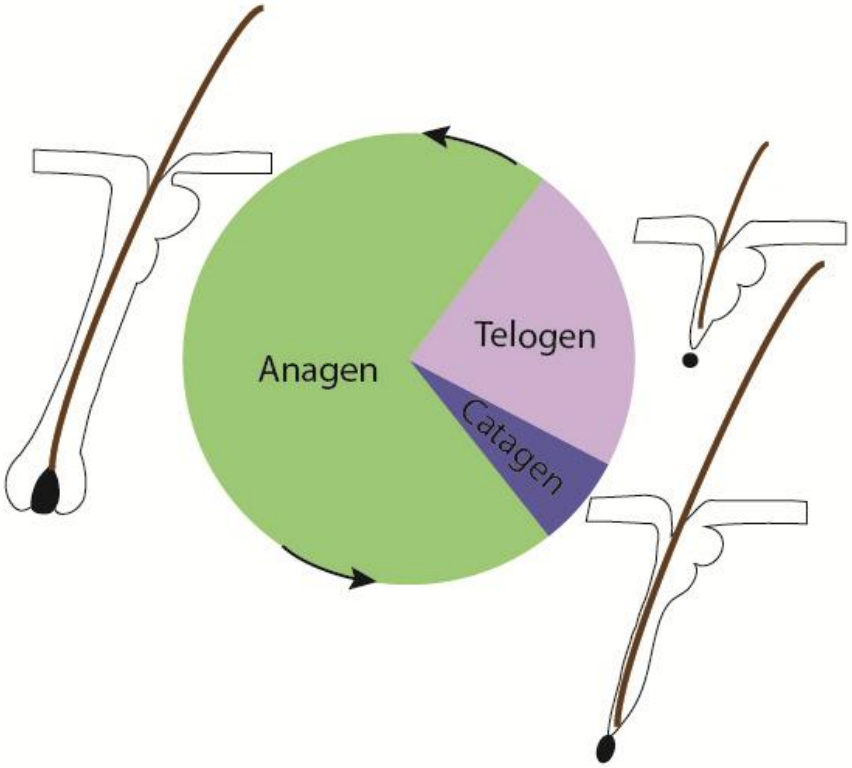

Figure 1.3 Schematic representation of different stages of mouse hair cycle (adapted from Porter, 2003)[31].

1.1.3.1.1Anagen phase

Anagen is the growth phase of hair cycle. In mice, the duration of anagen phase is ~ 1-4 weeks[29]. In human, the length of anagen controls the length of the hair shaft and this allows a wide diversity of different hairs in different body sites[29]. Anagen is divided into six different stages defined by specific morphological criteria (i.e. increasing the size of dermal papilla from anagen I to VI). The main characteristic feature of this phase is a rapid proliferation in the bulb to form the inner root sheath and hair shaft[29].

1.1.3.1.2 Catagen phase

Catagen (regression phase) is the dynamic transition phase between the anagen and telogen, in mice it lasts ~ 2 days (starts at day 16 and completed on day 17 after birth), in human it lasts ~ 2-3 weeks[29]. During catagen, the lower part of hair follicle undergo rapid regression by apoptosis of the matrix, inner root sheath and outer root sheath (ORS) while the stem cells in the bulge, the sebaceous gland and infundibulum remain. Eventually, the lower part of the hair follicle is reduced to an epidermal strand which brings the dermal papilla (DP) up into close proximity with the bulge. The old hair shaft (also known as the club) normally remains in its canal even while the new hair erupts through the same orifice [29].

1.1.3.1.3 Telogen phase

Telogen phase is referred to as the resting phase due to relative quiescence of the cells during this stage. In mice, it lasts about 11 days [29], whereas in humans, the telogen phase lasts up to three months before the hair follicles restart anagen phase and the cycle is repeated again. A signal for the next anagen stage is thought to pass between the dermal papilla and the stem cells in the bulge to initiate the next anagen stage and down growth of the hair follicle epithelium. The enlarged dermal papilla is soon encapsulated by epithelial cells and the production of inner root sheath and hair shaft lineages begins while the follicle is still growing down into the subcutaneous adipose tissue in the case of terminal hairs and mouse pelage but not vellus hairs[29].

As shown above (**figure 1.2**), the hair production originates from proliferating germinative epithelial cells located in the hair follicle bulb, which is under the control of the dermal

papilla. Complex cell signalling between the germinative cells of the hair follicle bulb and the dermal papilla instructs lineage restricted differentiation[19,20].

1.1.4 Common types of hair Loss

Hair loss (Alopecia) is a common problem that affects up to 50% of both sexes throughout their lives[32]. This condition can occur anywhere on the body but it is more common on the scalp where patients are presented mainly for cosmetic concerns[32]. Hair loss is broadly divided into focal or diffuse hair loss (**table1.1**)[33]. Focal hair loss is further sub-divided into scarring or non-scarring depending on the underlying cause. The main cause of non scarring focal alopecia is tinea capitis or alopecia areata. Whereas, patchy hair loss is caused by traction alopecia or trichotillomania. Scarring alopecia is a rare condition and mainly caused by discoid lupus erythematosus[33].

Table 1.1 Common types and clinical feature of hair loss (adapted from Mounsey, 2009) [33].

Type of hair loss	Subtype	Clinical feature
Diffuse	Female pattern hair loss	Hair thinning Intact frontal hair line Negative pull test
	Male pattern hair loss	Hair thinning Frontal line involved (M pattern) Negative pull test
	Diffuse alopecia areata	More patchy distribution Positive pull test
	Alopecia totalis or universalis	Total scalp hair loss and/ or body
	Telogen effluvium	30-50% hair loss, three months after precipitating event Positive pull test
	Anagen effluvium	90% of sudden hair loss two weeks after chemotherapy
Focal, Non scarring	Alopecia areata (AA)	Normal scalp with surrounding exclamation point hair
	Tinea capitus	Scaly Scalp, Positive KOH test (fungus visible on KOH examination)
	Traction alopecia	Patchy, +/- scaring, related to hair practice
	Trichotillomania	Patchy, +/- scaring, associated psychological disturbance
Focal, **scarring**	Cicatricial alopecia	Scaring, atrophy of the scalp (e.g. DLE, discoid lupus erythematosus)

Alopecia areata (AA) is defined as non scaring sudden hair loss that ranges from a single oval patch to multiple patches that become confluent. It can occur at any age and both sexes are equally affected. Studies showed that there is genetic predisposition to AA with a polygenic pattern of inheritance[34]. Alopecia areata is considered as an organ specific auto immune disease most probably mediated by autoreactive T cells which affect the hair follicle and the surrounding area[35]. It is commonly associated with other autoimmune diseases such as autoimmune vitiligo, thyroid disorders, type 1 diabetes, rheumatoid arthritis and discoid lupus erythematosus[33].

On the other hand, diffuse hair loss (generalized hair loss) is also known as telogen effluvium. It occurs when an increased number of hairs enter the telogen (resting phase) of the hair cycle from the anagen (growing) phase and these hair are lost about three months later[33]. Telogen effluvium may be precipitated by severe illness, infection, injury, surgery, childbirth thyroid disorders, psychological stress, iron deficiency anaemia and drugs. However, in about third of patients, no cause can be found[36]. Thyroid disorders including both hypo and hyper thyroidism can cause telogen effluvium; it is usually reversible when the thyroid status is corrected. The patient presents with increased numbers of hair in their hair brush or shower, they may also present with thinning of hair in the scalp, axillary, and pubic area. A detailed history and a careful examination may indicate the cause of hair loss[36].

1.2 Normal Thyroid Biology

1.2.1 Anatomy, histology and morphogenesis

"The thyroid gland develops from a tubular invagination of the embryonic pharynx, and migrates towards the neck where it develops into a thyroid gland. The thyroid is composed of two lateral lobes joined across the midline by an isthmus; a pyramidal lobe of varying size extends upward from the isthmus and represents the point of attachment with the thyroglossal duct. The thyroid is closely attached to thyroid cartilage and to the upper end of the trachea, and thus moves on swallowing[37,38].

Macroscopically, the thyroid is firm, reddish brown in colour, smooth and surrounded by a fibrous capsule that bonds together with the deep cervical fascia, and weighs between 20-25g[37]. Microscopically, the thyroid is composed of closely packed follicles, which are

separated by a rich vascular supply and a little intervening stroma. These follicles are lined by cuboidal epithelioid cells and contain colloid; a proteinaceous material composed mainly of thyroglobulin (TG) and provides the matrix for thyroid hormone biosynthesis and a vehicle for its subsequent storage[39]. The gland has a rich blood supply from superior and inferior thyroid arteries. Dispersed between the thyroid follicles are the parafollicular or C cells, and these secrete calcitonin, a hormone involved in the regulation of circulatory calcium[39] The thyroid follicular cells co-express the three thyroid specific transcription factors. Thyroid transcription factor1 (TTF1 also known as NKX2.1), thyroid transcription factor 2 TTF2 (also known as FOXE1), and Pax8 (a member of the paired box family of DNA binding proteins), which are all required for the thyroid morphogenesis. In the absence of the mentioned factors, morphogenesis is thoroughly impaired[40,41,42].

1.2.2 The Thyroid function

The thyroid plays a vital role in the intermediary metabolism of virtually all tissues, and is of fundamental importance for the normal growth, mental and sexual maturation[43]. The main function of thyroid hormones is to control the overall metabolic turnover. Moreover, it plays a crucial role in the growth and development of the nervous system of the developing fetus and the new born[43]. The widespread effects of the thyroid result from the biosynthesis and secretion of two rather unique iodine-containing hormones, triiodothryonine (T3) and thyroxine (T4)[44].

The thyroid hormones modify the enzyme systems that affect the intermediary metabolism of carbohydrate, lipid, protein and the rate of terminal oxidative metabolism by direct and indirect mechanisms. The net effects of thyroid hormone actions are therefore to increase the cell's metabolism by enhanced turnover of the carbohydrate, protiens and lipids thus

regulating body weight, maintaining the core body temperature by production of metabolic heat, and the regulation of calcium metabolism of bone[45]. In addition, thyroid hormones are of particular importance in the long term adaption to stress, including prolonged exposure to cold[43,45].

1.2.3 Regulation of thyroid function

The anterior pituitary thyroid stimulating hormone (TSH) is the major stimulus of thyroid hormone secretion[46]. TSH secretion in turn is controlled by the hypothalamus which produces thyrotropin releasing hormone (TRH) (a positive regulator) and somatostatin (a negative regulator)[46]. The secretion of TRH and TSH are regulated via a negative feedback loop (hypothalamic pituitary thyroid axis) responding to the amounts of the thyroid hormones circulating in the blood and intra-hypothalamic and intra-pituitary T3 levels[46] .

TSH is a pulsatile secreted hormone with a marked circadian rhythmicity with a characteristic nightly surge[43]. Activation of the sympathetic branch of the autonomic nervous system directly stimulates the thyroid gland while, somatostatin and cortisol inhibit TSH secretion, whereas, iodine (I) directly inhibits growth of the thyroid gland. At physiological levels by negative feedback mechanism, the thyroid hormones reduce TSH secretion. T3 binds to the anterior pituitary nuclear receptors, and because most of the intracellular T3 is derived from circulating free T4, the pituitary gland is more sensitive to changes in plasma T4 than to T3 concentration[46].

1.2.4 Thyroid hormones biosynthesis and secretion

Thyroid hormones are synthesized in the thyroid gland by iodination and coupling of two molecules of the amino acid, tyrosine (Tyr). The pituitary thyrotropin (TSH) level controls the rate, and all steps of thyroid hormone synthesis in the blood. TSH also induces an increase in the number and size of thyroid follicular cells, this is achieved by its binding to the thyroid stimulating hormone receptor (TSHR) and activating downstream signal cascades, mainly cAMP [45]. The synthesis of thyroid hormones is fundamentally dependent on the adequate iodine (I) supply. TSH is the principle factor determining the rate of (I) uptake by the thyroid and as a result thyroid hormone secretion[44].

Iodide transport into the thyroid cytoplasm is an active transport process against an electrochemical gradient carried out by the sodium iodide symporter (NIS). The NIS couples the inward "downhill" translocation of Na^+ with the inward uphill translocation of iodine[47]. The driving force of this process is the inwardly directed Na^+ gradient generated by the Na^+/K^+ adenosine triphosphatase (ATPase). Once inside the cell, the I^- is then passively trans-located through the putative I^- channels across the apical membrane into the colloid, in the follicular lumen (I^- efflux) where it is oxidized by thyroid peroxidase (TPO), to a higher state (TPOI) as a result transforming into an effective iodinating agent[47]. Within the thyroid follicular lumen, the thyroid hormones are then formed in a two stage process. Firstly; the tyrosine molecule on TG are singly or doubly iodinated to form monoiodotyrosine (MIT) or diiodotyrosine (DIT). Subsequently, Triidothyronine (T3) is formed by joining MIT and DIT and similarly, Thyroxin is formed by joining two DIT **(figure 1.4).**

The iodination and coupling of iodotyrosyl precursors are mediated by TPO, and the thyroid hormones (still incorporated in TG) are stored within the colloid of the thyroid follicle[44]. When required, the thyroid hormones are retrieved by endocytosis and both T3, T4 are released by cleavage, with the proteolytic enzymes allowing the hormones to enter the circulation. The I^- is then released from MIT and DIT and is re-circulated[44].

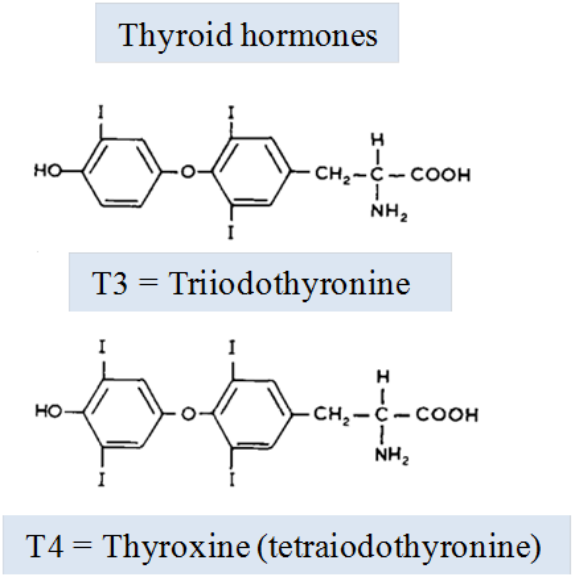

Figure 1.4: Chemical structure of Triiodothryronine (T3) and Thyroxine (T4)(adapted from Carrasco, N. et al, 1993)[44].

1.2.5 Thyroid hormone transport and metabolism

When released into the circulation, the thyroid hormones are immediately bound to plasma proteins. More than 99% of plasma T3 & T4 are bound to plasma proteins[48]. The thyroxine binding globulin (TBG) carries about 70% of T3 & T4 because of its high affinity for both hormones, while about 15-20% are bound to para-albumin and about 10-15% are bound to transthyretin or "thyroxine-binding pre-albumin" (TTR or TBPA) which has a lower affinity binding, thus allowing the thyroid hormone to disassociate more rapidly. This fraction is responsible for much of the immediate delivery of T3 & T4[48].

Thyroid hormone receptors (THr) are located in the nuclei of the cells and, the affinity of the receptors to T3 is higher than that of T4. In the peripheral tissues (liver and kidney), the majority of the secreted T4 is deiodinated (removal of an iodine atom from the outer β ring) to a more active form T3 and approximately 80% of plasma T3 is formed in this way. The remaining 20% is secreted by the thyroid gland. Deiodination of the inner α ring of the T4 produces reverse T3 (rT3) that is inactive. While T4 has independent capability, T3 binds more avidly to thyroid receptors and is the main active form[48].

1.3 Disorders of thyroid gland

The most common clinical presentations of thyroid disorders are as a result of excessive hormone secretion (Hyperthyroidism), deficient hormone secretion (Hypothyroidism) and Goitre (diffuse or nodular) in which case there may or not be abnormal thyroid hormone secretion[49]. Normal level of thyroid hormones is variable, different testing laboratories may have different reference ranges.

1.3.1 Hypothyroidism

Hypothyroidism is a medical condition characterized by low levels of thyroid hormones (T3 and T4) and high levels of TSH causing a general slowing of the BMR (basal metabolic rate), which manifests itself clinically as weight gain, cold intolerance, fatigue, lethargy, depression, hoarseness of voice, dry skin, decreased appetite and menstrual disturbances[49]. It is classified as primary, due to a decrease in thyroid hormone levels resulting from a disease process in the thyroid gland or secondary resulting from failure of

pituitary TSH secretion. A reduction of thyroid hormone synthesis and secretion at birth is known as cretinism, while myxedema in adults[49].

Congenital hypothyroidism (Cretinism) is an uncommon disease of childhood (1-4000 live births), it is screened for in all newborns (Guthrie test) as early diagnosis and immediate treatment by thyroxin administration is crucial in order to avoid irreversible developmental defects. The main causes of congenital hypothyroidism include: 1) thyroid gland dysgenesis: ectopy, agenesis, hypoplasia, hemiagenesis 2) failure of thyroid hormone synthesis due to severe dietary iodine deficiency (maternal during pregnancy or after birth); 3) failure due to the presence of dietary substances (goitrogens) that block hormone synthesis: 4) failure of synthesis due to autosomal recessive enzyme deficiency (sporadic cretinism)[49] .

Hypothyroidism in adults is caused by: 1) Hashimoto autoimmune thyroiditis; 2) secondary hypothyroidism due to pituitary failure; 3) hypothyroidism due to anti thyroid drugs or ablation of the gland by surgery or radiation; 4) failure of hormone synthesis due to extreme dietary iodine deficiency. This is usually compensated by hyperplasia of the thyroid gland via the TSH feedback mechanism and the enlarged gland maintains adequate hormone secretion[49].

1.3.1.1Cutaneous manifestation of Hypothyroidism

The skin manifestations vary and depend on the extent, duration of the disease and the ethnicity. The skin is cold, pale, due to cutaneous vasoconstriction and reduced core temperature, patients may have, dry, thick, rough, hyperkeratotic skin[50]. The most striking skin changes are due to dermal accumulation of mucopolysaccharides causing diffuse

generalized myxedema[51]. However, the hands and periorbital region of the legs are more commonly affected. Unlike the pretibial myxedema of Graves' disease, the generalized myxedema of hypothyroidism is fully reversible with thyroid hormone therapy[52,53].

The facial changes are almost pathognomonic; nonpitting swelling or puffiness around the eyes with a very characteristic loss of the outer third of the eyebrows (Madarosis), drooping of eye lids. Furthermore, malar flush and yellow discolouration of skin especially palms, soles and naso-labial folds. The scalp hair may be thin, dull, coarse and brittle resulting in a diffuse, partial alopecia (alopecia areata), axillary and pubic hair may be sparse[34]. The nails are thin, brittle and striated with both longitudinal and transverse grooves[51].

1.3.2 Hyperthyroidism

It is a medical condition characterized by high levels of thyroid hormones (T3 and T4) and supressed TSH. The most common causes of hyperthyroidism are Graves' disease (GD) and toxic thyroid adenomas, both causes produce continuous activation of the TSHR (**figure 1.5**)[54].

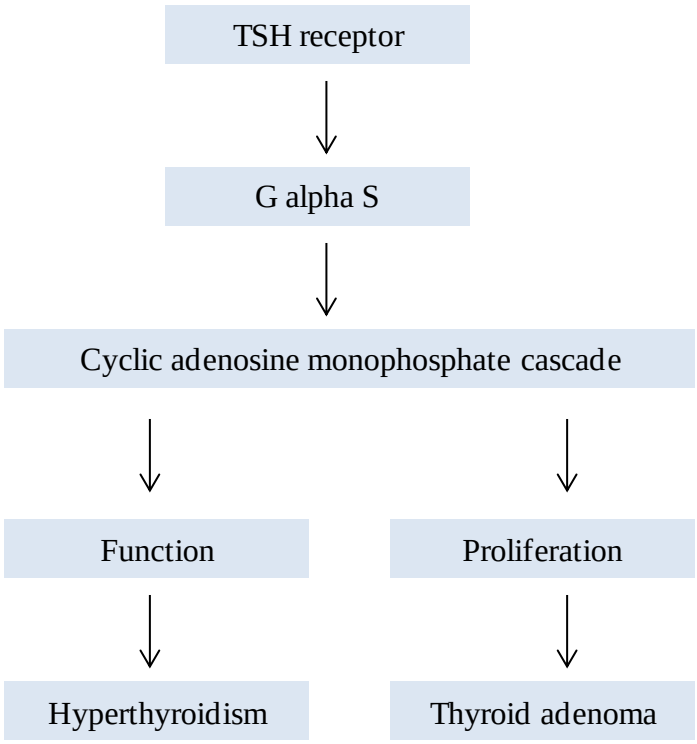

Figure 1.5: Consequences of activation of TSHR. The TSHR is coupled mainly via the G protein S to the cAMP cascade. The cAMP cascade positively regulates thyroid hormone production and thyroid epithelial cell proliferation and thereby mediated hyperthyroidism as well as the formation of thyroid adenoma (adapted from Paschke et al, 1996[54]).

GD is diffuse autoimmune thyroid hyperplasia characterized by the presence of IgG auto-antibodies which stimulate each thyrocyte in the gland to produce excess thyroid hormones. These thyroid stimulating antibodies (TSAbs) mimic the effects of the TSH on the thyrocytes causing inappropriate production of cAMP with subsequent hyperfunction and goitre[55].

The toxic thyroid adenoma is a circumscribed benign tumour with monoclonal origin. This condition is characterized by an inappropriate production of cAMP started in a single cell, which often harbours an activating TSHR mutation and then experiences clonal expansion leading to the generation of the hyper-functioning nodule. When the thyroid

hormone production by this nodule exceeds the normal daily production, the normal tissue surrounding the adenoma is put at rest as a consequence of suppressed TSH levels[54]. Other causes of hyperthyroidism include: 1) Toxic Multi-nodular goiter (MNG); 2) TSH secreting pituitary adenoma (known as pituitary hyperthyroidism); 3) Sub-acute thyroiditis (De Quervian's) 4) Germline tumors such as chorio-carcinoma or teratoma 5) An active follicular carcinoma (rarely) [49].

1.3.2.1Cutaneous manifestation of Hyperthyroidism

The skin manifestations vary and can include; warm, moist erythematous, silky texture, and frequently pruritic skin[56]. The warmth is caused by increased blood flow and peripheral vasodilatation may be responsible for episodic facial flushing and palmer erythema[56]. The epidermis is thin but not atrophic with generalised hyperhydrosis which is more prominent in palms and soles[51]. Diffuse or localized hyper- pigmentation and vitiligo of a variable degree can occur and the latter is seen especially with Graves' disease, it is thought to be part of the autoimmune response. Diffuse hair loss occurs in about 20-40% of patients with hyperthyroidism and the severity of the loss is not directly related to the severity of the disease. Loss of axillary, pubic, eyebrows in addition to alopecia areata may be seen[51]. The nails become soft, shiny, rapidly growing and friable [26,57]. Onycholysis occurs in many patients, it is a distal separation of nail plate from its underlying bed with upward curvature; so called Plummer's nail [26,57]. Onycholysisis is not specific to hyperthyroidism, it may be observed in patients with hypothyroidism, psoriasis, contact dermatitis and trauma[26,57].

1.3.3 Autoimmune thyroid disease

Graves' disease (GD) is the most common autoimmune thyroid disorder and is characterized by the presence of thyroid stimulating auto antibodies (TSAbs) which mimic the effects of the TSH leading to stimulation of the thyroid follicle via the TSHR to produce excess thyroid hormone[49,55]. Hashimoto autoimmune thyroiditis is the cause of most cases of primary hypothyroidism, and is the result of an auto immune destruction of the thyroid by a cytotoxic T-cell-mediated hypersensitivity reaction[49].

1.3.3.1Cutaneous manifestation of autoimmune thyroid disease (Thyroid Dermopathy)

The dermatologic manifestations of Graves's disease are thought to be due to autoimmune mediated reaction rather than elevated thyroid hormones levels[51,58]. In addition to the fore mentioned cutaneous features of hyperthyroidisim, patients with Graves' disease have distinctive cutaneous manifestation such as pretibial myxedema and acropachy[51]. Table 1.2 summarizes the clinical presentation of thyroid disease.

Pretibial myxedema is also known as thyroid dermopathy and usually occurs in hyperthyroid patients. However, it can also occur in euthyroid patient[59,60]. It is characterized by dermal fibroblast proliferation resulting in immune reaction and the release of local glycosaminoglycans and cytokines which causes mild to moderate skin thickening[50]. The most common site of myxedema is the anterior tibia and dorsa of feet. However, other areas of the body can be affected such as face, pre-radial area, scalp, neck extremities and torso[59,60]. It was suggested that local physical and anatomical factors such as local trauma, oedema on a background of a usually subclinical, systemic, connective

tissue inflammation may aggravate pretibial myxedema [61]. It is diagnosed clinically by its characteristic features; the early lesions may be unilateral or bilateral, non-pitting, scaly, firm, with a peau d' orange[51]. The lesions may coalesce to form hyperkeratotic or verruocus plaques, and may appear pink or purple, hyperhidrosis and hypertrichosis may be present. It is usually non progressive and may partially or completely regress in time[62]. Biopsies in general should be avoided as the lesions may not heal. Histologically, staining with hematoxylin and eosin shows mucin production in the lower dermis and a reduction in elastic tissue. Acropachy is characterized by a clinical triad consisting of digital clubbing, soft tissue swelling of the hands and feet and periosteal new bone formation, it occur in 0.1-1% of patients and it almost always occurs in association with ophthalmopathy and pretibial myxedema[51].

Table 1.2 Summary of clinical presentation of thyroid disease. (Adapted from Safer, JD, 2011[63]).

Low T3,T4 and High TSH	**HighT3,T4 and low TSH**	**Autoimmune reaction**
Cold intolerance	Heat intolerance	Heat intolerance
Pallor	Warm skin	Acropachy
Dry, scaly skin	Increased sweating (hyperhydrosis)	Urticaria, pruritis
Generalized myxedema		Pretibial myxedema
Diffuse alopecia Loss of hair of lateral eye brow	Hypertrichosis	Alopecia areata
Purpura	Erythema	Vitiligo
Drooping of upper eyelid	Hyperpigmentation	Pernicious anaemia
Nerve entrapment syndromes	Telengictasia	Bullous disorders
		Eczema
		Connective tissue disease.

1.3.3.2 Treatment of thyroid dermopathy

Generally, localized lesions of pretibial myxedema are asymptomatic and most patients require no treatment. The indications for treatment are cosmetic concern, functional impairment or local discomfort[64]. Topical application of corticosteroids is the preferred therapy; however, as the extent of the lesion increases the likelihood of successful treatment is decreased and the severe elephantiasic forms may lead to significant limb enlargement and impair function[64]. Surgical treatment should be avoided because scarring may aggravate the dermopathy, and the benefits are equivocal. Compression wraps or stockings that provide 20-40 mm Hg of pressure can be useful as an adjunctive[65,66]. Systemic steroids or other immunosuppressive therapy is not indicated for patients presenting with only localized myxoedema, it is indicated when presented with both ophthalmopathy and myxedematous lesion[62,67].

The long term outcome for patients with localized myxedema varies. It is not known to what extent treatment promotes remission of the lesions[64] . Long term remission appears to depend on the severity of the initial disease rather than the effect of the therapy[65]. The available therapeutic modalities are palliative at best and a better and safer means of immune modulation are needed to treat this extra thyroidal manifestation of autoimmune thyroid disease.

1.3.4 Inflammatory thyroid disease

Sub acute thyroiditis is an uncommon inflammatory condition of the thyroid; the most likely cause is viral origin, histologically characterized by extensive destruction and fibrosis of the thyroid follicles with aggregation of macrophage and giant cells around the fragments of colloid[49]. Riedel's disease is a rare chronic condition, not involving thyroid

auto-antibodies, associated with fibrosing lesions of mediastinum and retroperitonium. It is suggested that this condition may be a systemic disease involving the fibroblast[49].

Other forms of thyroid dysfunction are: Diffuse non-toxic, Multinodular goiter (MNG) represents a compensatory thyroid hyperplasia as a result of the accumulation of mild deficiency of thyroid hormone production. Hyperplasia corrects the hormone deficiency and maintains the euthyroid state. Endemic goiter is the result of iodide deficiency and sporadic goiter is usually due to increase of physiologic demand for thyroxine during pregnancy or at puberty[49].

1.4 Effect of thyroid hormones on different parts of the skin

It is commonly believed that most of thyroid associated skin symptoms are related to autoimmune reaction rather than disturbance of thyroid hormone level[58]. This section describes the effect of thyroid hormones on different parts of the skin which are summarized in **(table 1.3)**.

Table 1.3 Summary of effect of thyroid hormones on different parts of skin. (Adapted from Safer, JD, 2011[63]).

Skin changes	Low T3,T4 and high TSH	High T3, T4 and low TSH
Epidermal changes	Coarsened, thin, scaly skin	Smooth, thin skin
Dermal changes	Non pitting oedema (myxedema) Oedema (hands, face, eyelids) Carotenemia Pallor	
Hair and nail changes	Dry, brittle, coarse hair Alopecia Loss of lateral third of eye brows Coarse, dull, thin, brittle nails	Fine hair (loses waves), hypertrichosis Shiny, soft, friable nails (Onycholysis, Plummer's nails)
Sweat gland changes	Dry skin (xerosis) Decreased sweating	Excessive sweating.

1.4.1 Epidermal effect

High levels of T3 and T4 causes thinning of the epidermis (not atrophic). However, one report showed epidermal thickening in skin biopsies from thyrotoxic subjects[68]. Tissue culture studies show that T3 stimulates growth of both epidermal keratinocytes and dermal fibroblasts[69,70]. However, thyroid hormone mediated inhibition of keratinocyte growth has been observed when the keratinocytes were co-cultured with dermal fibroblasts[71].

In addition, in vitro keratinocyte studies have demonstrated that depletion of T3 causes elevation of transglutaminase level, which is involved in the formation of the cornified envelope. Moreover, it was also observed that T3 depleted keratinocytes have reduced levels of plasminogen activator, an enzyme involved in the corneocyte shedding process[72]. Low levels of thyroid hormones in hypothyroid status may affect the epidermal barrier function. Studies of thyrodiectomized rats have suggested that sterol synthesis (which is

associated with scaling dermatoses) is altered in epidermal keratinocytes deprived of thyroid hormone[73]. It is believed that thyroid hormones accelerate the barrier formation of the skin by enhancing the enzyme activities in the cholesterol sulphate cycle[74]. It was also suggested that hypothyroid status may affect the development of the lamellar granules, which are vital for the development of normal stratum corneum in fetal mice[75].

Thyroid hormones have a direct control over keratin genes, which encode the intermediate filaments and make up about 30% of the protein of the epidermis, at a nuclear level through hormone response element in their upstream promoters[75,76]. It stimulates the expression of proliferation associated keratin genes (K6a,K16,K17) both in vivo and vitro[77]. However, only negative thyroid response elements have been identified for these genes[78].

1.4 .2 Dermal effects

Most of the dermal changes in hyperthyroid patients are derived from autoimmunity rather than direct thyroid hormone action while most of the dermal changes in hypothyroid patients are thought to be because of low thyroid hormone rather than autoimmune reaction[58]. In hypothyroid patients, pale skin is due to dermal mucopolysaccharides and water content. However, a prominent yellow hue of palms, soles and nasolabial fold is caused by dermal carotene[63]. The main causes of thyroid dermopathy (myxedematous state) are accumulation of hyaluronic acid, the extravascular albumin accumulation (due to increase of its trans-capillary escape) and an inadequate lymphatic drainage[79]. Hyaluronic acid (HA) is the major glycosaminoglycan that is produced by 3 synthase enzymes and accumulates in myxedema, its hygroscopic nature allows it to swell when it is hydrated [80,81].

The effect of thyroid hormones on dermal fibroblast is a debatable issue. Tissue culture studies showed that thyroid hormones stimulate the proliferation of dermal fibroblast[71,82]. However, other groups showed inhibiting synthesis of hyaluronic acid, fibronectin and collagen in cultured fibroblast[83,84]. Moreover, animal studies using rat treated with triiodothyronine (T3) administrated topically or intra-peritoneally suggested increased dermal thickness[69,71]. Another study reported increased collagen thickness in mice treated topically with the thyroid hormone analog, tri-iodothyroacetic acid (Triac)[85].

1.4 .3 Effect on wound healing

It is believed that topical thyroid hormone may have a useful effect to accelerate wound healing rate. Safer JD et al demonstrated that topical application of supra-physiological does of T3 accelerate wound healing in normal mice[86]. Another clinical report showed that human wound healing formulation requires T4 in addition to growth hormone and insulin[87].

1.4 .4 Effect on hair and nail

Studies show that thyroid hormone affects the hair cycle. Animal treated by intra-peritoneal administration of T4 showed decreased telogen (resting phase) and anagen phases (growth phase) of hair cycle[88]. In vitro studies suggested increased hair growth rate in Hyperthyroidism; DNA flow cytometry of dissected anagen hairs from thyrotoxic patients compared with follicles taken from euthyroid controls demonstrated a 30% increase in the S and G2+M phases of the cell cycle[89]. Moreover, a pilot study showed topical application of T4, insulin and growth hormone enhances hair growth over 6 months in male patients with androgenic alopecia[90]. Another animal study revealed that topical

application of T3 for short periods produced increased hair counts whereas, animal made thyrotoxic with systemic T3 showed decreased hair counts[69,71].

On the other hand, in hypothyroidism the hair is coarse, dry, brittle and slow growing (diffuse alopecia) and with localized hair loss (similar to AA)[91]. The hypothyroidism related alopecia may be mediated by hormonal effect initially as well as the duration of hair growth. However, there is evidence that associated autoimmunity and thyroid dysfunction may be involved[92]. Therefore, tests to detect thyroid autoantibodies are relevant in alopecia areata patients[92]. Nail changes are characterized by concave contour associated with distal onycholysis (Plummer's nails)[26].

1.4.5 Effect on sweat glands

In hypothyroidism, the skin is dry due to decrease in eccrine gland secretion. The mechanism of deceased sweat gland secretion is not clear yet. Histological analysis shows atrophy of the sweat glands. Moreover, it was suggested that accumulation of periodic acid-Schiff (PAS) positive material may play a role[93].

Hyperthyroidism is associated mainly with generalized hyperhydrosis which is usually more prominent in palms and soles. It is believed that hyperhydrosis is a reflection of the underlying metabolic status; the other suggested causes are increased sympathoadrenal activity caused by synergistic action between catecholamines and thyroid hormones[94]. Localized hyperhydrosis has been documented in patients with pretibial myxedema, it is caused by inappropriate stimulation of the sympathetic nerves by perineural infiltration of mucin[95].

1.5 The glycoprotein hormones family

Glycoproteins are proteins that contain oligosaccharide chains (glycans) covalently attached to polypeptide side-chains. The carbohydrate is attached to the protein in a cotranslational or posttranslational modification. This process is known as glycosylation. Secreted extracellular proteins are often glycosylated. The glycoprotein hormones family involves human thyrotropin (TSH), follitropin (FSH), lutropin (LH), and chorionic gonadotropin (CGH). TSH, FSH and LH are synthesized and stored in a specific group of cells in the anterior pituitary and are released in response to a specific releasing hormone secreted by the hypothalamus, whilst CGH is produced predominantly by the placenta during pregnancy[48]. These glycoprotein hormones form the basis of the classic pituitary peripheral target feedback mechanism and, TSH, specifically, plays a crucial role in metabolism and physiological function of virtually all tissues via its regulation of T4/T3 production, while, the CGH is important during pregnancy[96,97]. Structurally the glycoprotein hormones are classified as part of the cysteine-knot growth factors (CKGF) super family of structurally related proteins with important biological activities[98]. Furthermore, the glycoprotein hormones are heavily glycosylated heterodimers comprised of non-identical subunits coupled by noncovalent interactions, glycoprotein hormone α1 subunit (GPHα1) which is common to all members of this family and a glycoprotein hormone specific β subunit (GPHβ) which is unique and confers biological specificity to each hormone, the formation of α/β dimers is necessary for their biological function[99, 96,100].

As mentioned above, an important structural component of glycoprotein hormones is their N-linked oligosaccharides or their carbohydrate moiety. The N-linked glycosylation is the attachment of a sugar molecule (a process known as glycosylation) to a nitrogen atom in an amino acid residue in a protein. The N-linked oligosaccharides of these hormones are

necessary for proper folding, assembly, secretion, metabolic clearance and biological activity[101]. The common α- subunit has two asparagines (N)-linked oligosaccharides, and the β-subunit has one (in TSH and LH) or two in (CG and FSH)[102,103].

The heterodimers of glycoprotein hormones are stabilized by a unique segment of the β subunit termed "seat belt" segment because it wraps around α subunit long loop. The human TSH-β subunit has three disulfide bridges from cysteine-knot motif that determines the core structure, two of the disulfide bridges are involved in the seat belt formation and the third one links the two β- hairpin loops[104]. This additional stabilization by the seat belt results in doubling of the subunit interface. Moreover, these hormones are also shown to activate specific G protein–coupled receptors in the thyroid and gonads by activating the thyrotropin receptor (TSHR) and FSH and LH/ CG receptors respectively[96,105].

1.5.1 TSH structure

The thyroid stimulating hormone (TSH) is a member of glycoprotein hormone family, it is 28- to 30- kDa glycoprotein produced in the thyrotroph cells (basophil cells) of the anterior pituitary gland[100,105]. Its synthesis and secretion is stimulated by thyrotropin releasing hormone (TRH) and inhibited by thyroid hormones T3 & T4 in a classic negative feedback mechanism[100,105]. Both TSH subunits are synthesized from separate mRNAs encoded on different chromosomes, the common human α1 subunit and TSH-β subunit are encoded by genes located on chromosome 6 and 1 respectively[100]. The α1 subunit gene is 9.4 kb in length, consists of four exons and three introns whereas, the TSH-β subunit gene is 4.9 kb in length, consists of three exons and two introns[99].

1.5.2 TSH Function

The TSH controls thyroid growth and function upon its interaction with the G protein-coupled TSH receptor (TSHR)[43]. The physiological role of TSH includes the stimulation of different thyroid functions, such as iodide uptake and organification, the release of thyroid hormones from thyroid gland, and promotion of thyroid growth[106]. It also plays a critical role as a thyrocyte survival factor and protects the cells from apoptosis[107].

1.6 Thyroid stimulating hormone receptor (TSHR)

1.6.1 Structure of TSHR

The TSHR is a G-protein coupled receptor (GPCR) characterized by large glycosylated extra cellular domain (residues 21-415) and N-amino terminus responsible for high affinity binding of TSH[45,108,109]. The TSHR shares with other GPCR a common molecular architecture of seven trans-membrane segments (three extracellular loops and three intracellular loops plus the carboxyl terminus) responsible for the G coupling and the signal transduction[108,110]**(figure 1.6).**

At protein level, the human full length TSHR is made up of amino acids 21-764 amino acids. The TSHR contains six putative glycosylation sites and the first 20 amino acids are the signal peptide[109]. It contains two subunits; A subunit, corresponding to the extracellular domain (ECD) (residues 21-415) and, the B subunit, is mainly the transmembrane domain (TMD) (residues 416-764)[111-114].

Post translation proteolysis splits the TSHR into two subunits (A and B subunits) linked to each other by disulfide bonds[115]. These A and B subunits are formed by intermolecular cleavage of the C peptide and formation of S-S bridges between cysteines, apparently at two sites (site1 & site 2)[115] with removal of an intervening polypeptide segment of approximately 50 amino acids known as the "hinge" region[113,114,116](**figure 1.6**).

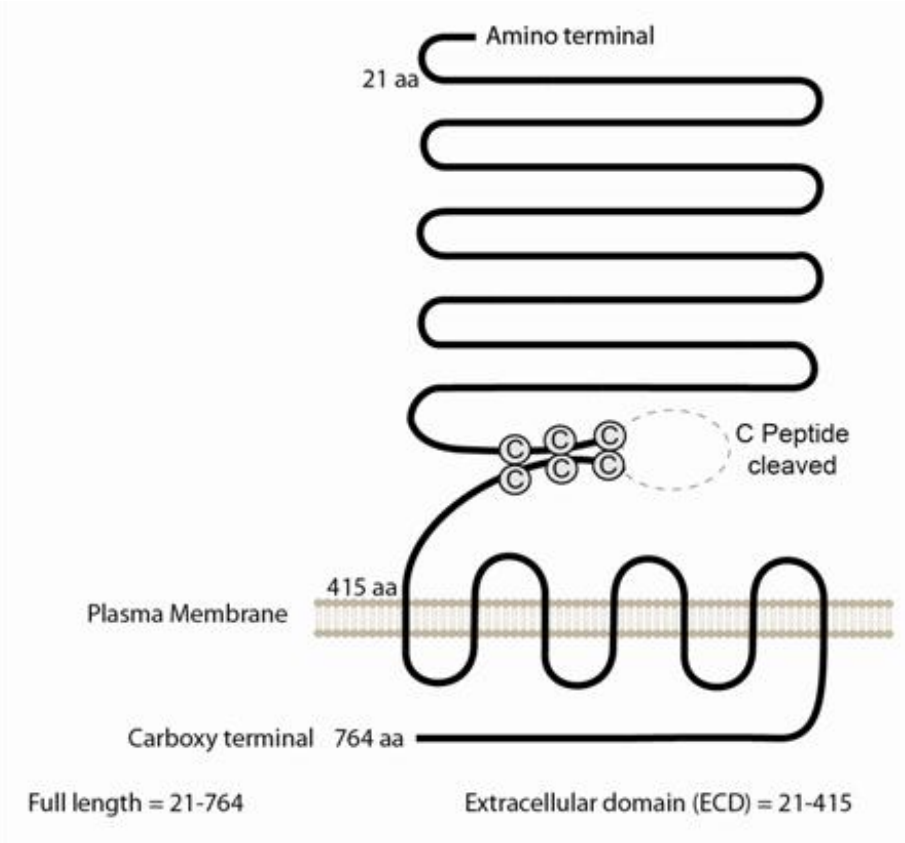

Figure 1.6: Structure of TSHR protein: showing seven trans-membrane spanning loops, intra and extra cellular domain.(Adapted from Rapoport, B,1998)[109].

Furthermore, the extra cellular domain consists mainly of nine leucine-rich repeats (LRRs) and an N-terminal tail forming the binding domain for TSH. Whereas, the seven trans-membrane domain are joined intracellularly by connecting loops that interact with G proteins when the receptor is activated[117]. Each LRR consists of 20–24 amino acids (aa), which combine to form a horseshoe-like structure with a concave inner surface which

determines its ligand specificity[118]. The LRRs are characteristic to the subgroup of GPCRs such as TSHR, LH-R, FSH-R[45,109].

Unlike the other members of this subgroup of receptors, the extra cellular domain of the TSHR has two very unique regions. These regions are in the N-terminus of the ectodomain ~10 amino acids (residues 38-45) and, in the C-terminus of the ectodomain ~ 50 amino acid (residues 316-366)[109]. It is believed that the cysteine clusters in this N-terminus is important for appropriate folding and intercellular trafficking of the receptor. While, cysteine clusters at the C-terminus of the ectodomain serve in disulfide bond formation after intermolecular cleavage which produce the receptor's A and B subunits[109].

1.6.2 Genomic structure of TSHR

At the genomic level, the full length TSHR is located on chromosome 14q3[110] , sequence reference number (NM_000369). It spans over 60 kilobases (kb) which is split into 10 exons. It consists of two subunits generated by cleavage of a single gene product, linked by disulphide bridges[119]. The A subunit (A), corresponding to the extracellular domain (ECD), is encoded by exons 1-9 plus the first 300 base pairs (bp) of exon 10, and a B subunit (B), which is a trans-membrane domain region (TMD), important for signal transduction via cAMP, encoded by the remaining 1000bp of exon 10[120](**figure 1.7**).

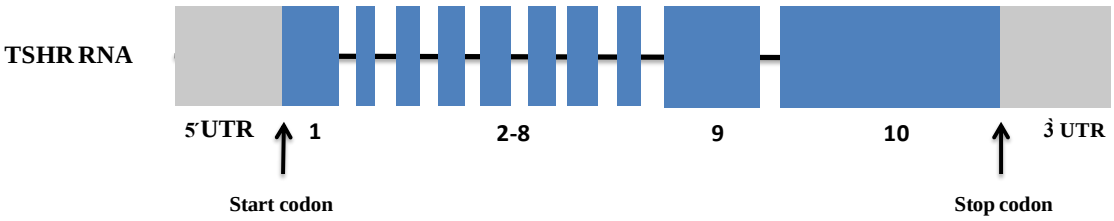

Figure 1.7 Structure of Human TSHR gene (adapted from Paschke, R et al,1996)[54]. Blue boxes indicate the translated region (exons1-10), Black horizontal line indicates introns, and grey boxes represent untranslated regions.

1.6.3 Cleavage and shedding of TSHR

As mentioned above, the TSHR comprises two subunits held together by di-sulphide bonds. These two subunits are formed by intermolecular cleavage from a large precursor, apparently at multiple sites[114,115]. This cleavage is associated with the loss of an intervening C peptide segment corresponding approximately to 50 amino acids (amino acids 316-366) that are uniquely present in the TSHR and not LH and FSH receptors, **(figure 1.6)**[109]. The fact of TSHR cleavage into 2 subunits is thought to explain why the TSHR is so easily activated by autoantibodies and mutations[109].

Under certain conditions the disulphide bonds holding the A and B subunits are reduced most probably by protein disulfide isomerise leading to release of the A subunit from the membrane bound receptor [116,121]and possibly progression of B subunit degradation towards the membrane[113]. This phenomenon of releasing of A subunit is referred to as receptor shedding and it produces a soluble form of ligand binding protein[122].

1.6.4 Post-translational TSHR modifications

The recombinant full length glycosylated TSHR determined by SDS-PAGE appears to be ~ 100-120 Kilo Dalton (kDa), this mature glycosylated form of TSHR receptor is expressed on the plasma membrane and undergoes cleavage[109]. The molecular weight of the un-glycosylated TSHR deduced from the amino acid sequence corresponding to ~ 84 kDa[109].

1.6.5 Activation of TSHR

The thyrotropin receptor basically acts as a transducer molecule whereby ligand binding (TSH or TSAbs) triggers the activation of the G protein (guanine –nucleotide –binding protein). The N-terminus of the ECD contributes to TSH binding but the trans-membrane spanning region and the carboxyl terminus are responsible for G protein coupling and signal transduction[123]. When the TSHR is preferentially coupled to the α subunit of the stimulatory G protein (Gs α), it activates the adenylate cyclase and increases the accumulation of cyclic AMP (cAMP) **(figure 1.8)**[55].

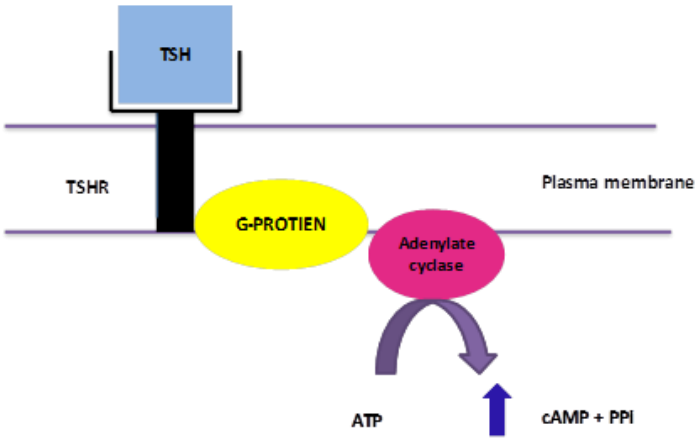

Figure 1.8: Schematic figure showing activation of adenylate cyclase by TSHR activation.

Both the growth and function of the thyroid are stimulated by cAMP[55]. This second messenger indirectly regulates the expression of the thyroglobulin (TG) and thyroid peroxidase (TPO) genes, whose promoters contain binding sites for the transcription factors TTF-1 and TTF-2 and Pax8[124]. Therefore, continued stimulation of the cAMP pathway (as occurs in patients with Graves' disease) causes hyperthyroidism and thyroid hyperplasia[124]. TSH has been documented to induce not only cAMP activation but also to the induce protein kinase C pathway in thyroid cells[125].

1.6.6 TSHR expression in the skin

It is well known that skin development and function are regulated by thyroid hormones. However, thyroid dysfunction can cause alteration in skin architecture and haemostasis[50,126]. For example thyroid hormone dysfunction can effect fetal epidermal differentiation, barrier formation, hair growth, sebum production, wound healing, epidermal oxygen consumption, keratinocyte proliferation, and keratin gene expression [127,128,77,126,129-131]. Traditionally the skin/skin appendages conditions associated with thyroid dysfunction have all been attributed to the effects of too much or too little thyroid hormone and several thyroid hormone responsive genes have been identified in the skin[53]. However a role for TSH and autoantibodies has also been suggested but this would require the presence of the TSHR in the skin. More recently, elements of the hypothalamic- pituitary – thyroid axis genes[53] have been demonstrated in the skin with TSHR expression shown to occur in different cell types, including the epidermal keratinocytes, dermal papillae fibroblasts[132], hair arrector pili muscle, sweat glands, sebaceous gland cells, vascular endothelial cells, Schwann cells[133].

1.7 TSHR variant

A number of TSHR splice variants or isoforms of variable length have been described for the TSHR[134], LH/hCG receptor[135,136] and FSH receptor[137, 138]. TSHR variants have also been described in other vertebrates including mouse (NM_001113404.1), dog[139] and embryonic chicken thyroid[140]. The pathophysiologic importance of these variants is not clearly known[141]. Graves and his team were able to clone and sequence a 1.3kb TSHR variant namely TSHR isoform 2 precursor which codes for amino acid residues (21-253) (NM_001018036.1)[134] and, found that it comprised exons 1-8 and a new "tail sequence". This transcript variant encodes the extracellular ligand binding domain but lacks the trans-membrane domain and is therefore not capable of signalling[134]. Furthermore, another TSHR variant with deletion of exon 3 has been described[139] with deletion of exon 3 known as TSHR isoform 3 precursor which codes for amino acid residues 21-274 (NM_001142626.1)[139]. The isoform variants differ in the 3' UTR and coding sequence compared to isoform 1. The resulting protein variants have a shorter and distinct C-terminus compared to isoform 1[134].

The splice variants for the glycoprotein hormone receptors family described in the literature so far comprise nearly the entire extracellular domain of the receptors[134,138], and parts of the carboxyl terminal intracellular domain[135,136]. Therefore, studies trying to detect full length TSHR by PCR should be undertaken with primers spanning exons 1-10. Studies trying to detect full length TSHR using primers spanning shorter segment could carry a considerable risk of amplifying the TSHR variant instead of the full length receptor as these short segment primers could not distinguish between the full length form and the variant form[141].

The level of expression of these receptors varies depending on the functional state of the target tissue for LH and FSH[142,143]. Using primer specific for human 1.3kb variant transcript described by Graves and his team in 1992[134] in a reverse polymerase chain reaction and southern blotting analysis[134], Paschke and his team were able to demonstrate the presence of 1.3kb variant transcript in many locations including normal thyroid tissue, Graves' thyroid, peripheral blood mononuclear cells (PBMC) and also in extra ocular muscles and to a lesser extent in fat and cultured ocular and dermal fibroblasts[141]. However, it is not known whether TSHR variants actually exert a physiological role in the body. Similarly, the exact cellular location of TSHR variant expression is also not known yet. In addition to the possible modulatory effects of TSHR variants on TSH/TSHR interactions is still not clear.

1.8 Thyrostimulin

1.8.1 Thyrostimulin discovery

A new glycoprotein hormone known as thyrostimulin or corticotroph-derived glycoprotein hormone has been described[144]. Based on Genbank search, Nakabayashi et al, 2002[144], identified two novel human glycoprotein hormone-like genes The first one was named GPHα2 due to its structural similarity to the common glycoprotein α-subunit and, the second one was named GPHβ5 as the potential fifth member of glycoprotein hormone β-subunit family, accession numbers for α2 and β5 are AF403384 and AF403430, respectively[144] . This new hormone was named thyrostimulin.

Human α2 is located on chromosome 11q13 and β5 is located on chromosome 12[145]. Both α2 and β5 subunits were capable of activating TSHR in vitro and in vivo with an affinity

similar to that of thyroid stimulating hormone (TSH). However, they have limited effect on LHR and FSHR[144]. The pathophysiological role of thyrostimulin is still unclear. However, its expression in the anterior pituitary suggests a paracrine signaling mechanism[144,146].

1.8.2 Structure of Thyrostimulin

Thyrostimulin consists of non-covalent heterodimers of a novel α subunit and unique β subunit[144]. Unlike other glycoprotein hormone which shares a common α subunit GPH α 1, this novel α subunit does not form a heterodimer with any of the known β subunits (TSH-β, LH-β, FSH-β, CG-β)[144]. They contain cysteine residues that form a cystine knot structure, which is common to all glycoprotein hormone subunits important for the formation of the disulphide bond[144,147,148]. However, the thyrostimulin is less stable than the other glycoprotein hormones during the SDS-PAGE analysis[144], because the β5 lacks the disulfide bond necessary for the seat belt formation[145].

This typical framework consists of four cysteine residues with a cysteine spacing of Cys-$(X)_3$- Cys and Cys-X-Cys, important for a ring structure formed by eight amino acids. The cystine knot family members contain two additional cysteines (C1,C4) that form a third disulfide bond that penetrates the ring structure, thus forming a cystine knot with 10 amino acids of which six are cysteine residues[149]. Cysteines 2, 3, 5, and 6 form a ring by disulfide bonding between cysteines 2 and 5 as well as 3 and 6. The third disulfide bond, formed by cysteines 1 and 4, penetrates the ring, thus forming a knot[148]. The arrangement of the cysteine knot folding of these domains in sequence motifs for GPHα2 forms a three-dimensional structure and has been referred to as a "hand" containing two fingers and a middle heel (**figure 1.9**)[147]. Two of them, between cysteines 1 and 2, as well as 4 and 5,

consist of anti-parallel β-strands that form finger-like projections, whereas the third domain between cysteines 3 and 4 usually contains an α-helical structure[147].

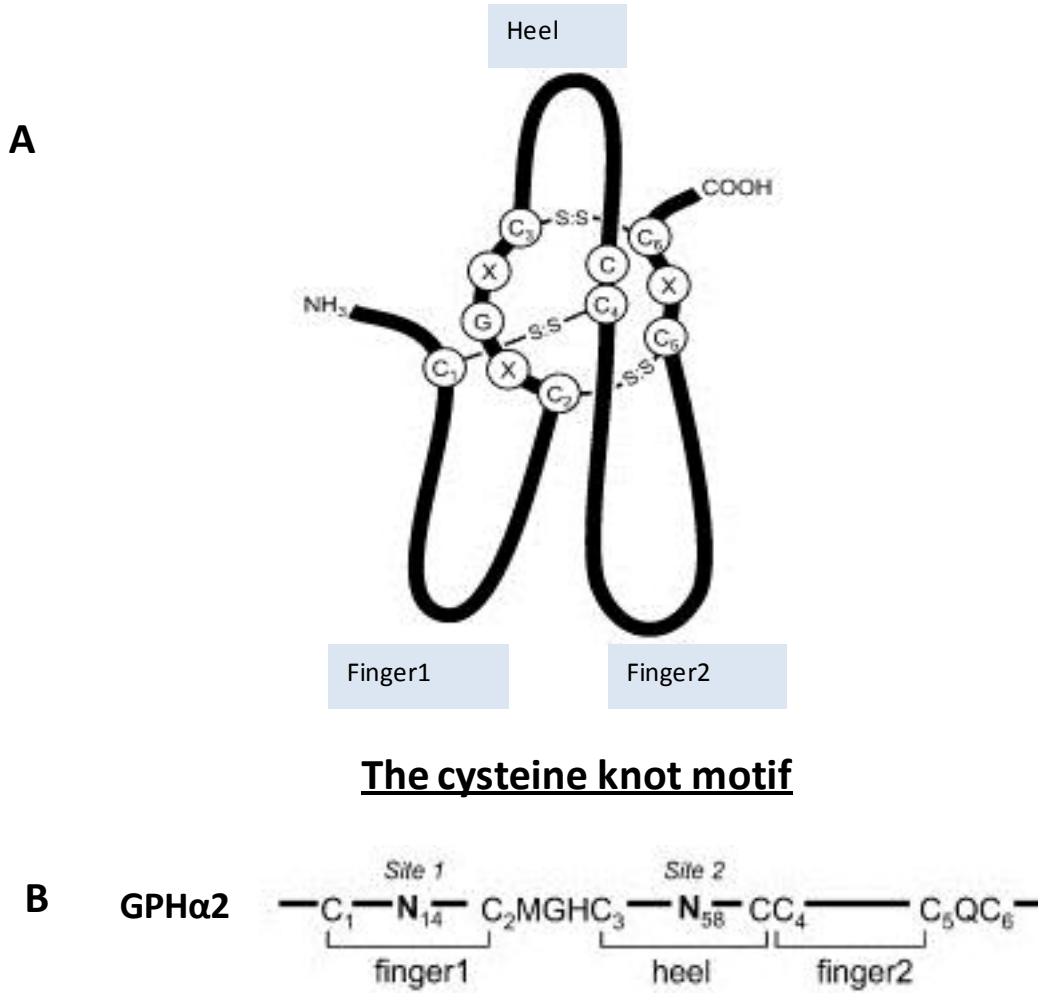

Figure.1.9: Schematic diagram showing the cysteine knot structure of thyrostimulin (adapted from Okajima,Y. et al,2008)[147]. (A) Consensus sequence for the 10-membered cysteine knot structure. Due to the arrangement of the domains, the three-dimensional structure of these proteins has been referred to as a "hand" containing two fingers and a middle heel. (B) Sequence motifs for GPHá2 showing oligosaccharide attachment sites[147].

1.8.3 Role of N-linked glycosylation motifs in thyrostimulin regulation

The oligosaccharides of glycoprotein hormones have been reported to be significant for their bioactivities[101]. Loss of these oligosaccharides may cause disruption of protein folding and /or disulfide bond formation, consequently altering the peptide stability and increase the peptide sensitivity to proteases[101]. The GPHα2 and GPHβ5 subunits of thyrostimulin have three N-linked glycosylation motifs, which play a crucial role in thyrostimulin regulation. They are located at positions (Asn14 and Asn 58) of GPHα2 and (Asn63) of GPHβ5[**147**].

Okajima and his colleague studied the role of thyrostimulin N-linked oligosaccharide subunit expression, secretion and assembly by using site directed mutagenesis (site specific disruption) which allows selective and complete inhibition of oligosaccharide attachment at each site[147]. Deletion of both oligosaccharide motifs in GPHα2 (α2n 14,58q) and deletion of the solitary oligosaccharide in GPHβ5 (β5n63q) significantly decreased the expression level, secretion and stability of both subunits in the conditioned medium and cell lysate[147]. This was consistent with the previous finding that removal of the oligosaccharide chain in GPHα1 of all glycoprotein hormones and TSH-β of the TSH significantly reduced the secretion and expression level to negligible amounts[150,151].

1.8.5 Tissue expression of Thyrostimulin

Tissue expression of thyrostimulin is highly controversial. Expression profile analysis using RT-PCR and immuno-histochemistry showed that both Thyrostimulin subunits α2 and β5 are expressed in the pituitary of different vertebrates also in different tissues outside the HPT axis[144,145]. In general, tissue analysis demonstrated that α2 showed wider

range of distribution than β5, immuno-histochemistry analysis showed both Thyrostimulin subunits were co-localized in the rat pituitary, central nervous system, adrenal gland, stomach, duodenum, pancreas and testis[145,146,152]. A further report by Nakabayashi and his colleagues, where by endpoint RT-PCR analysis of a panel of rat tissue mRNA found α2 and β5 transcripts in diverse tissues outside the HPA and HPT axes. However, they reported that β5 expression was observed in the brain, pituitary, thyroid, oviduct and the heart and not in testis or adrenal gland[144]. In contrary, a different group used northern analysis and quantitative real-time PCR was able to detect expression of α2 and β5 in different set of human tissues[153]. The reason for the difference in the expression pattern of thyrostimulin subunits in various reports is unclear, it could be explained by antibody specificity (Anti- α2 vs. Anti- β5), the sensitivity of the methods used and, alternatively, species differences (rat vs. human) might also account for the variable results.

Thyrostimulin is thought to be expressed in corticotroph cells of the human anterior pituitary[153]. Nakabayashi and his colleagues reported co-localization of α2 and β5 to the anterior pituitary cells using double fluorescent immuno-staining, they did not, however, identify the specific cell type co-expressing the two subunits .In this study, the α2 positive cells did not show co-staining with adrenocorticotropic hormone (ACTH), growth hormone (GH), prolactin (PRL), LH-β or TSH-β secretory cells[144].

Furthermore, Okada et al further advocated this point and reported that Thyrostimulin is expressed in the anterior pituitary, in an attempt to specify the cells which secrete Thyrostimulin they used double immuno-histochemical methods to stain for the co-localization of β5 with any of the markers for cell types in the anterior pituitary, including GH, PRL, LH-β, FSH-β, and ACTH. They reported co localization of β5 with ACTH

which, according to the author, strongly suggests that thyrostimulin is produced in human pituitary by corticotrophs which are known to secrete ACTH. This was an interesting observation because these cells were not thought to have a direct role in thyroid activation[153]. These results contradict with another study which reported that thyrostimulin α2 mRNA is diffusely expressed in the anterior lobe of rat pituitary by using in situ hybridization and, did not co-localize with any of the other anterior pituitary hormone mRNAs[146]. The author suggested that α2 might be expressed in an unidentified cell type and, thyrostimulin β5 mRNA was not detected in rat anterior pituitary by using the same method. This divergence from the immunohistochemical data might be explained by: firstly, thyrostimulin β5 might be stored in the pituitary but its expression is undetected in normal conditions. Secondly, cross reactivity of antisera with other antigen[146].

1.9. Thesis Hypothesis & Aims

Thyroid dysfunction is often accompanied by skin problems. We are hypothesizing that the changes that accompany thyroid dysfunction in the skin are not simply due to the changes in the thyroid hormone levels. We think that TSHR activation might also be important but we are suggesting that there might be a novel ligand which is the thyrostimulin which may be providing the TSHR activation. The signaling through TSHR may be important in skin biology as well as thyroid function, this would require a functional TSHR in skin.

We will investigate this hypothesis and address the following aims

1. Is there a functional TSHR in the skin
2. Are α2 and β5 subunits of thyrostimulin expressed in the skin

Chapter two

Expression of TSHR and agonist (Thyrostimulin)

2. Chapter two

2.1. Introduction

Almost all people with thyroid dysfunction experience aberrant activation or increased signalling of the TSHR. This is either because of high TSH in hypothyroidism or from thyroid stimulating antibodies in Graves' disease[49]; or due to rare cases of familial non – auto-immune hyperthyroidism which is caused by germline activating TSHR mutations[154]. Since TSHR is expressed in the skin its activation might be the cause of skin disease associated with thyroid dysfunction rather than changes in thyroid hormone levels.

TSHR RNA has been clearly detected in extra-thyroidal tissues including the skin[132], adipose tissue[155], cultured human hair follicle keratinocytes, human dermal papilla fibroblasts[133], human skin fibroblast, and melanoma cell lines[53]offering an alternative explanation for dermatopathology associated with thyroid disorders. TSHR immunoreactivity (using monoclonal TSHR antibodies) has been observed in the dermis of both patients with pretibial myxedema and unaffected individuals[61]. All of these data lead to the question of whether the TSHR is of functional importance in normal skin or not?

The thyroid-stimulating hormone receptor (TSHR) belongs to the superfamily of G-protein-coupled receptors, characterized by the presence of a large extracellular domain and an extracellular amino terminus, jointly comprising the ligand binding site; and a seven trans-membrane spanning domain plus the carboxyl terminus responsible for the G coupling and the signal transduction[45,109,111].

The full length TSHR consists of two subunits generated by cleavage of a single gene product, linked by disulphide bridges[119]. The A subunit, corresponding to the extracellular domain (ECD) and B subunit, which is a trans-membrane domain region, important for signal transduction via cAMP[45,156]. The TSHR gene is located on chromosome 14q31, and spread over 60 kb and it spans 10 exons. The ECD is encoded by first nine exons (exons 1-9) and part of the last exon, whereas the transmembrane and the intracellular domains are encoded entirely by the last exon (exon10)[100].

A number of TSHR alternative splicing or truncated isoforms have been detected on Northern blot analysis of human thyroid cells. Different other variant forms has been described in the literature which were shorter and longer than the cloned 4.3kb variant these are; (1.7kb variant), (1.3kb variant)[134]. Moreover, another TSHR variant with deletion of exon3 has also been described[139], amongst these 1.3kb is the most abundant form therefore, we will be focusing on this form in this project.

The TSHRv1.3 transcript has been shown to be expressed in normal and Graves' thyroid extra-ocular muscle, PBMC, and, to a lesser extent in fat and fibroblasts[141]. The major human TSHR variant transcript (TSHRv1.3) (NM_001018036.2) is 1.3 kb in human and is comprised of exons 1-8 of the major mRNA species plus a unique 3`-sequence of DNA tract, presumably an intron, predicted to encode further amino acids and a polyadenylated tail[134]. This transcript variant not only lacks the trans-membrane domain or signalling capability but also if expressed it is not expected to couple to G-proteins[134]. The exact pathophysiologic importance of the variant isoforms is not known yet. However, a possible biological role of truncated isoforms in modulating TSH signals is suggested by their occurrence in other species, including mouse, dog and chicken[157].

The TSHR variant isoforms are formed by alternative splicing of the full length TSHR mRNA. Alternative splicing of eukaryotic pre-mRNAs is a mechanism for generating potentially many transcript isoforms from a single gene; the exons of the RNA produced by transcription of a gene (a primary gene transcript or pre-mRNA) are reconnected in multiple ways during RNA splicing. The resulting different mRNAs may be translated into different protein isoforms; thus, a single gene may code for multiple protein products (**figure 2.1**). The alternative splicing was thought to be unimportant and maybe even an in-vitro artefact[157]. Currently its importance in generating novel and different proteins is increasingly recognised[157].

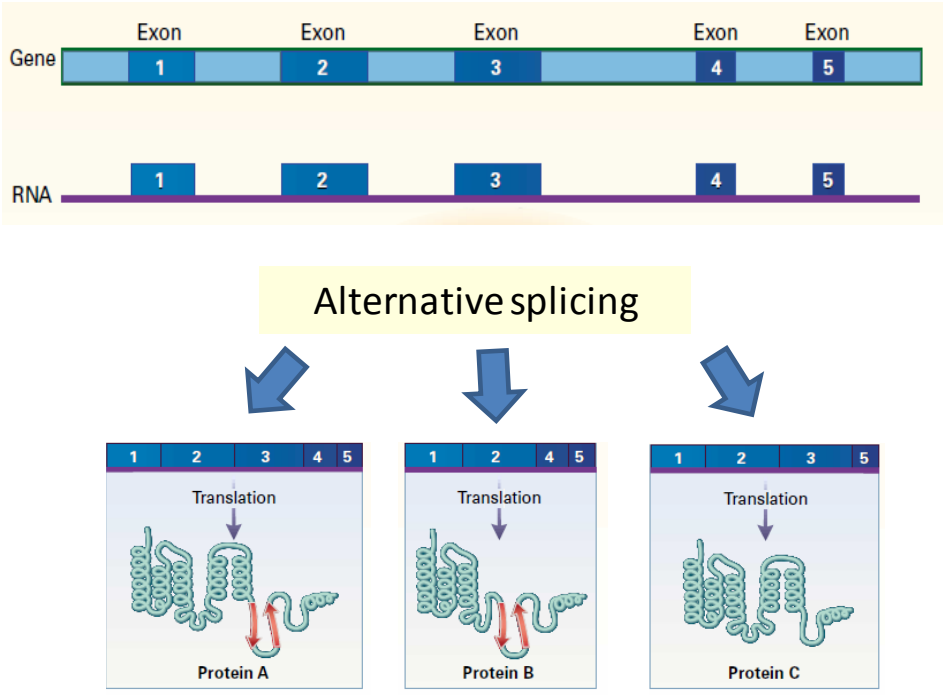

Figure 2.1, Schematic diagram showing alternative splicing. A single gene can produce multiple related proteins, or isoforms by means of alternative splicing (Adapted from A Guttmacher,2002[158]).

This process includes joining of different 5' and 3' splice sites where two or more alternative 5' splice sites compete for joining to two or more alternate 3' splice sites, other types of common gene splicing events includes exon skipping and intron retention[158]. Taking that into consideration, as the full length TSHR transcript comprises 10 exons and is 4.3Kb and a smaller variant transcript comprises exons 1-8 of 1.3 Kb of the receptor gene, then as a result of alternative splicing, a smaller part of intron 9 is removed leading to creation of an alternative exon that codes for 22 unique amino acids (aa) in hTSHR and 15 unique amino acids (aa) in (mTSHR) before reaching an alternative STOP codon[134] (**figure 2.2)**.

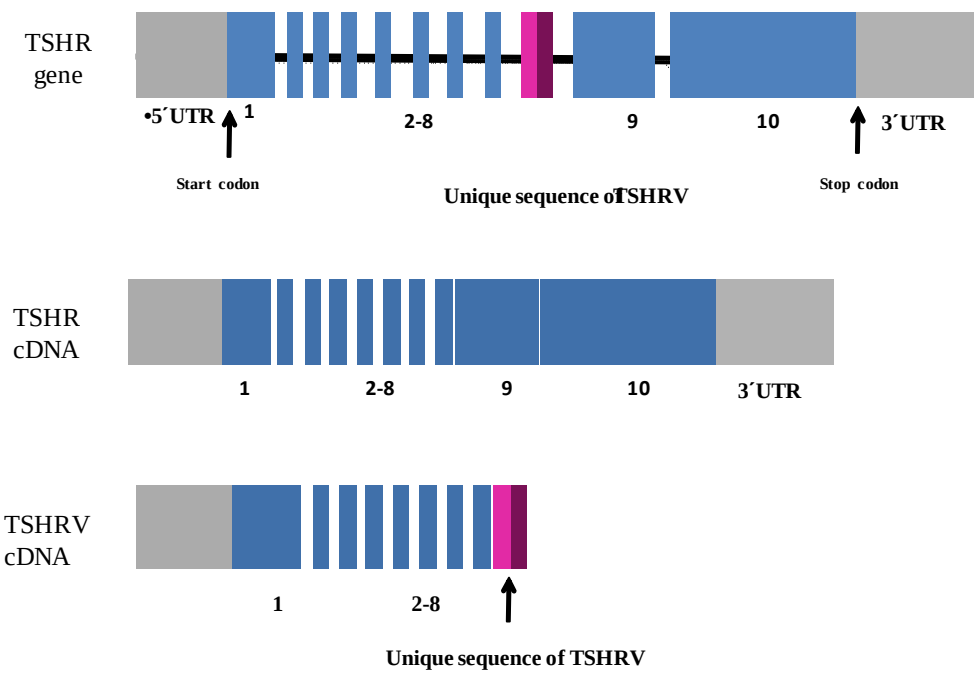

Figure 2.2. Structure of Human TSHR gene and TSHR splice variants. Blue boxes indicate exons1-10, Black horizontal line indicates introns, and light pink box represents unique sequence in TSHRV, dark pink box indicates alternative stop codon.

Several studies were undertaken to detect the expression and the localization of full length TSHR in the skin[53,132,133]. In 2002, Slominski et al, demonstrated TSHR transcripts in cultured keratinocytes, epidermal melanocytes and melanoma cells using an exon 6 forward and exon10 reverse primers[53]. While, Bodo et al, 2009[133], used an exon 1 forward primer and an exon 2 reverse primer and found transcript in normal human scalp skin and human hair follicle mesenchyme. Furthermore, Cianfarani and his colleagues, 2010[132], amplified the TSHR with forward primers located in exons 4/5 and reverse primer located in exons 7/8 in cultured keratinocytes and dermal fibroblast (**figure 2.3).**

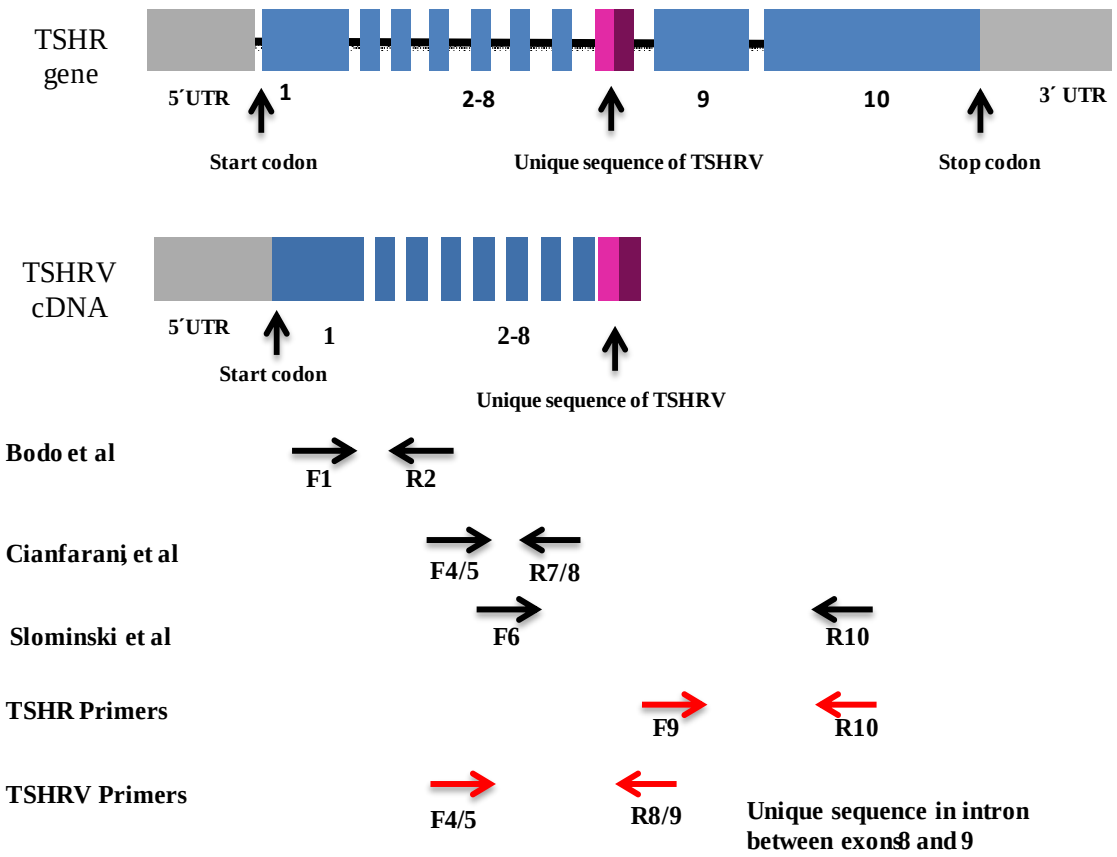

Figure 2.3: Primers used in different reports to study TSHR expression. Blue boxes indicate exons1-10; pink box represents unique sequence in TSHRV, dark pink box indicates alternative stop codon (**F**) Represents forward primer, (**R**) represents reverse primers. Black arrows represent primers used in different reports; Red arrows represent primers used in this study (Adapted from Paschke R,1994[141]).

Generally, attempts to detect a full-length TSHR by PCR should be undertaken with primers spanning exons 1-10. For example, as shown in (**figure 2. 3**) Bodo et al, 2009 and Cianfarani et al, 2010 tried to detect the full length TSHR with primer pairs spanning shorter segments as this may carry a considerable risk of amplifying TSHR variants, instead of full-length TSHR.

In this project we used RT-PCR technique for detection of full length and the variant isoform of TSHR in the skin, thyroid and different cell lines and we tried to minimize the risk of amplifying the wrong gene and, avoid false positive results, for that reason the amplification strategy we employed was to use specific primers which distinguish between the full length and variant isoform for TSHR. Full length human TSHR primer pair were designed to amplify 254 bp product, exons (9 to 10) while, the variant isoform primer pair were designed to amplify 338 bp product, exons 4/5 to the initial part of exon 8/9 (**figure 2.3**) primer positions are shown in TSHR & TSHR variant sequences (**see appendix**).

The biological role of thyroid-stimulating hormone (TSH; thyrotropin) as an agonist of the TSH receptor (TSHR) in the hypothalamic–pituitary–thyroid axis is well known[132]. However, this receptor can also be activated by other pathological elements; the TSHR is considered as a major primary autoantigen in autoimmune thyroid disease[111]. In particular, the TSHR is the target of the immune response in patients with Graves' disease in which thyroid stimulating antibodies mimic the action of TSH and cause hyperthyroidism and goitre. While, other autoantibodies can inhibit its activation by TSH in some cases of Hashimoto's thyroditis[159]. Both germline and somatic mutations, commonly located in the transmembrane regions, may induce constitutive activation of the receptor, resulting in congenital hyperthyroidism or the development of actively secreting thyroid nodules

respectively[55,160]. Similarly, mutations leading to structural alterations may induce constitutive inactivation and congenital hypothyroidism[55,160].

Based on Genbank searches, a new TSH-like hormone was identified named thyrostimulin because of its ability to activate the TSH receptor in vivo and in vitro[144]. This hormone is comprised of two novel human glycoprotein hormone like genes named GPHα2 (α2) and GPH-β5 (β5) based on chronological order of discovery. The Genbank accession numbers for α2 and β5 are AF403384 and AF403430 respectively[144]. The two thyrostimulin subunits are characterized by the potential for, in vitro, heterodimerization by using a yeast-two hybrid assay. Immunological analysis confirmed that both subunits colocalize in anterior pituitary cells. Recombinant thyrostimulin activates human TSHR but not LH and FSH receptors with high affinity to TSHR in a radioligand receptor assay[144]. The two recombinant thyrostimulin subunits stimulate cAMP production, thymidine incorporation by cultured thyroid cells and have an in vivo thyrotropic activity by increasing serum thyroxin levels in TSH suppressed rats following intravenous administration[144].

The potential physio-pathological role of thyrostimulin hormone is still awaiting elucidation. However, it was suggested that this hormone may play a role in a paracrine – signalling mechanism in the anterior pituitary and other extra-thyroidal tissues expressing TSHR[161,162], suggesting that thyrostimulin could play a role as a locally acting factor in activating the TSHR.

2.1.1Aims of chapter two

The aims of this chapter are:

Firstly, to investigate the site of expression of full length signalling competent TSHR receptor in other tissues apart from the thyroid especially in the skin, if so, which cell type. Secondly, to explore the possibility of TSHR variant expression in the skin and its role as a potential TSH or thyrostimulin binding protein, and finally to investigate whether the transcripts for the α2 and β5 subunits of thyrostimulin are co-expressed with the TSHR as a first step in determining the likelihood of thyrostimulin to serve as an alternative ligand of TSH for activating TSHR or TSHRV in the skin and in a variety of mouse tissues. However, its exact role is still unknown.

2.2. Materials and Methods

2.2.1 Tissues and cells used in this project

2.2.1.1 Human tissues

Since ethical approval is extremely time consuming and would have delayed the start of this project, human thyroid tissue and normal human skin tissue was purchased from a commercial source, AMS Biotechnology (Europe) Ltd, UK. Some skin samples were from the Dermatology Department, Cardiff University and were collected for research purposes with patient consent prior to the 2004 human tissue act.

2.2.1.2 Mouse tissues

For easy access of different mouse tissues, mouse tissues were used collected from adult C57Bl/6 mice aged 2-10 weeks (males and females). Mice were sacrificed using CO_2 asphyxiation (schedule 1) and tissues were dissected and immediately, frozen on dry ice. Tissues were stored at -80ºC until required. Prior to RNA extraction the tissues were cut up finely using a surgical scalpel on dry ice.

2.2.1.3 Cell culture

As skin is a combination of lots of cell types we used different cell lines, each cell line representing one cell type and are in vitro equivalents of the cell types found in the skin (**table 2.1**). The cell lines used in this project were to extract RNA or proteins. They were kindly prepared and provided by colleagues in the Dermatology and Endocrinology laboratories.

Table 2. 1. Summary of different cell lines used in this project.

Cell line	Cell Type	Culture Medium	Source	Reference
HaCaT	Human keratinocyte cell l*i*ne**.** Cell passage number was 38-40.	DMEM (high glucose) supplemented with L-Glutamine, 10% fetal calf serum (FCS). Medium for differentiation experiments.	Cell Lines Service (CLS), Germany.	Boukamp et al, 1988[163].
HCA2	Human dermal fibroblast cell line	Same as HaCaT but used heat inactivated FCS.	Dr David Kipling, Cardiff University	Wyllie et al. 2000[164].
3T3L1	Mouse preadipocyte cell line	DMEM/F12 10% FCS (complete medium, CM).	ATCC* (Atlanta,USA)	Zhang et al, 2006[165].
3T3	Mouse embryonic fibroblast cell line	DMEM + 10% FCS	Dr Joachim Bugert, Cardiff University	Todaro GJ, Green H, 1963[166].

*ATCC= American Type Culture Condition

2.2.1.4 Cell culture conditions

Specific culture medium and conditions for each cell type used is shown in the summary table above (table2.1). Generally, the cells were grown in 80 cm^2 Nunclon™ delta surface flasks [Nunc, UK] containing 10 ml culture medium. The medium consisted of Dulbecco's modified Eagle medium (DMEM) (with 4.5 g/L glucose, L-glutamine and without sodium pyruvate) supplemented with 10% heat-inactivated Fetal calf serum (FCS) (EU approved), 50 U/ml penicillin, 50 µg/ml streptomycin and 2.5 µg/ml fungizone (amphotericin B) [all reagents from Cambrex, Berkshire, UK]. The cells were kept in a humidified 5% CO_2 atmosphere at 37°C, and the culture medium was routinely replaced every 2 days.

2.2.1.5 Trypsinisation of cells

The cells were passaged when they reach 80% confluence. The culture medium was removed and the cells washed three times with 10 ml sterile PBS. Then 2ml of trypsin-EDTA (Lonza, Slough,UK) was added and the flask incubated at 37 ºC until the majority of the cells were in suspension (~ 5-10 min). To aid the release of the cells the flask was lightly tapped every couple of minutes. Once in suspension, 20 ml DMEM with 10% FCS was added to inactivate the trypsin. The cells were then reseeded in a fresh flask, if split 1:5 they were ready to passage again within 7 days (for HaCaT cell line). For other cell lines, this varies between 4-8 days.

2.2.1.6 Cryo-preservation of cells

The cells were trypsinised as described above and the resulting suspension of cells centrifuged at 1000 rpm for 5 minutes at room temperature. The cell pellet was then resuspended in 0.5 ml culture medium and 0.5 ml freezing mixture (FCS with 20% dimethyl sulfoxide (DMSO) [Sigma-Aldrich Company Ltd, Dorset, UK] and transferred to 2 ml sterile cryotube. The cryotube was placed in an insulating polystyrene freezing box containing isopropanol [Fisher Scientific UK Ltd, Leicestershire, UK] (ensuring a cooling rate of 1°C/min) and placed in an -80°C freezer overnight. The next day the cryotube was transferred to liquid nitrogen (-190°C) for long-term storage.

Experiment designs: to study the expression of TSHR and agonist (thyrostimulin) in HaCaT cell line we used two experimental designs. The first experiment was based on the use of calcium for cell differentiation[167]and, the cells were harvested before and after adding calcium and the second experiment was based on confluence for the stratification

and differentiation to be initiated and similarly the cells were harvested at different time points.

2.2.1.7 Calcium-Shift Induced Differentiation of HaCaT

The day that the cells were plated was designated day 0. Following trypsinisation of an 80% confluent T75 flask, the resulting cell suspension was centrifuged at 1000 rpm for 5 mins at room temperature. The cell pellet was resuspended in 20 ml KGM® (keratinocyte growth medium) KGM® SingleQuots® supplemented with (Bovine pituitary extract, human epidermal growth factor, insulin and hydrocortisone) [Cambrex, Berkshire, UK] and 0.06 mM CaCl2 [Sigma-Aldrich Company Ltd, Dorset, UK]. This was repeated to ensure all traces of the DMEM (Lonza, Slough, UK) and serum were removed. The volume of medium was then adjusted to give a cell density of 4.5×10^5 cells per dish in 6 ml of low calcium medium. The cells were plated in 10 cm wells at a cell density of 4.5×10^5 cells per dish. The cultures were maintained in a humidified 5% CO_2 atmosphere at 37°C and the DMEM culture medium replaced every two days. When the cells reached 80% confluency (usually around day 6) the medium used was switched to KGM® supplemented with KGM® SingleQuots® and 1.8 mM $CaCl_2$, and the cells were maintained for a further 10 days in this high calcium medium (bovine pituitary extract, human epidermal growth factor, insulin and hydrocortisone) [Cambrex, Berkshire, UK]. The cells were plated into six dishes: the first one which is in low Ca^{+2} and harvested around 3 days when the cells are about 30% confluent; the second one which is collected on the day of shift when the cells are 80 % confluent (usually day 6); and the third one which is kept in low Ca^{+2} for the whole experiment (16 days total), then 3 other dishes which are taken at (6 days + 3), (6 days + 6), and (6 days + 10) post shift in high Ca^{+2} as illustrated in (**figure 2.4**).

2.2.1.8 Confluence induced differentiation of HaCaT

Similarly, the day that the cells were plated was designated day 0. Following trypsinisation of an 80% confluent T75 flask, the resulting cell suspension was centrifuged at 1000 rpm for 5 mins at room temperature, The cell pellet was resuspended cells in a Dulbecco`s modified Eagle`s medium DMEM (Lanzo, Slough, UK) (high calcium) supplemented with a mix of 10% fetal calf serum (FCS) (Biosera, South America), 2μmol/L l-glutamine, 20 mmol/L HEPES buffer, 5μg/ml insulin, 5μg/ml transferrin, 0.4 μg/ml hydrocortisone and 5 ng/ml sodium selenite The cells were plated in 10 cm wells at a cell density of 4.5×10^5 cells per dish. Cells were grown at 37°C in a humid condition with 5% CO2 and 95% air and the Fresh culture medium containing 10% FCS was replaced every two days until cells were fully confluent. The cells were harvested when pre-confluent state (usually day 1), on day 3 when the cells are about 30% confluent; and (3 day + 1), (3 days + 3) ,(3 days + 7), (3 days + 10) post confluent, see (**figure 2.4**)

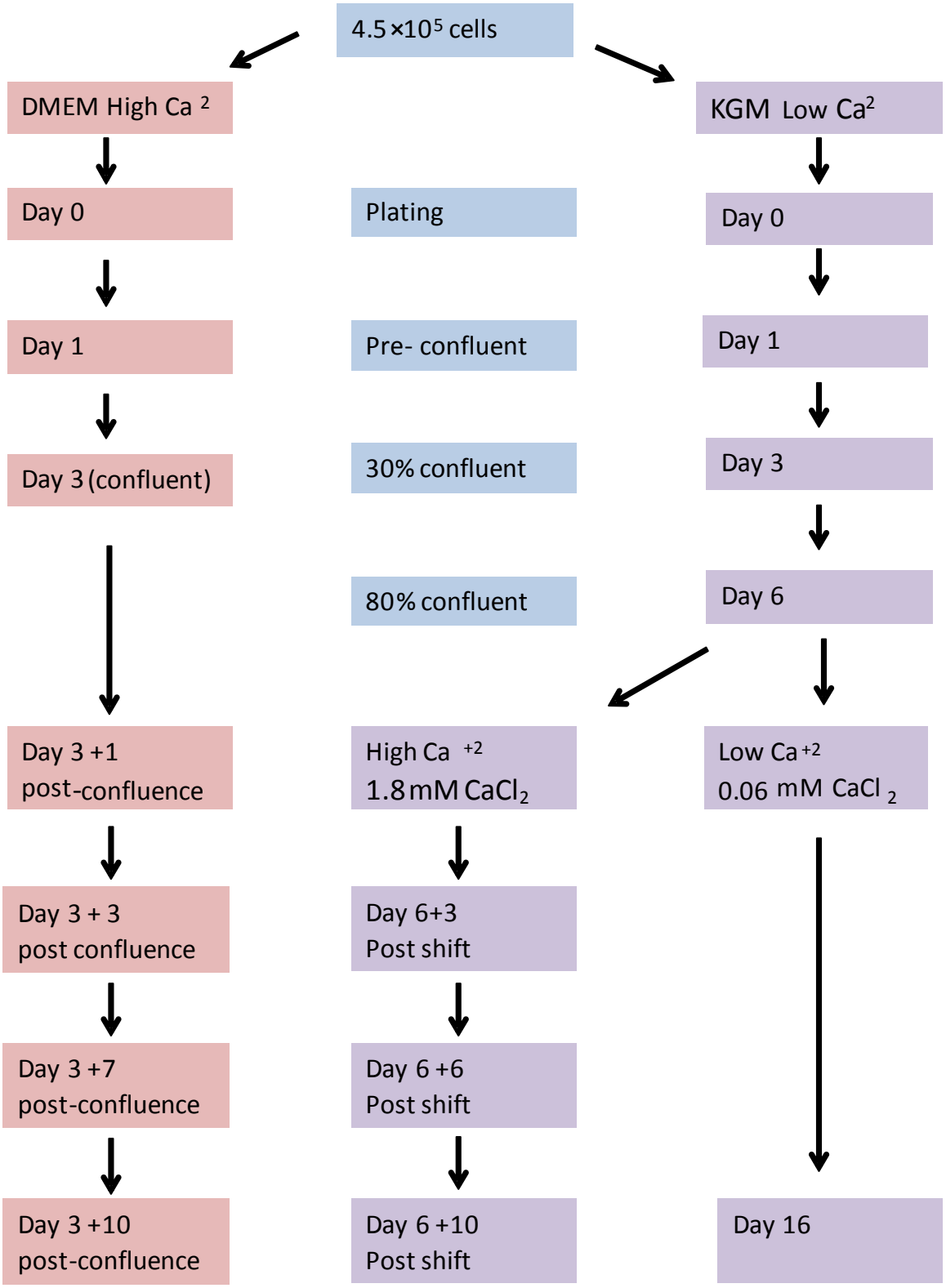

Figure 2.4: Schematic diagram showing HaCaT differentiation experiment design. Showing where the cells were plated in KGM, DMEM medium and harvested at different time points.

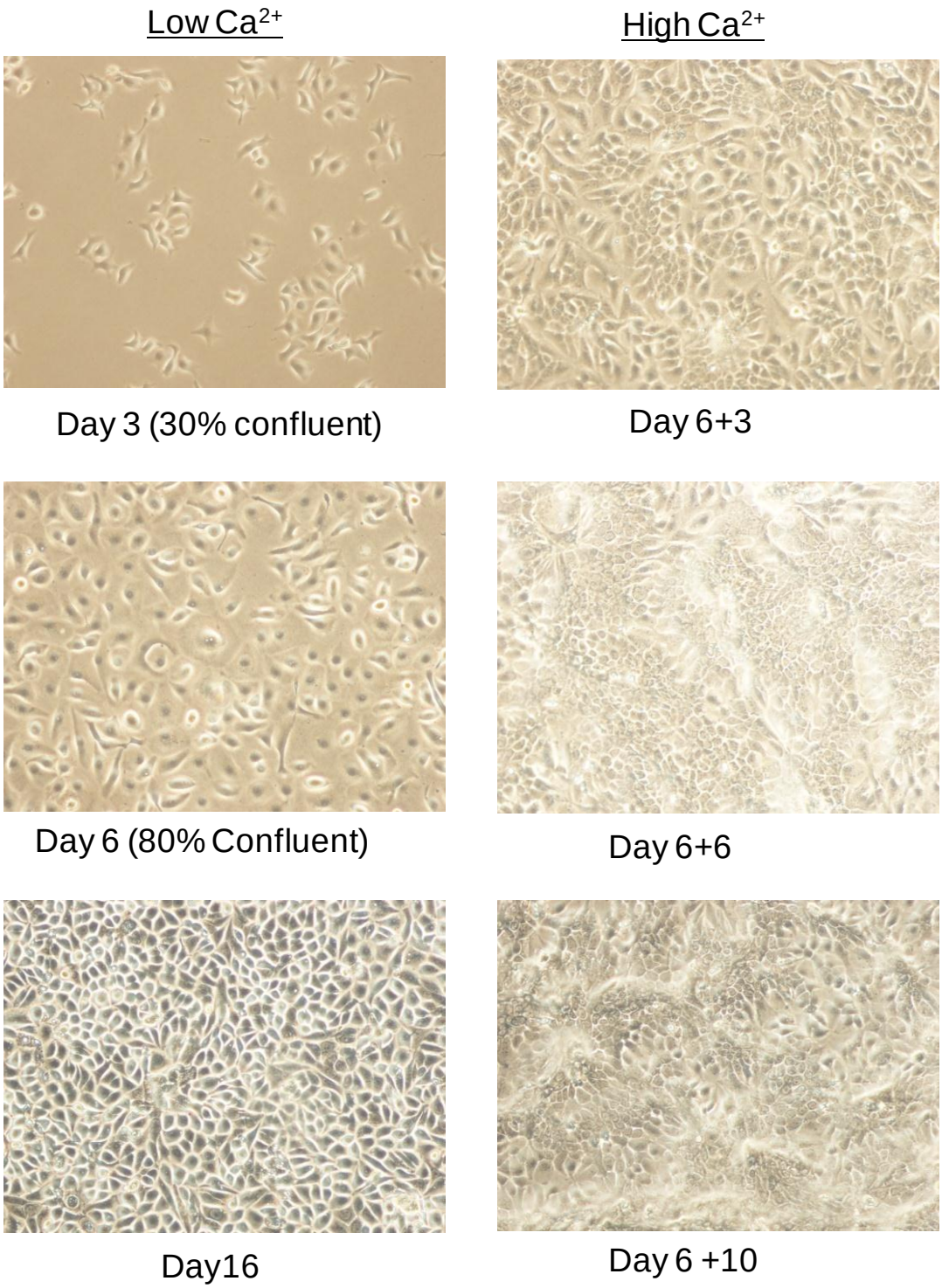

Figure 2.5: Calcium-Shift Induced Differentiation of HaCaT.
Showing live images of HaCaT cells plated in KGM medium at different time points before and after adding calcium.

2.2.1.9 Isolation of Total RNA from HaCaT Cells

RNA samples were collected on day 1 (pre confluent), day 3 (30% confluency), day 6 (80% confluency), (day 6 + 3) post-shift, (day 6 + 6) post-shift and (day 6 + 10) post-shift. Additional samples were also collected for the other experiment on day 1 (pre confluent), day 3 (confluent), (3 days + 1), (3 days + 3), (3 days + 7) and (3 days + 10) post confluent.

In each case, the culture medium was removed and the cells washed three times with 1 ml Phosphate Buffered Saline (PBS). Total RNA was isolated using Invitrogen's Trizol reagent (Invitrogen, life technologies ltd, Paisley, UK) according to the manufacturer's instructions. The cells were lysed by the addition of 1 ml Trizol reagent and passing the cell lysate several times through a pipette. Visual inspection was performed using light microscopy to ensure complete cell lysis. To allow the dissociation of nucleoprotein complexes the cell lysate was transferred to a nuclease-free 1.5 ml microtube, and left for 5 minutes at room temperature (RT). The RNA was separated from DNA and protein by adding 200 µl chloroform [Fisher] and mixing the solutions vigorously. This was followed by incubation for 3 minutes at RT and then centrifugation at 12,000×g for 15 minutes at 4°C. The upper aqueous phase (~500µl), containing the RNA, was transferred to a fresh nuclease-free 1.5 ml microtube and the RNA precipitated by adding 500 µl isopropanol [Fisher]. The sample was vortexed briefly, incubated for 10 minutes at RT, and then centrifuged at 12,000×g for 10 minutes at 4°C. The supernatant was removed and the RNA pellet washed with 1 ml 75% ethanol [Fisher]. The sample was vortexed and then centrifuged at 7,500×g for 5 minutes at 4°C. The supernatant was removed, the RNA pellet air-dried and resuspended in 20 µl nuclease-free water [Promega]. Total RNA quantity and integrity were assessed by spectrophotometer [GeneQuant, GE Healthcare] and 2 % agarose gel analysis. RNA samples were stored at -80°C until required.

2.2.2 Reverse Transcription Polymerase Chain Reaction (RT-PCR)

The messenger RNA is first reverse transcribed into its complementary DNA (cDNA) using the enzyme reverse transcriptase. By means of semi-quantitative PCR, the resulting cDNA was used to amplify the regions of TSHR, TSHRV, α2 and β5 subunits of thyrostimulin and a housekeeping gene.

2.2.2.1 RNA extraction

The initial and key step is to obtain high quality, intact RNA. The total RNA from human skin, thyroid, and mouse tissues was isolated with Trizol reagent (Invitrogen, life technologies ltd, Paisley, UK) according to the manufacturer's instructions as described earlier.

2.2.2.2 Reverse-Transcription

The reverse transcription reaction was carried out by adding 5 µl (1µg RNA in 5µl of sterile dH_2O) of mRNA to 1µl of Oligo-(dT) primers (Promega). The reaction was transferred to a thermocycler (GeneAmp9700, Applied Biosystem) and heated to 70°C for 10 minutes to denature the RNA secondary structure. Reactions were cooled to 42°C and then 14 µl of a mixture of pre-prepared RT mix was added to each tube: 1 µl of reverse transcriptase AMV-RT (50 units/reaction) (Promega, Southampton, UK), together with 1 µl of the RNAase inhibitor (Promega, Southampton, UK), 4 µl x5 Buffer (QIAGEN), 4 µl dH_2O, 4 µl of deoxynucleotide triphosphate mixture (10Mm stock) (dNTP, Roche Diagnostics GmbH, Germany). The reaction was then incubated at 42°C for 60 minutes to

synthesise the cDNA and then at 70°C for 10 minutes to stop the reaction. The resulting cDNA was stored at -20°C until required.

2.2.2.3 Polymerase Chain Reaction PCR

PCR amplification was performed in a standard reaction volume of 50 µl with the use of Taq DNA polymerase (Qiagen, Crawley,UK) For each reaction 1 µl of cDNA template was added on ice to a microcentrifuge tube containing 49 µl of a master mix comprising the following reagents:

Table 2.2: Constituents of PCR mix.

PCR Mix	Volume
X 10 PCR amplification buffer	5 µl
dNTPs mixture (10 mM)	1 µl
Forward primers (0.1µg/µl)	2 µl
Reverse primers (0.1µg/µl)	2 µl
$MgCl_2$ (see $MgCl_2$ optimization)	Variable
Q Solution	Variable
Taq DNA polymerase (5units/µl)	0 .25 µl
Nuclease free water	Up to 50µl

All the primers were synthesised by Sigma Genosys (Sigma-Aldrich, Dorset, UK) and designed from sequences obtained from NCBI Genbank. A summary of the primers used are shown in the (**table 2.3)** below. The PCR tubes containing the PCR mix were capped and briefly centrifuged to collect the contents then transferred to MJ Research PTC-200 Peltier thermal cycler. The Thermal cycling conditions for PCR: Denaturation for 5 minutes at 95ºC was followed by 40 cycles of PCR amplification as follows: denaturation at 94ºC for 30 seconds, annealing at a temperature specific to each primer pair (**table2.3**)

for 30 seconds, extension at 72ºC for 30 seconds. The reaction products were maintained at 4ºC after completion of cycles.

2.2.2.4 $MgCl_2$ optimization

The $MgCl_2$ concentration was optimized for each set of primers used in this project to get the maximum efficacy of the PCR. In summary, in addition to the $MgCl_2$ in the PCR buffer (15mM); 0 µl, 2µl, 4 µl, or 6 µl of $MgCl_2$ (25mM) stock solution was added to the PCR mix to give final concentrations of 1.5mM minimum and 6.5 mM maximum. PCRs were run on an agarose gel and the intensity and purity of the amplicon compared. The PCR conditions giving the most intense single amplicon of the correct molecular weight was used for the same set of primers throughout the project.

2.2.2.5 Calculating approximate annealing temp

The annealing temperature of each set of primers was calculated according to the following equation: (4xGC) + (2xAT) – 5 = º C

Table 2. 3: Summary of primers for genes of interest and housekeeping genes used in this project

Species	Gene	NCBI Reference Sequence	Amplicon size	Sequence direction	Primers	Exon	Annealing Temp	$MgCl_2$ cycles
Human	HTSHR	NM_000369	254bp	Forward primer	5'-GTGTCACTGCCCTTCCATCCA	Exon 9	60ºC	40 cycles
				Reverse primer	5'-GGGGCTATTCAAGGCATTCACAGA	Exon10		
	HTSHRV2	NM_001018036.2	338bp	Forward primer	5'-CCTCCTAAAGTTCCTTGGCATT	Exon 4/5	60ºC	40 cycles
				Reverse primer	5'-AGGACTTTCTTCCAAGAGGTAG	Unique sequence in intron between exons 8/9		
Mouse	mTSHR	NM_011648	540bp **166bp**	Forward primer	5'-ACGCATTCCAGGGCCTATGC **5'-TCTTACCCGAGCCACTGC**	Exon 6 **Exon9**	60 ºC	40 cycles
				Reverse primer	5'-AGTTGCTTGGGCTCTCCTGG **5'-TGTCACCCGGATCTTCTTCATA**	Exon10 Exon10		
	mTSHRV2	NM_001113404	232bp	Forward primer	5'-ACGCATTCCAGGGCCTATGC	Exon 6	55 ºC	40 cycles
				Reverse primer	5'-TCCTAGATTTGTGCCTGGTGG	Exon 8		
Human	APRT	NM_000485	245bp	Forward primer APRT (F1)	5'-GCTGCGTGCTCATCCGAAAG	Exon3	60ºC	35 cycles
				Reverse primer APRT (R1)	5'-GTGGCCAGCAGATCATCCAC	Exon4		

Mouse	β- Actin	NM-007393	458bp	Forward primer	5’-GGTGGGAATGGGTCAGAAGG	Exon3	55 ºC	30 cycles
				Reverse primer	5’-CACGCTCGGTCAGGATCTTC	Exon4		
	ARP	NM_007475	347bp	Forward primer, F2	5`CTCGCTTTCTGGAGGGTGTC	Exon5	55 ºC	30 cycles
				Reverse primer, R1	5`AAGCAGGCTGACTTGGTTGC	Exon7		
Human	α2	BC093960	400bp	Forward primer	5’-CTCGGAAGTGATGCCTATGGC		60ºC	40 cycles
				Reverse primer	5’-CTAGTAGCGAGAGAGGCGACA			
	β5	AF403430	296bp	Forward primer	5’-ATGAAGCTGGCATTCCTCTTC		60ºC	40 cycles
				Reverse primer	5’-CAGTTGGGCAGCTTGACAGTC			
Mouse	α2	NM_130453	355bp	Forward primer	5’-GAGTCTTGCTCCTTTGCCTGC	Exon2	60ºC	40 cycles
				Reverse primer	5’-CGGCACATATCACACTGGCAG	Exon4		
	β5	NM_175644	447bp	Forward primer	5’-TGAAGCCAGCGTTGTCACAGC		60ºC	
				Reverse primer	5’-ATGGGCATCCTTGTGAGCCAG			

2.2.2.6 DNA (Agarose) gel electrophoresis

The products of the PCR were analysed by size fractionation using agarose gel electrophoresis. To prepare an agarose gel an appropriate amount of agarose (Sigma-Aldrich, Dorset, UK) (2%) was dissolved in x2 Tris-acetate-EDTA (TAE) buffer (**table 2.4**) by heating the solution in a microwave oven for one minute until boiling. When the agarose had cooled sufficiently to touch, 5µl of Ethidium bromide (10mg/ml) (Sigma-Aldrich, Dorset, UK) was added and, the gel cast into a AGT1 gel tank (VWR International, UK) with a comb inserted at either end and left to set for around 30 min on a level surface. When set, the agarose gel was immersed in x2 TAE buffer. DNA samples were loaded (the Qiagen PCR buffer already contains gel-tracking dyes, ready for loading) into the wells of the 2% agarose gel together with a well containing standard size DNA ladder marker (New England Biolabs 100 bp or 1 kb ladder). A constant voltage of 50V (approximately 120 mAmps) was applied until the tracking dye had migrated to the desired distance towards the positive electrode (about half an hour). The DNA was then visualised on an UV transilluminator, and photographed using Alpha Innotech Multi Image II, Alpha Imager HP, and wave length of 365 nm. The molecular weight was compared with the DNA ladder markers.

Table 2. 4: X 50TAE (Tris-acetate-EDTA) buffer (stock solution)

Tris	242g
Acetic acid	57.1 g
0.5 M EDTA PH 8	100 ml

X 2 TAE was prepared by mixing 20 Parts stock with 480 parts H_2O.

2.2.2.7 Sequencing of PCR products

The identity of the PCR products and specificity of the primers for thyrostimulin and different types of TSHR in both species (human and mouse) were verified by DNA sequencing carried out by the Central Biotechnology Services (CBS) http://medicine.cf.ac.uk/cbs/, Cardiff University, Wales, and analyzed using A/B Applied Biosystem by life technology Software to confirm that they were 100% identical to their relevant cDNA sequences.

The Modified Automated Sequencing Method using Big Dye v 3.1 & ABI 310 was applied. The forward and the reverse primer used for sequencing are listed in primer (**table 2.3)**. Briefly, the PCR product was run in 2% Agarose gel to check that the bands were strong and clear and with the appropriate size. The following components were added to a nuclease-free 500 µl microtube: 20 µL of PCR product was mixed with 24 µL of PEG (Polyethylene glycol) (26% PEG 8000, 6.6 Mm $MgCl_2$, 0.6 M NaOAc, pH5.2), the mixture was allowed to precipitate at room temp for 10 minutes then centrifuged at 13.000 rpm for 25 minutes at room temperature, the supernatant was carefully pipetted out (invisible pellets) The pellets were washed twice with 200 µL of ice cold 70% ethanol then centrifuged for 2 minutes at 15.000 rpm. The supernatant was carefully removed and the samples were left to dry at room temperature for 5 minutes max. At this time point the sequencing oligonucleotide dilutions were made up (7µL primer + 13 µL of nuclease free water) and kept on ice and the master mix was prepared (2 µL of x5 Big Dye buffer, 2 µL Big Dye (v3.1), 1 µL of nuclease free water). The reaction mix was prepared on ice by mixing 4 µL of the DNA sample, 1 µL of primer, and 5 µL of master mix. The reaction mix was transferred to the PE Applied Biosystems 9700 thermocycler.

2.2.2.7.1 Thermocycler protocol for sequencing

28 cycles of	Denaturation:	96°C for 10 sec
	Annealing:	50°C for 5 sec
	Extension:	60°C for 4min
		4°C

DNA samples were precipitated by the addition of 1 µL 3M Na^+ Acetate (NaOAc) and 25 µL ice-cold 95% ethanol, then left at -20°C for 15 minutes. Samples were centrifuged (15,000 rpm at 4°C for 30 minutes), and DNA pellets washed twice with 180 µL ice-cold 70% ethanol. Finally, the pellets were re-suspended in 10 µL ice-cold 70% ethanol for subsequent analysis on ABI 310 DNA sequencer, (Life Technologies Ltd, Paisley, UK).

2.3. Results

2.3.1. TSHR and agonist (α2 and β5) expression in human skin and human cell lines

A number of tissues outside the thyroid express the TSHR including the skin suggesting that its activation might be the cause of skin diseases associated with thyroid dysfunction rather than changes in thyroid hormone levels. The aim of this experiment was to investigate whether TSHR, α2 and β5 thyrostimulin subunits are co-expressed in the skin and if yes, to determine in which cells type (s) they are expressed using appropriate cell lines.

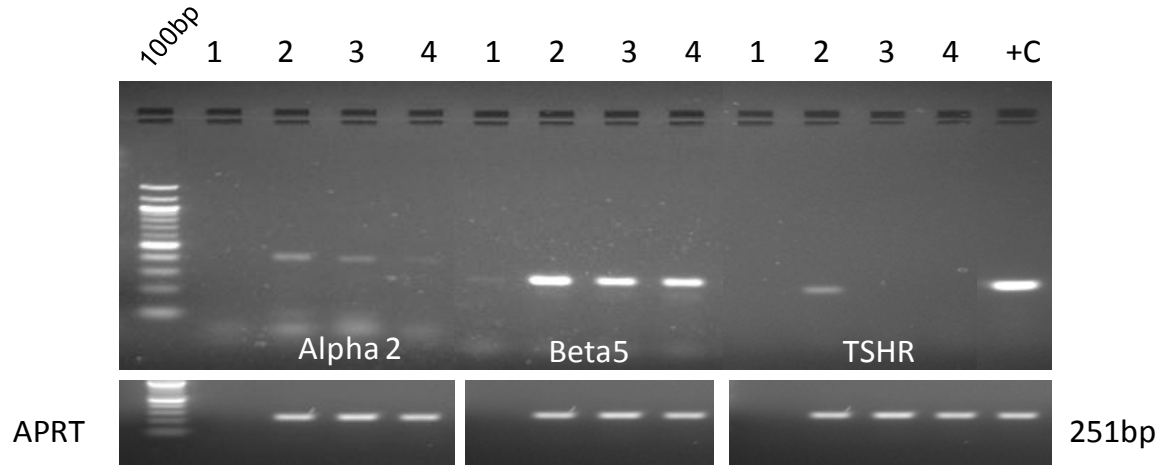

Figure 2.6: Transcript Expression of TSHR and thyrostimulin in human skin and human cell lines. Ethidium bromide stain of PCR amplification products separated on 2% agarose gel analysis of α 2 (410 bp), β 5 subunits (296 bp) of thyrostimulin and the thyrotropin receptor (TSHR) (254 bp) **Lane 1)** negative control (H_2O) lane **2)** Human skin, **lane 3)** HaCaT keratinocyte cell line, **lane 4)** HCA2 fibroblast cell line, **+ C)** positive control (Human thyroid) for TSHR, APRT (251bp) = Housekeeping gene. The first lane contains the 100bp DNA ladder.

As shown in figure 2.6, H_2O was used as a negative control while human thyroid was used as a positive control for the TSHR. The ideal positive control for thyrostimulin would have been the human pituitary but this was difficult to obtain, and so not used in these experiments. APRT was used as a house keeping gene and the presence of the expected 251bp product shows that the RNA of all the samples tested was of reasonable quality and was reverse transcribed efficiently. The full length TSHR, of the correct amplicon size, is expressed in human skin, but it is not expressed in HaCaT keratinocyte and HCA2 fibroblast cell lines. On the other hand, both α2 and β5 subunits of thyrostimulin of the correct amplicon size are expressed in human skin, HaCaT keratinocyte and HCA2 fibroblast cell lines. No additional bands were observed.

2.3.2. TSHR and agonist (α2 and β5) expression in mouse skin and mouse cell lines

The aim of this experiment was to investigate whether TSHR, alpha2 and beta5 are co-expressed in mouse skin and in which relevant mouse cell lines they are expressed.

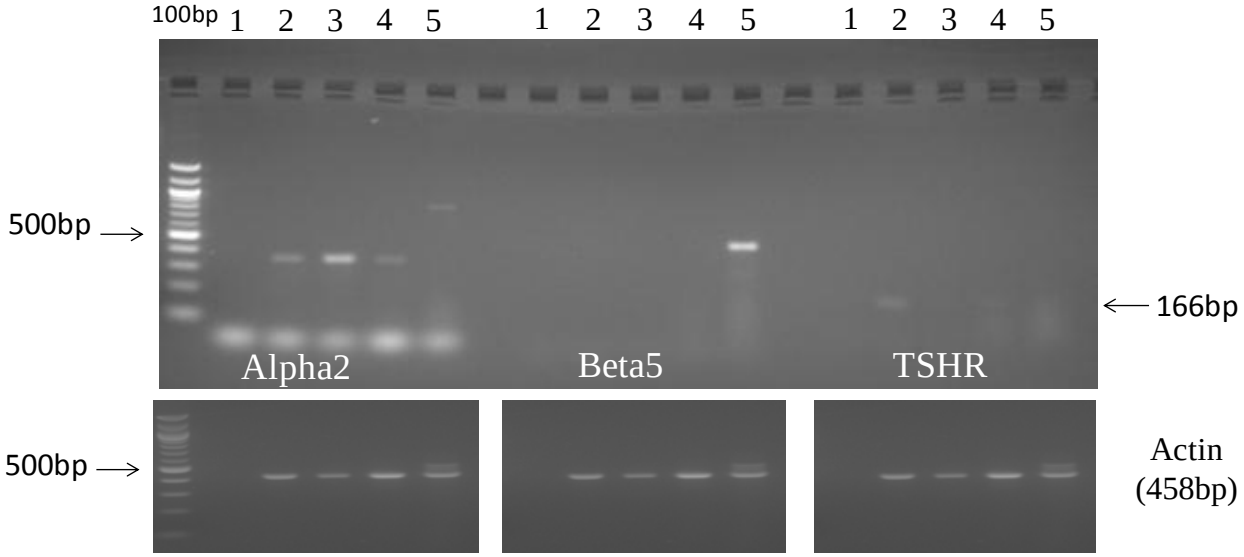

Figure 2.7: Transcript Expression of TSHR and thyrostimulin in mouse skin and mouse cell lines. Ethidium bromide stain of PCR amplification products separated on 2% agarose gel analysis of α 2 (313bp) and β 5 subunits (447bp) of thyrostimulin and the thyrotropin receptor (TSHR) (166bp) from mouse skin and mouse cell lines: **Lane 1)** negative control (H_2O) **lane 2)** Mouse skin (1), **lane 3)** Mouse skin (2), **lane 4)** Mouse embryonic fibroblast cell line (3T3), **lane 5)** Pre-adipocyte cell line (3T3L1), Actin (458bp) = Mouse housekeeping gene. The first lane contains the 100bp DNA ladder.

As shown in figure 2.7, H_2O was used as a negative control (lane 1). The ideal positive control for the TSHR would be the mouse thyroid and, mouse pituitary gland for thyrostimulin. Mouse thyroid was used in most experiments. However, we were not able to isolate the mouse pituitary due to technical reasons. A parallel PCR analysis of β-actin provided a quality check for RNA integrity and RT efficiency for all samples. The TSHR and α2, (but not β5) are expressed in mouse skin of the correct amplicon size. Whereas, TSHR was not expressed in the mouse embryonic fibroblast cell line (3T3) nor in pre-adipocyte cell line (3T3L1). On the other hand, α2 was expressed in mouse skin and embryonic fibroblast cell lines (3T3) but not in the pre-adipocyte cell line (3T3L1). An additional band was seen in lane 5 α2 (740bp) which is most likely due to amplification of genomic DNA.

2.3.3. TSHR and agonist (α2 & β5) expression in different mouse tissues

To facilitate our investigation of possible TSHR expressing tissues which might also be targets of thyrostimulin we applied ex vivo analyses of murine tissue aiming to investigate the expression of TSHR, α2 and β5 subunits of thyrostimulin as well.

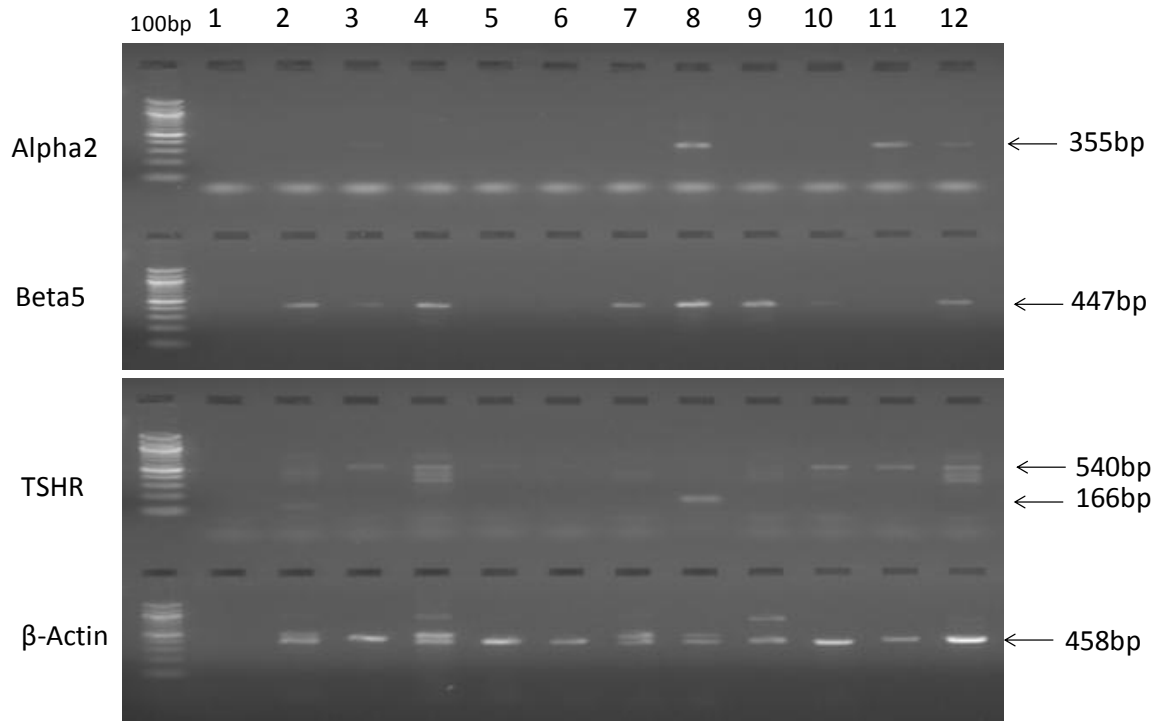

Figure 2.8: Transcript expression of TSHR and thyrostimulin in different mouse tissues.
Ethidium bromide stain of PCR amplification products separated on 2% agarose gel analysis of alpha 2 (355bp) and beta 5 (447bp) subunits of thyrostimulin and the thyrotropin receptor (TSHR) (540bp & 166bp), β-actin (458bp) = Mouse housekeeping gene. : **Lane 1)** negative control (H_2O), **Lane 2)** heart, **Lane 3)** lung, **Lane 4)** kidney, **Lane 5)** spleen, **Lane 6)** stomach, **Lane 7)** small Intestine, **Lane 8)** eye, **Lane 9)** brain, **Lane 10)** thyroid, **Lane 11)** ovary, **Lane 12)** testis, the first lane contains the 100bp DNA ladder.

As shown in figure 2.8, H_2O was used as a negative control. A parallel PCR analysis of β-actin provided a quality check for RNA integrity and RT efficiency for all samples. The TSHR transcript is expressed in lung, eye, kidney, thyroid, ovary and testis, TSHR in lane 8 (amplicon size 166 bp) was amplified using different set of primers. The α2 subunit (355bp) is only expressed in eye, ovary and testis. On the other hand, β5 subunit is expressed in most of the tissues tested of the expected size (447bp) such as heart, lung, kidney, small intestine, eye, brain, ovary and testis. However, all three transcripts were only co-expressed in the eye and testis. Additional bands were amplified by TSHR primers in particular in heart, kidney, and testis samples. The additional band amplified by β actin primers in kidney and brain samples (872bp) is most likely due to amplification of genomic DNA.

2.3.4. TSHR expression in mouse hair cycle

This experiment was conducted to try to identify the skin component responsible for the observed TSHR transcript expression in mouse skin. RT-PCR was carried out at different stages of mouse hair cycle. In the mouse, the hair cycle is synchronised making the different stages of the hair cycle easy to analyse[29]. Utilizing this we compared the expression levels of the TSHR during mouse hair cycle including; early anagen (4 weeks), late anagen (5 weeks), and telogen (7-10 weeks) in C57B1/6 mice.

Due to certain circumstances this experiment was conducted in different laboratory and different setting from where the experiment was originally started. Therefore, optimization of different PCR conditions (annealing temp and $MgCl_{2)}$ was essential at this stage as shown below (**table 2.5**).

2.3.4.1 Optimization of PCR annealing Temp in a different laboratory

The annealing temperature of genes of interest was optimized using TC-512 Techne PCR machine, Barloworld scientific Ltd, Stone Staffordshire, UK.

Table 2.5: Optimization of annealing temperature in a different laboratory.

Gene	Annealing Temp	Delta	Best result
H.TSHR	58.5°C	15°C	60°C
M.TSHR	50.0°C	15°C	55.9°C
Human α2	58.0°C	15°C	61.9°C
Human β5	58.0°C	15°C	53.9°C

2.3.4.2 Optimization of $MgCl_2$ level in a different laboratory

As described earlier in the materials and methods, the $MgCl_2$ concentration was optimized by using a range of the $MgCl_2$ concentration, between 0 µl and 2.5 µl of $MgCl_2$ (25mM) stock solution was added to the PCR mix to get the maximum efficacy of the PCR. The PCR conditions giving the most intense single amplicon of the correct molecular weight was used.

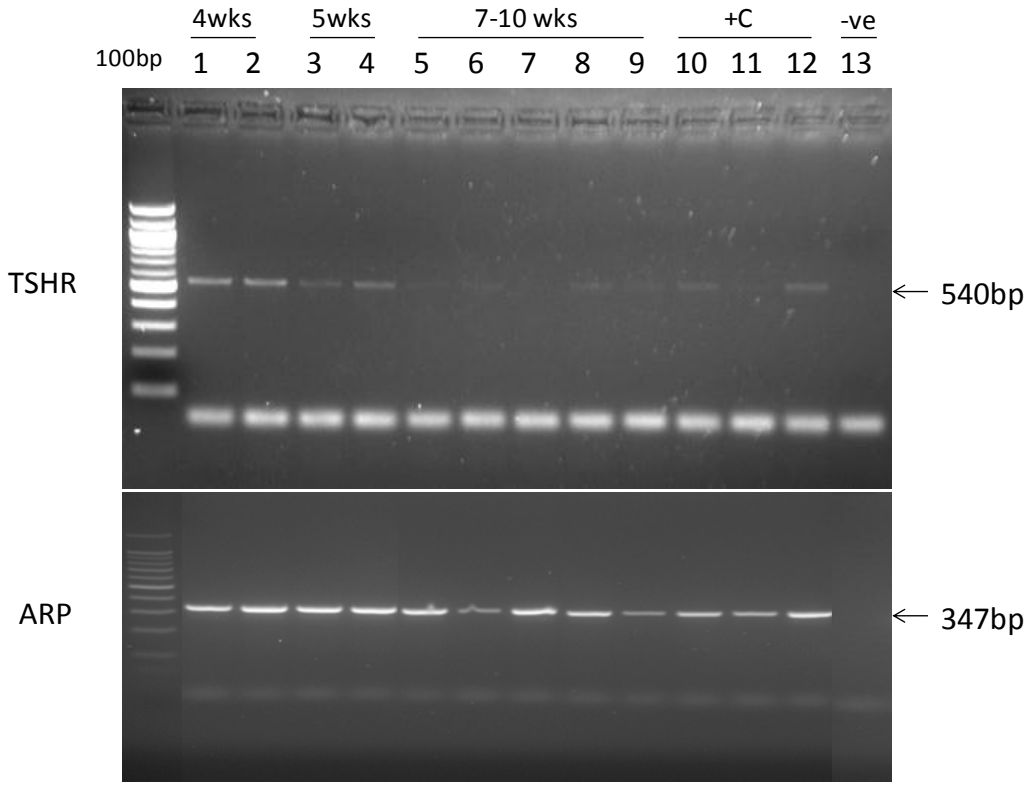

Figure 2.9.Transcript Expression of TSHR during mouse hair cycle.

Ethidium bromide stain of PCR amplification products separated on 2% agarose gel analysis of mouse TSHR (540bp). ARP (347bp) = mouse housekeeping gene. **Lane (1&2)** 4 weeks (early anagen), **lane (3&4)** 5 weeks (late anagen), **lane (5-9)** 7-10 weeks (telogen), **lane (10-12)** positive control (mouse thyroid), **lane (13)** negative control (H2O). The first lane contains the 100bp DNA ladder.

As shown in figure 2.9, H_2O was used as negative control; three different samples of mouse thyroid were used as positive control. A parallel PCR analysis of ARP housekeeping gene provided a quality check for RNA integrity and RT efficiency for all samples. The levels of TSHR were higher in early anagen than in late anagen and relatively low in telogen. Please note that at the lower part of the ARP gel, the DNA marker and the negative control were loaded in different gels.

2.3.5 TSHR and TSHR variant expression in 3T3L1 during adipogenesis

In the mouse, the hair cycle is synchronised making the different stages of the hair cycle easy to analyse[29]. Due to adipogenesis, the thickness of both dermis and the subcutaneous layer increase during anagen to accommodate the hair follicle[29], as shown in **(figure 2.10)**. Recently, Festa et al, 2011 reported that de novo adipogenesis parallels follicular stem cell activity which leads to anagen[168]. The mouse 3T3L1 preadipocyte cell line is capable of undergoing adipogenesis and provides a useful model for the process in primary depots.

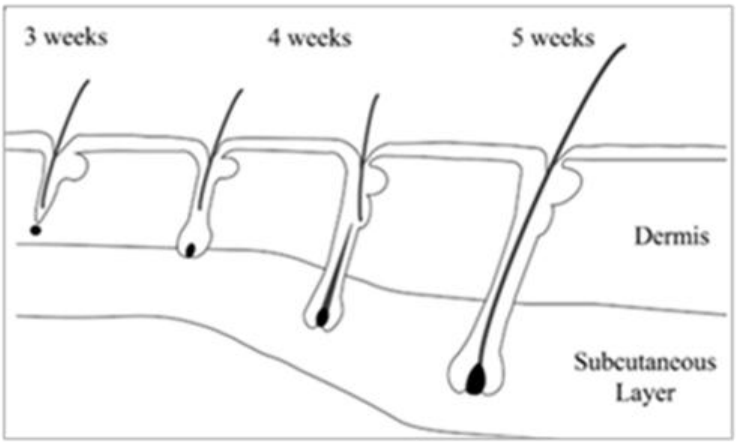

Figure 2.10: Subcutaneous layer changes during the mouse hair cycle.
Schematic diagram to showing the increase in the thickness of the subcutaneous layer to accommodate the hair follicles during the synchronised anagen phase of mouse hair cycle.

The aim of this experiment is to compare the levels of gene expression of both TSHR and TSHRV in 3T3L1 during adipogenesis. This experiment was carried out by others in the laboratory (**figure 2.11**).

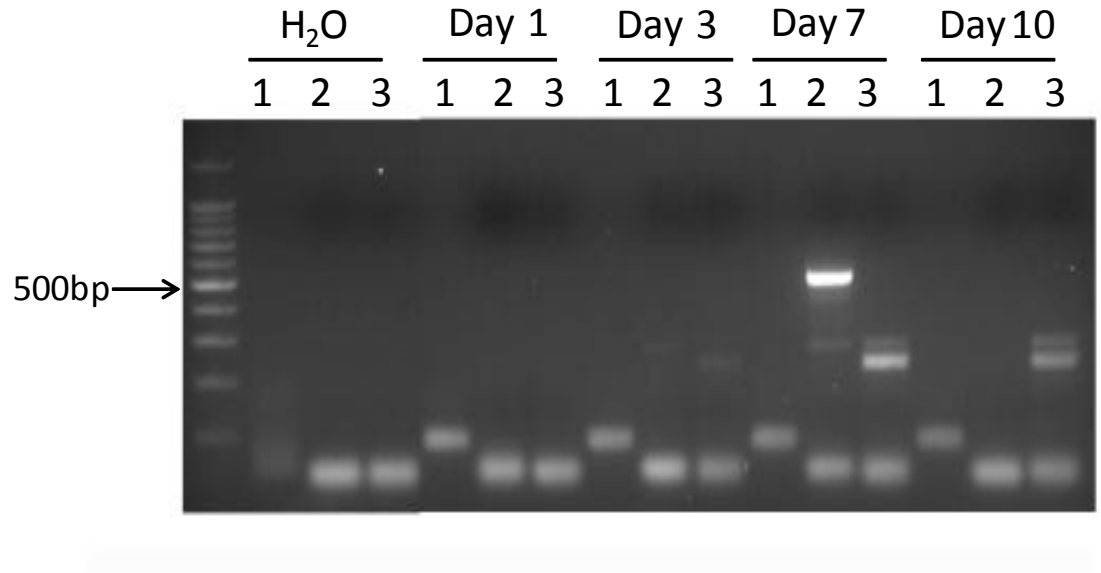

Figure 2.11: TSHR and TSHR variant expression in 3T3L1 during adipogenesis.
Ethidium bromide stain of PCR amplification products separated on 2% agarose gel analysis of: **lane 1)** ARP housekeeping gene, **lane 2)** TSHR (540bp), **lane 3)** TSHRV (232bp). **D1** = day 1, **D3**= day 3, **D7**= day 7, **D10**= day10. The first lane contains the 100bp DNA ladder

As shown in figure 2.11, H_2O, was used as negative control, a parallel PCR analysis of ARP housekeeping gene provided a quality check for RNA integrity and RT efficiency for all samples. The RT-PCR showed TSHR transcript was not expressed in 3T3L1 at early stages of differentiation but on day 7 when adipogenesis is clearly apparent in these cells the TSHR expression appears to be strongly expressed (switched on). TSHRV expression occurs earlier at day 3 and persists until day 10, longer than TSHR**.**

2.3.6 TSHRV expression in human skin

To our knowledge, TSHRV expression has not been explored in skin before. The few studies that have investigated the role of TSHR in the skin present conflicting results and show evidence of signalling using unnaturally high levels of TSH[132,133]. These studies do not distinguish between full length and truncated variant. The aim of this experiment was to clarify the abundance of TSHR variant isoforms in the skin by using unique sequence primers in intron between 8/9 of the isoforms that are not present in full length TSHR in order to distinguish between transcripts coding for signalling competent TSHR and TSHRV. If TSHRV is expressed in the skin, it has the potential for binding TSH or thyrostimulin.

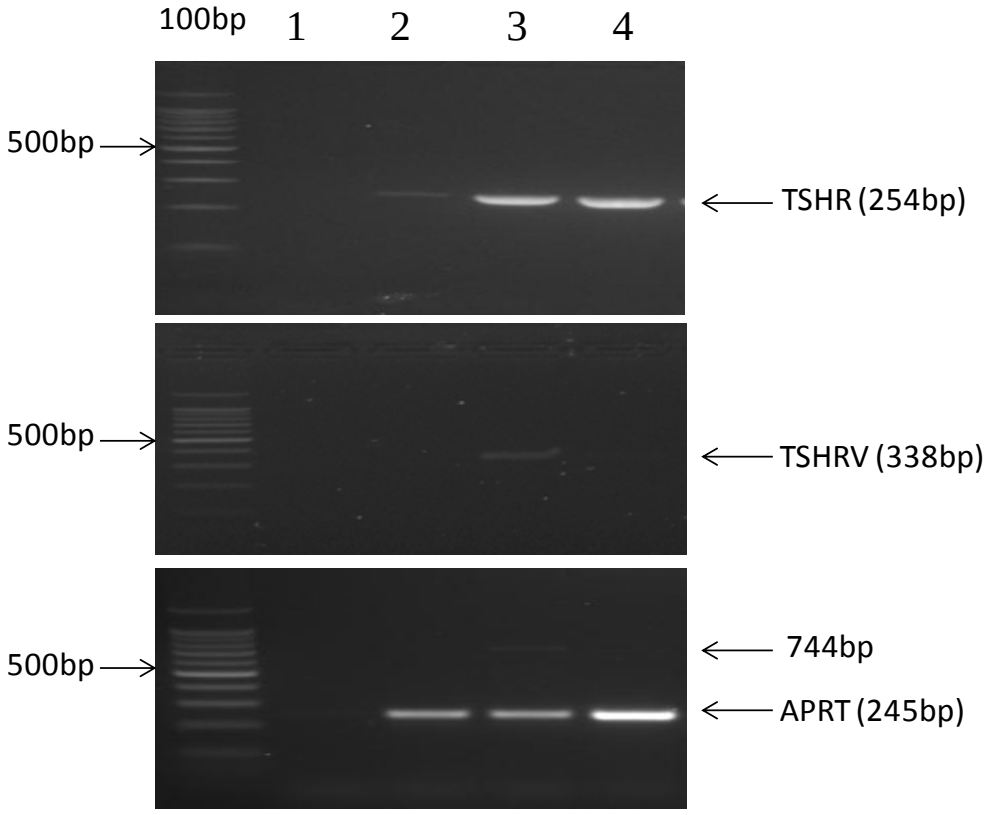

Figure 2.12. Expression of TSHR and TSHR variant in human skin.

Ethidium bromide stain of PCR amplification products separated on 2% agarose gel analysis of TSHR (254 bp) and TSHRV (338 bp) of human skin and human thyroid. APRT (245 bp) = human housekeeping gene. **Lane 1**) negative control (H_2O), **lane 2)** human skin, lane **(3& 4)** human thyroid. The first lane contains the 100bp DNA ladder.

As shown in figure 2.12, H_2O was used as negative control; two different samples of human thyroid were used as positive control. A parallel PCR analysis of APRT housekeeping gene provided a quality check for RNA integrity and RT efficiency for all samples. RT-PCR revealed high levels of TSHRV in some of human thyroid samples but not in human skin. Additional band was seen in APRT, lane 3 (744bp) which is most likely due to amplification of genomic DNA.

2.3.7 TSHRV expression in mouse skin

This experiment was conducted to determine which TSHR variant isoform is expressed in mouse skin and whether its expression varies with the hair cycle. We investigated the TSHRV expression in hairy mouse skin at different time points of the hair cycle, and compared it with hairless skin (foot sole) (**figure 2.13**).

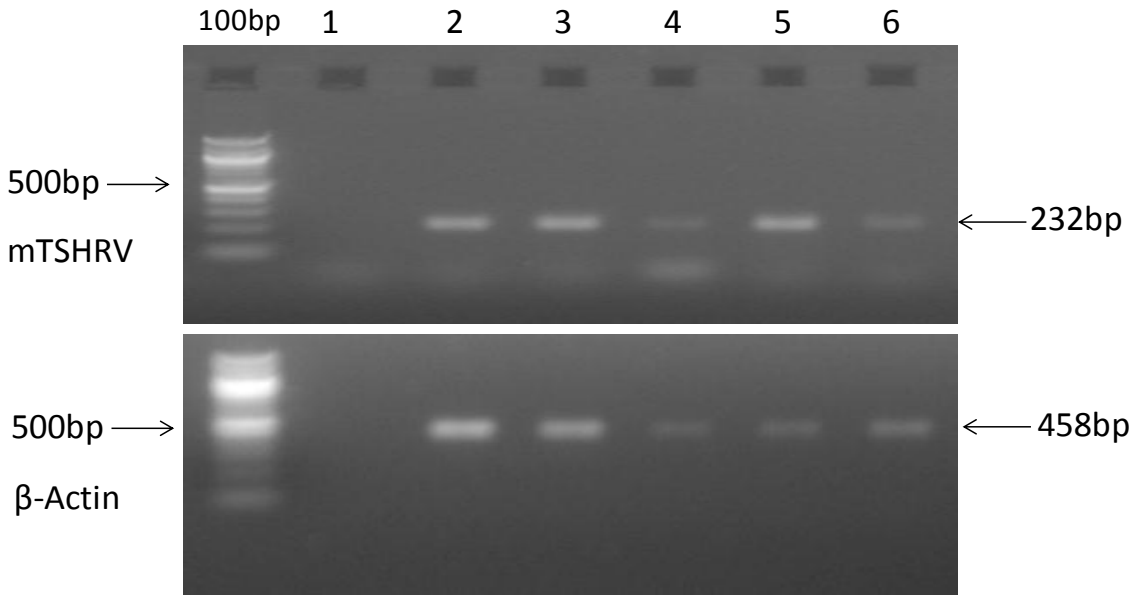

Figure 2.13. Expression of TSHR variant in mouse skin.

Ethidium bromide stain of PCR amplification products separated on 2% agarose gel analysis of mouse TSHRV (232 bp) in mouse skin, β-Actin (458 bp) = mouse housekeeping gene. **Lane 1)** negative control (H_2O), **Lane 2)** 2 weeks (anagen), **Lane 3)** 3.5 weeks (telogen), Lane **4)** 7 weeks (telogen), **Lane 5)** 8 weeks (telogen), **Lane 6)** Paw (hairless foot sole skin). The first lane contains the 100bp DNA ladder.

As shown in figure 2.13, H_2O was used as negative control. A parallel PCR analysis of β-Actin housekeeping gene reveals a variable quality for RNA integrity for all the samples. The RT-PCR revealed TSHRV transcript expression in dorsal skin (hairless foot sole skin) of variable degree at various ages of mouse skin corresponding to different stages of the hair cycle.

2.3.8 TSHRV expression in different mouse tissues

Further to the previous mouse tissue expression experiment, we asked whether the TSHRV is also expressed in mouse tissues other than the skin which might also be a potential target of TSH and thyrostimulin. We applied ex vivo analyses of representative samples of murine tissues (**figure 2.14**).

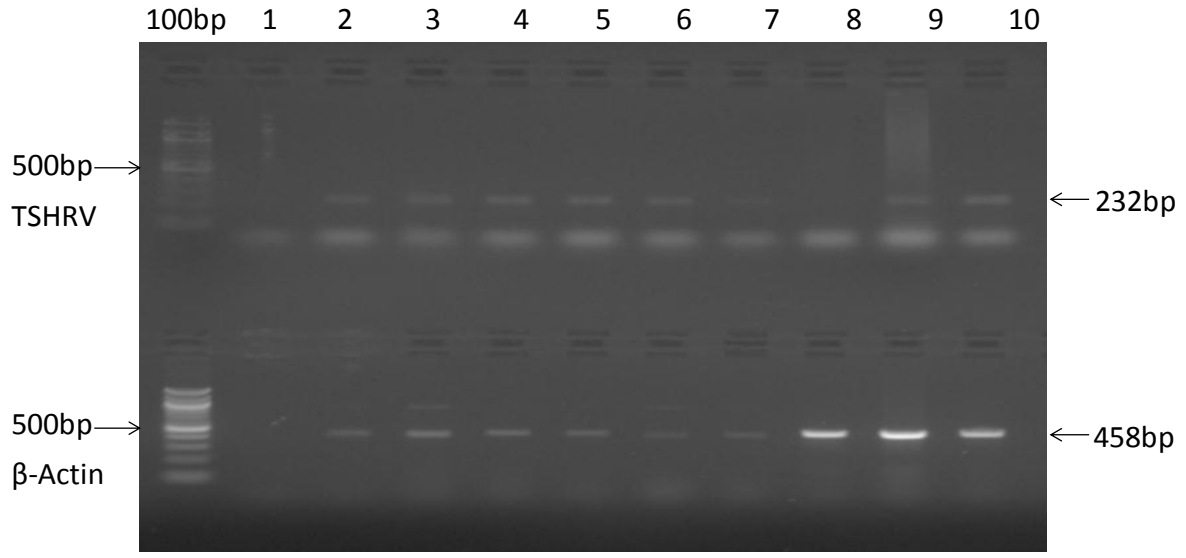

Figure 2.14. TSHR variant transcript expression in mouse tissues.

Ethidium bromide stain of PCR amplification products separated on 2% agarose gel analysis of TSHRV (232bp) in different mouse tissues, β-Actin (458bp) = mouse housekeeping gene. **Lane 1)** Negative control (H_2O), **lane 2)** heart, **lane 3)** kidney, **lane 4)** spleen, **lane 5)** stomach, **lane 6)** pancreas, **lane 7)** brain, **lane 8)** small Intestine, **lane 9)** testis, **lane 10)** positive control(mouse thyroid). The first lane contains the 100bp DNA ladder.

As shown in figure 2.14, H_2O was used as negative control, mouse thyroid used as positive control. A parallel PCR analysis of β-Actin housekeeping gene provided a quality check for RNA integrity and RT efficiency for all samples. The TSHR transcript variant was expressed in most of mouse tissues of the expected size (232bp) by RT-PCR analysis. Primer dimers appear in the TSHRV gel. Additional bands were seen in some of β actin of lane 3 (kidney) and lane 6 (pancreas) samples (872bp) which is most likely due to amplification of genomic DNA.

2.3.9 TSHR, agonist (α2 and β5) expression HaCaT cell line

Cells of the human HaCaT keratinocyte line and primary keratinocyte cell line have been reported to express TSHR in culture. We asked the question whether TSHR, α2 and β5 subunits of thyrostimulin and TSHRV are expressed in human HaCaT cell line or not?

Expression was investigated in two *in vitro* models for examining keratinocyte differentiation. The HaCaT lines were grown at different concentrations of calcium, which is known to affect differentiation and stratification of keratinocytes in culture[167]. The experiments were carried out in either Dulbecco's Modified Eagle's Medium (DMEM) with 10% fetal calf serum (high calcium throughout) and harvested at different stages before and after confluence or in serum-free keratinocyte growth medium (KGM; low calcium) and harvested at different stages before (low calcium) and after shift or the addition of calcium (high calcium) when the cells are about 80% confluency usually at day 6.

This experiment was done in a different laboratory where the initial work was conducted hence; optimization of the RT-PCR conditions was required. In all experiments we included

amplification of a housekeeping gene to provide a quality control on the integrity of the mRNA and efficiency of the RT step. We selected APRT and the first step in these HaCaT differentiation experiments was to evaluate APRT transcripts in three different cDNA sets (A, B and C) of HaCaT cells at various time points since its expression may also be regulated by the in vitro induced differentiation.

2.3.9.1 Expression of APRT in HaCaT cell line in KGM

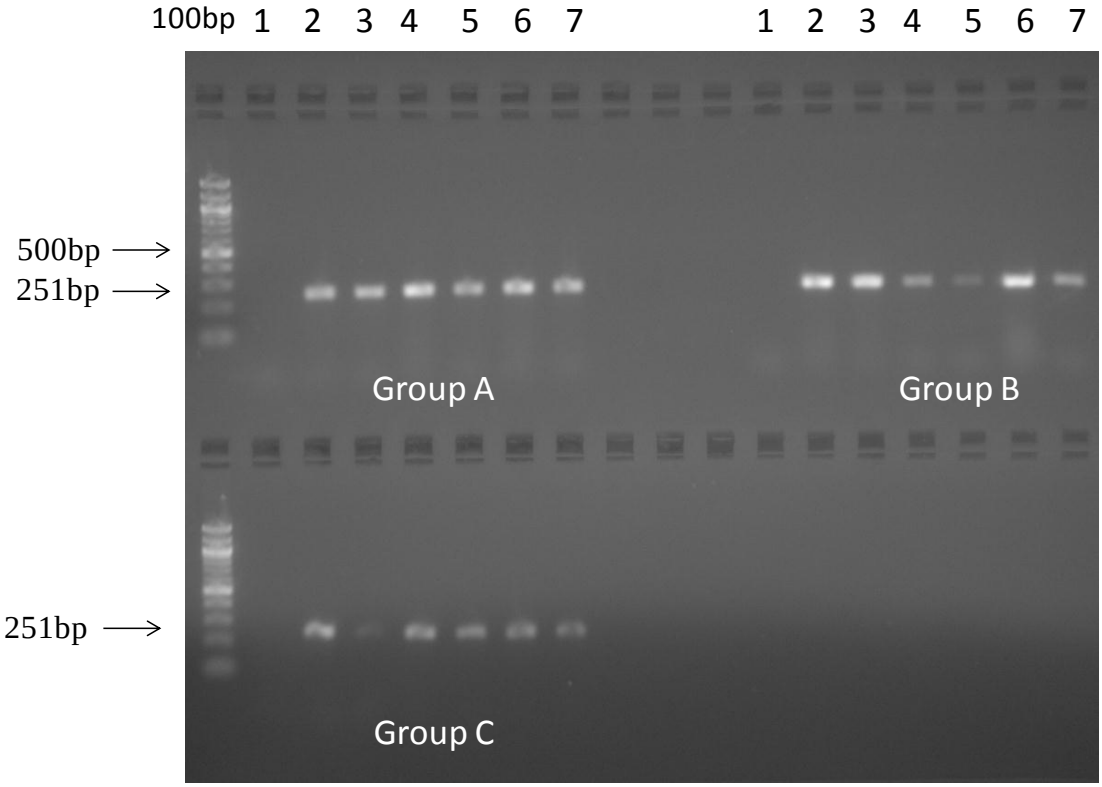

Figure 2.15*:* Expression of APRT housekeeping gene of three different sets of HaCaT cDNA in KGM (Calcium shift). Ethidium bromide stain of PCR amplification products separated on 2% agarose gel of housekeeping gene (APRT, 251bp) of different groups of HaCaT in KGM. **Lane 1)** Negative control (H_2O), **Lane 2)** Day1 (Pre-confluent), **lane 3)** Day 3 (30% confluent), **lane 4)** day 6 (80% confluent), **lane 5)** (Day 6 + 3) post-shift, lane **6)** (day 6 + 6) post-shift**, lane 7)** (day 6 +10) post-shift. The first lane contains the 100bp DNA ladder

As shown in the figure 2.15, H_2O was used as negative control. Amplification of the APRT house keeping gene provide a quality check for RNA integrity and reverse transcription efficiency for all samples. APRT was detected in all the three set of samples, but at variable levels in group B and C, being highest in group A with a similar strength of the signal in all lanes.

2.3.9.2. Expression of TSHR in HaCaT cell line in KGM

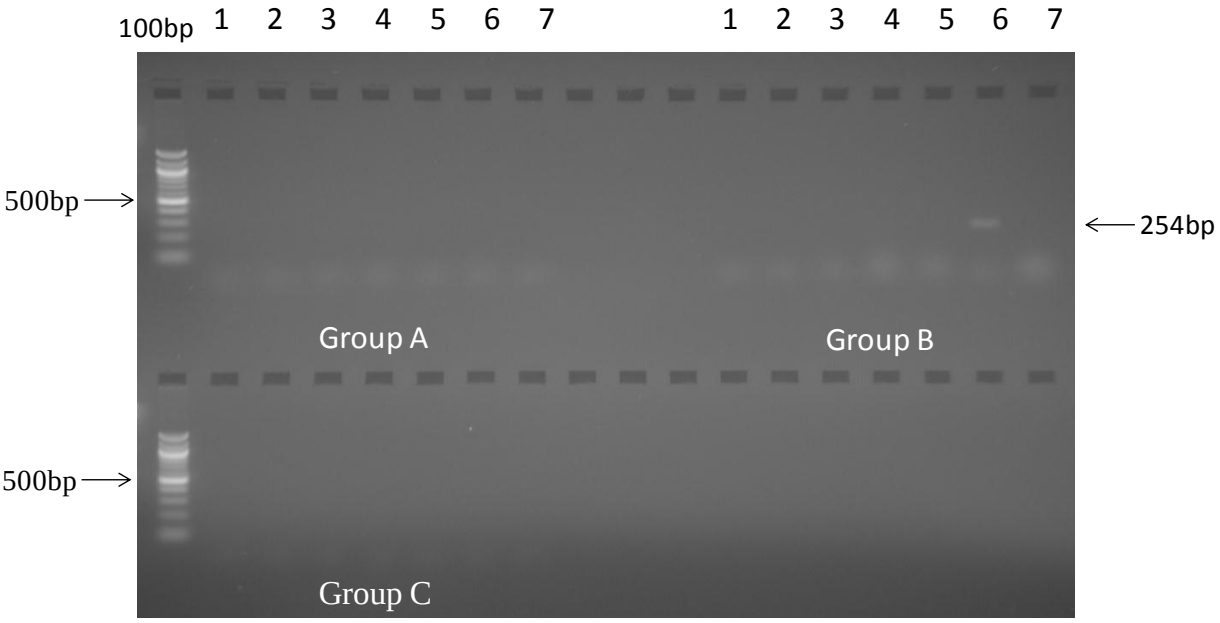

Figure 2.16: TSHR expression in different groups of HaCaT in KGM (Calcium shift)

Ethidium bromide stain of PCR amplification products separated on 2% agarose gel analysis of (TSHR, 254bp) of different groups of HaCaT in KGM. **Lane 1)** Negative control (H_2O), **Lane 2)** Day1 (Pre-confluent), **lane 3)** Day 3 (30% confluent), **lane 4)** day 6 (80% confluent), **lane 5)** (Day 6 + 3) post-shift, **lane 6)** (day 6 + 6) post-shift**, lane 7)** (day 10 + 6) post-shift. The first lane contains the 100bp DNA ladder.

As shown in the figure 2.16, H_2O was used as negative control. Due to some technical reasons at the time of doing this experiment the positive control of TSHR (human thyroid) was not used. The TSHR transcript was amplified at the same conditions in the three groups. However, only in group B a single band of relatively low strength post HaCaT differentiation at (day 6 + 3) post-shift of expected amplicon size (254bp) was seen. No other bands were seen in group A or group C.

2.3.9.3. Expression of TSHR in HaCaT cell line in DMEM

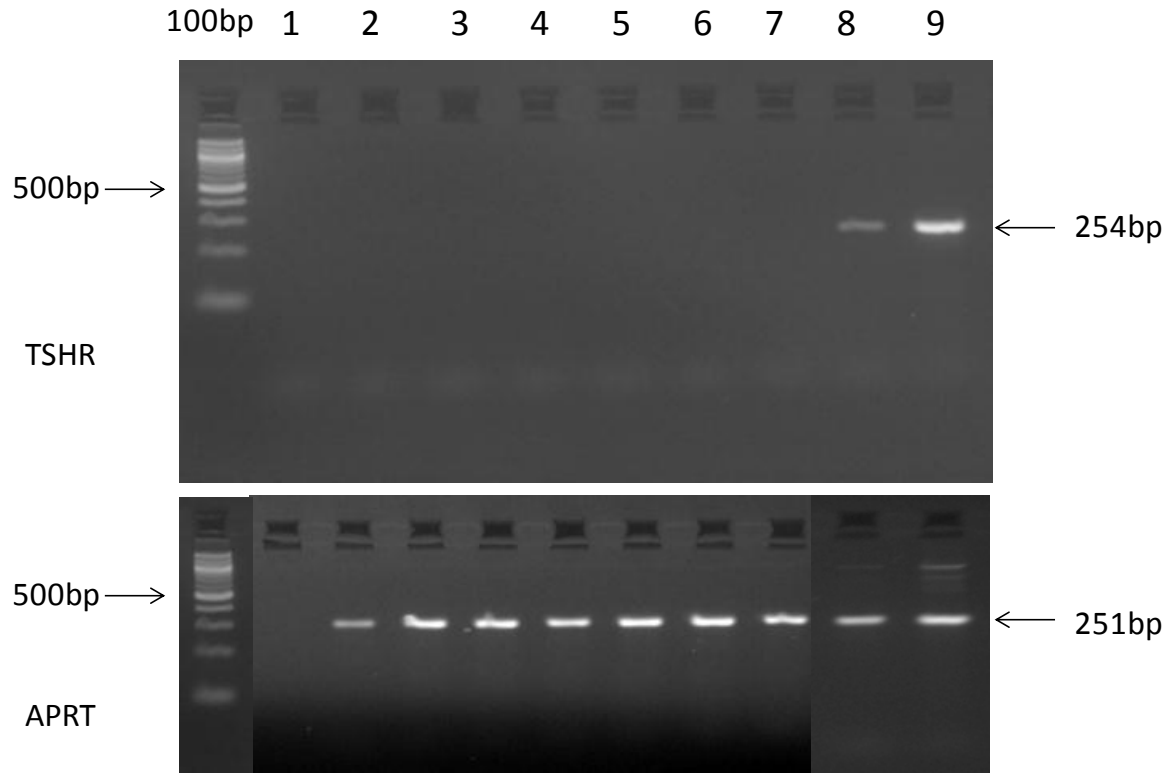

Figure 2.17: Expression of TSHR in HaCaT cell line in DMEM.

Ethidium bromide stain of PCR amplification products separated on 2% agarose gel analysis of PCR products of (TSHR, 254bp) and housekeeping gene (APRT, 251bp) of different groups of HaCaT in DMEM. **Lane 1)** Negative control (H_2O), **Lane 2)** day 1 (Pre-confluent), **lane 3)** day 3 (confluent), **lane 4)** (day 3 + 1) (Post-confluence), **lane 5)** (day 3 + 3) (Post-confluence), **lane 6)** (day 3 + 7) (Post-confluence), **lane 7**) (day3 + 10) (Post-confluence), **lane 8)** Human skin and **lane 9**) Human thyroid used as positive controls. The first lane contains the 100bp DNA ladder.

As shown in the figure 2.17, H_2O was used as negative control; human skin and human thyroid were used as positive control. Amplification of the APRT house keeping gene provided a quality check for RNA integrity and reverse transcription efficiency for all samples (the APRT gel was loaded in different occasions). The TSHR transcript is not expressed in HaCaT cell line in DMEM in all the time points investigated pre- and post confluence. Please note that at the lower part of the gel (the APRT) gel results were loaded in different gels.

2.3.10 Expression of Thyrostimulin (α2&β5) in HaCaT cell line

2.3.10.1 Expression of Thyrostimulin (α2 & β5) in HaCaT cell line in DMEM

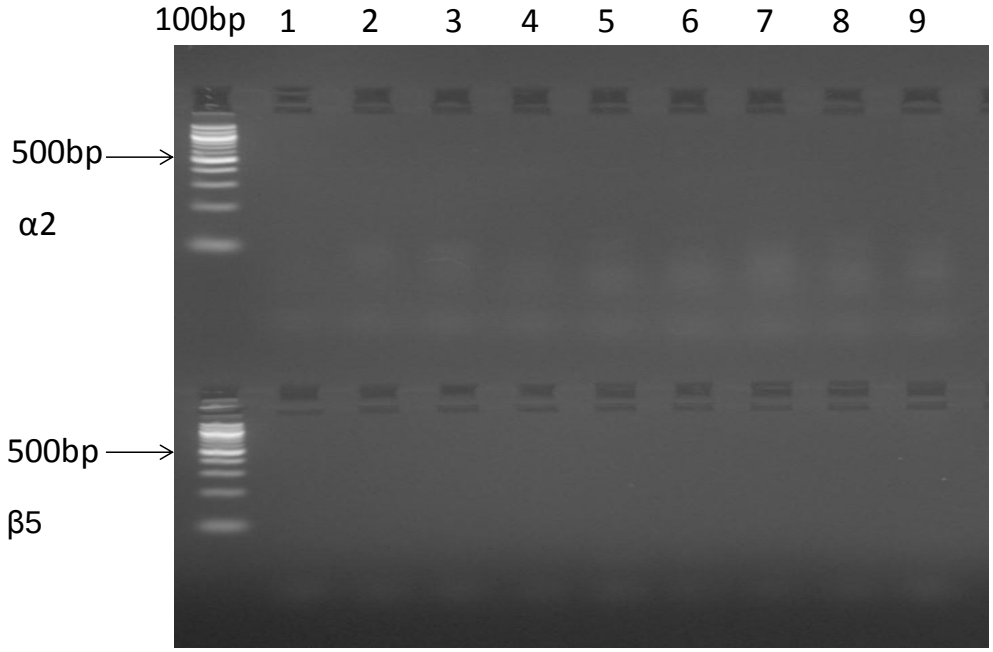

Figure 2.18: Expression of α2 and β5 subunits of thyrostiumulin in HaCaT in DMEM.
Ethidium bromide stain of PCR amplification products separated on 2% agarose gel analysis of α 2 (410bp) and β 5 (296bp) subunits of thyrostimulin in HaCaT in DMEM. **Lane 1)** Negative control (H_2O), **Lane 2)** day 1 (Pre-confluent), **lane 3)** day 3 (confluent), **lane 4)** (day 3 + 1) (Post-confluence), **lane 5)** (day3 + 3) (Post-confluence), **lane 6)** (day 3 + 7) (Post-confluence), **lane 7**) (day3+ 10) (Post-confluence), **lane 8)** Human skin and **lane 9**) Human thyroid used as positive controls. The first lane contains the 100bp DNA ladder.

As shown in the figure 2.18, H_2O was used as negative control; the ideal positive control for thyrostimulin is human pituitary which is difficult to obtain. Hence, in this experiment the human skin and human thyroid were used as positive control. Amplification of the APRT house keeping gene provided a quality check for RNA integrity and reverse transcription

efficiency for all samples (as shown in previous experiment). The initial result showed that alpha2 and beta 5 were not expressed in the HaCaT cell line in DMEM in all the time points tested. Both subunits of thyrostimulin showed negative bands, at this stage it was difficult to proceed any further without a positive control since the human thyroid used here is not the ideal positive control of thyrostimulin and the ideal positive control would be human pituitary which is practically difficult to get.

2.3.10 TSHRV expression in HaCaT cell line

2.3.10.1 TSHRV expression in HaCaT cell line in KGM

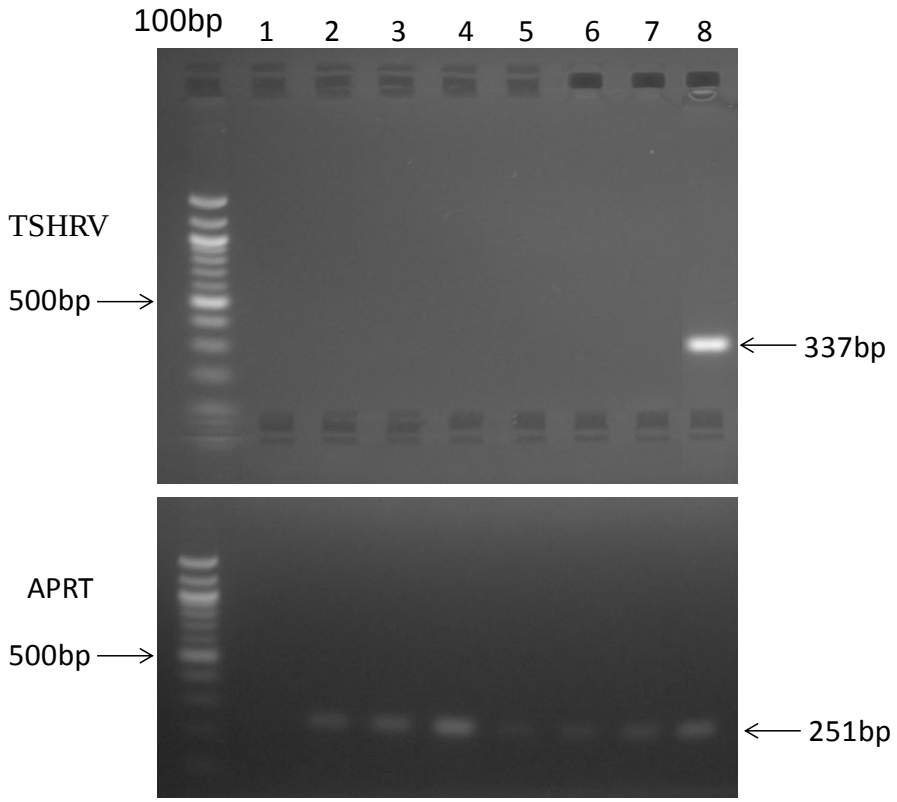

Figure 2.19: Expression of TSHRV in HaCaT cell line in KGM.

Ethidium bromide stain of PCR amplification products separated on 2% agarose gel analysis of 2% agarose gel analysis of PCR product of (TSHRV, 337 bp) and for housekeeping gene (APRT, 251bp) of HaCaT in KGM. **Lane 1)** Negative control (H_2O), **Lane 2)** Day1 (Pre-confluent), **lane 3)** Day 3 (30% confluent), **lane 4)** day 6 (80% confluent), **lane 5)** (day 6 + 3) post-shift, lane **6)** (day 6 + 6) post-shift**, lane 7)** (day 6 + 10) post-shift. The first lane contains the 100bp DNA ladder.

As shown in the figure 2.19, H2O was used as negative control; Human thyroid used as positive control. Amplification of the APRT house keeping gene provided a quality check for RNA integrity and reverse transcription efficiency for all samples. The TSHRV transcript was not expressed in HaCaT cell line in KGM in all time points investigated.

2.3.10.2 TSHRV expression in HaCaT cell line in DMEM

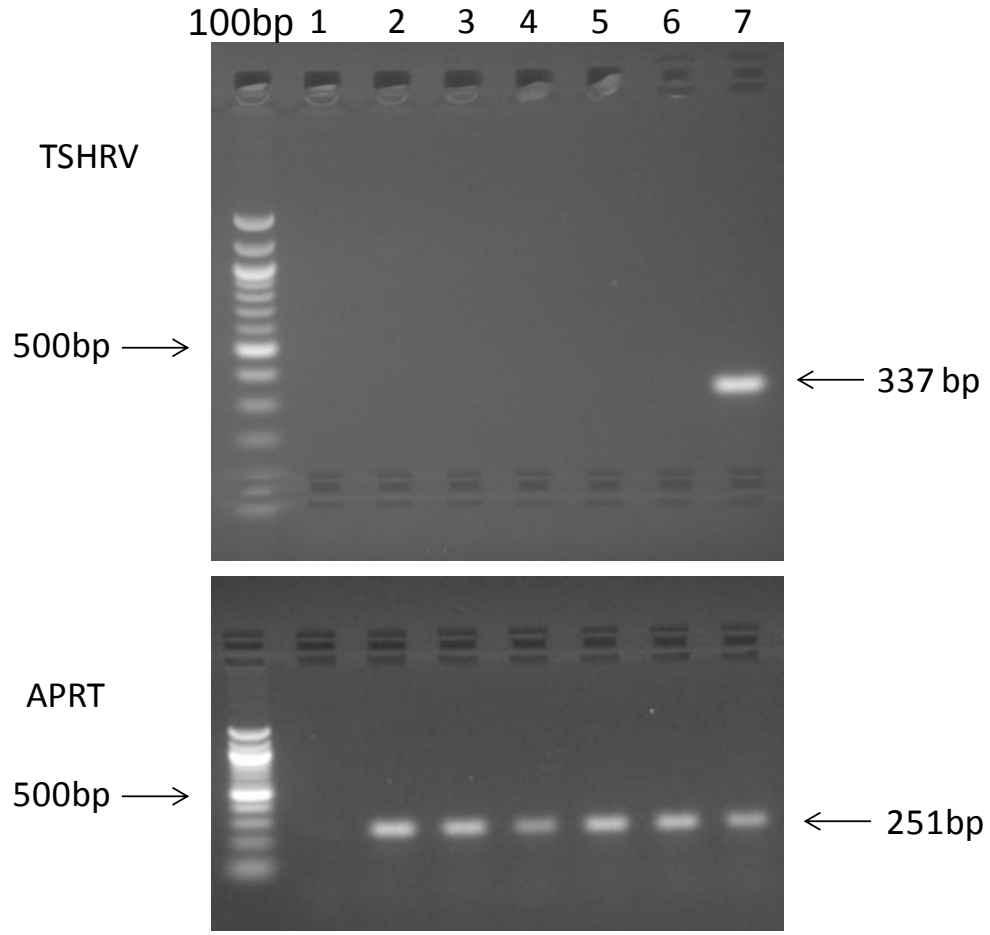

Figure 2.20. Expression of TSHRV in HaCaT cell line in DMEM.
Ethidium bromide stain of PCR amplification products separated on 2% agarose gel analysis of (TSHRV, 337 bp) and housekeeping gene (APRT, 251bp) of HaCaT in DMEM. **Lane 1)** Negative control (H_2O), Lane **2)** day 1 (Pre-confluent), **lane 3)** day 3 (confluent), **lane 4)** (day 3 + 1) (Post-confluence), **lane 5)** (day 3 + 3) (Post-confluence), **lane 6)** (day 3 + 7) (Post-confluence), **lane 7**) Human thyroid used as positive control. The first lane contains the 100bp DNA ladder.

As shown in the figure 2.20, H_2O was used as negative control; Human thyroid used as positive control. Amplification of the APRT house keeping gene provided a quality check for RNA integrity and reverse transcription efficiency for all samples. The TSHRV transcript was not expressed in HaCaT cell line in DMEM in all time points investigated.

Discussion

Expression of functional TSHR in the skin may have significant physiological and pathological implications particularly in autoimmune conditions associated with the production of stimulating antibodies against TSHR. Studies by Slominski and this team, 2002 revealed mRNA transcripts for full-length (has the potential to be functional) TSHR in cultured keratinocytes, epidermal melanocytes, and melanoma cells by RT-PCR and this was confirmed by northern analysis[53]. In addition, others have used highly sensitive methods to confirm TSHR protein expression in HaCaT this cell line[169].

In this chapter we were able to show the expression of the full length TSHR transcript in human skin and mouse skin (hairy and hairless skin). However, we were unable to detect noticeable levels of TSHR in HaCaT keratinocytes. The HaCaT cell line was either grown to different stages of confluency or at different concentrations of calcium, to induce differentiation and stratification of keratinocytes in culture[167]. These methods are known to induce early differentiation markers such as K1 and K10 but not later markers such as filaggrin[170]. In the first experiment, the cells were grown in Dulbecco's Modified Eagle's Medium (DMEM) with 10% fetal calf serum and high calcium all the way through. Here, cells were harvested at different stages before and after confluence. In the other culture condition, cells were grown in serum-free keratinocyte growth medium (KGM) and low calcium. In this case cells were harvested at different stages; before (low calcium) and after adding high calcium.

The occasional faint band shown in our data suggests that it might be related to HaCaT differentiation. The culture system employed was not completely in-vivo like since the cells were not fully differentiated and the later stages of differentiation were probably not

represented. It is well known that there are other more complicated methods of culture which induce further differentiation (like in vivo) which could have been tried, such as growing the keratinocytes on a fibroblast collagen matrix and at the air/liquid interface[171,172]. The TSHR transcript was not demonstrated in the undifferentiated mouse pre-adipocyte cell line (3T3L1). However, as 3T3L1 differentiate and the adipogenesis is clearly apparent, the TSHR appears to be strongly expressed **(figures 2.10).**

Studies by Bodo et al, 2009 [133] and Cianfarani et al, 2010[132] investigating the role of TSHR in the skin present conflicting results and showed evidence of signalling using unnaturally high levels of TSH (In the UK, guidelines issued by the Association for Clinical Biochemistry suggest a reference range of 0.4-4.5 mIU/L)[173] . In addition, these studies did not distinguish between full length and truncated variant. In our work, despite the use of unique sequence primers of the isoforms that are not present in full length TSHR in order to distinguish between transcripts coding for signalling competent TSHR and TSHRV, we were unable to detect the TSHR variant isoform transcript in human skin or HaCaT cell line by RT-PCR. However, a high level of TSHRV transcript expression was detected in mouse skin and at various ages of mouse skin corresponding to different stages of the hair cycle by the same method. The discrepancy between the human and mouse TSHRV results might be explained by differences in the hair cycle between species. The other possible explanation is the absence of hair follicles in the human skin samples used.

Semi-quantitative RT-PCR showed higher levels in TSHR expression observed in early anagen hair follicles in mouse pelage skin, than in late anagen and relatively low in telogen which is consistent with predominant expression in the human anagen hair follicle as observed by Bodo et al ,2009[133]. However, more accurate information about the level of

TSHR expression in hair follicles at different stages of mouse hair cycle could have been gained using a quantitative method such as a real-time q-PCR technique.

The α2 and β5 subunits of thyrostimulin were however readily expressed in human skin samples (α2 subunit in mouse skin) as well as in HaCaT keratinocyte and HCA2 fibroblast cell lines (figures 2.6 and 2.7). However, some experiments, failed to detect expression of thyrostimulin subunits in HaCaT. The inconsistency in thyrostimulin expression in HaCaT keratinocyte results could be related to the PCR conditions of each experiment as the RNA and the reverse transcription reaction used in these experiments were different in each experiment. It is known that RNA is very labile, and because the RNA extracted in different batches it might be of varying quality. In addition, the RT reaction will also vary from batch to batch, hence, housekeeper was included to provide some assurance of the quality RNA and that the RT reaction has worked. The main challenge with this experiment is the lack of positive control required for confirming the expression of thyrostimulin as the ideal positive control would be the pituitary which is practically difficult to obtain.

The results in this chapter showed TSHR transcript expression in a wide range of mouse tissues including lung, eye, kidney, thyroid, ovary and testis. The α2 subunit is only expressed in eye, ovary and testis. On the other hand, β5 subunit is expressed in most of the tissues tested as heart, lung, kidney, small intestine, eye, brain, ovary and testis. However, all three transcripts were only co-expressed the in eye and testis.

The results showed more expression of β5 transcript in different mouse tissues then α2 transcript. These results contradict with other reports where they showed α2 is more abundant than β5[144,145,153]. In this context, it is difficult to compare the relative levels of expression by

semiquantitative techniques and there may be differences in efficiency causing problems. Therefore, a real time qPCR would be a better technique for investigating the expression of thyrostimulin in these tissues.

Chapter three

Immunodetection of the TSHR protein

3. Chapter three

3.1 Introduction

As described in the general introduction, the TSHR has two main forms; the full length TSHR and the TSHR variant isoform. The full length TSHR contains two subunits; A subunit, corresponding to the extracellular domain (ECD) (residues 21-415) encoded by exons 1-9 and, the B subunit, is mainly the transmembrane domain (TMD) (residues 416-764) encoded by exon 10[111-114]. Post translation proteolysis splits the TSHR into two A subunits and B subunit linked to each other by disulfide bonds[115]. The TSHR variant is a 1.3 kb and comprise exons 1-8 and a new "tail sequence" and lack the transmembrane domain[134] (**figure 3.1**).

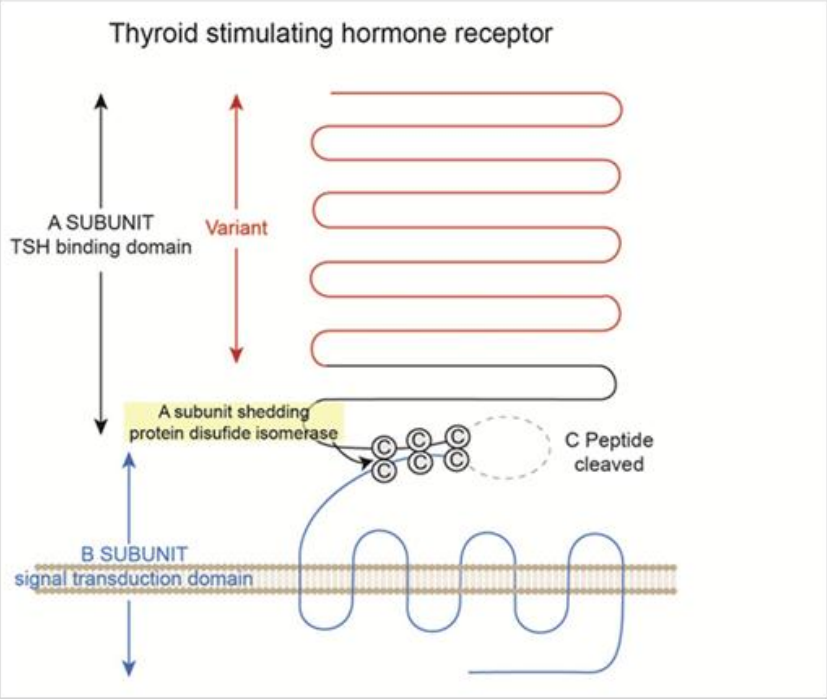

Figure 3.1: Schematic diagram showing structure of TSHR holoreceptor, TSHR isoform

Reports revealed TSHR is expressed in extra thyroidal locations including lymphocytes, extra ocular tissues[174], fibroblasts[61,175]; fat[165], human skin[132] and human scalp hair follicle[133]. Immunoreactivity to TSHR antibodies has been observed in the dermis of both patients with pretibial myxoedema and unaffected individuals. However, in the skin, it is not clear the exact site of this expression or the type of cell which expresses the TSHR.

Literature review revealed that different studies used different TSHR antibodies to study TSHR expression in skin, These studies mainly used antibodies which recognizes different parts of the extracellular domain of the TSHR[132,133,176-180] **(figure 3.2).** Furthermore, the two recently published papers utilised two different antibodies to the extracellular domain of TSHR showing contradictory results[132,133]. By using the (BA8) antibody which recognises the conformation of the whole extracellular domain, Bodo et al showed that TSHR was immunolocalized to the mesynchymal dermal component of the hair follicle, as well as the myoepithelial cells surrounding the sweat gland, the sebaceous glands, nerves and blood vessel endothelium . On the other hand, Cianfarani et al used an antibody A9, raised to a peptide corresponding to amino acid residues 147-228 of the extracellular domain, that immunolocalised to the epidermis and some cells in the dermis[132].

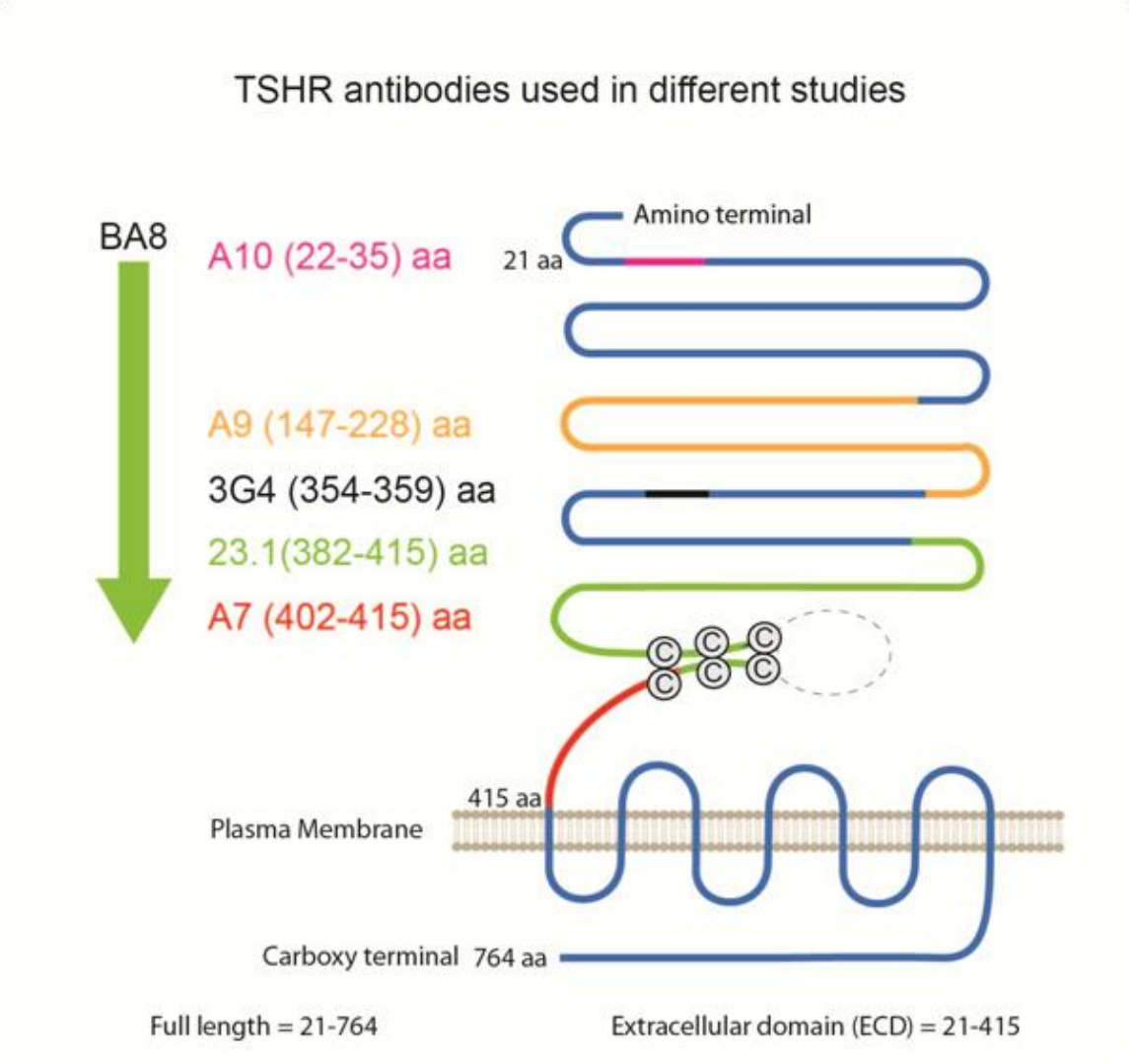

Figure 3.2: **Schematic diagram showing different binding sites of different TSHR antibodies used in immunohistochemical studies.**

As well as being inconsistent these results may not actually be immunolocalising the holoreceptor (TSHR), since these antibodies only detect the extra cellular domain and could also be detecting the truncated isoforms of the TSHR or the A subunit of the TSHR which can be shed by enzyme catalysed reduction of the disulphide bonds at the cell surface . As described in chapter two, we were able to amplify full length TSHR transcript from whole human skin, however, our RT-PCR revealed high levels of TSHRV transcript expression in human thyroid and mouse skin but not in human skin.

3.1.1 Aim of chapter three

The aim of this chapter is to determine the localisation of the signalling competent TSHR expression in the skin. Immunolocalisation of TSHR was carried out with two different monoclonal antibodies; the A9 antibody recognises amino acids 147-228 of the extracellular A subunit and, the A7 antibody recognises amino acids 402-415 of the last bit of ECD of TSHR or the initial part of B subunit. The thyroid tissue was used as a positive control.

NCBI Entrez Gene describes two alternatively splice variants, TSHR isoform 2 precursor (NM_001018036.1)[134], TSHR isoform 3 precursor (NM_001142626.1)[139]. As illustrated in (**figure 3.1**) the TSHRV (isoform2) spans (residues 21-253) which is the extreme carboxyl terminal of the ECD that doesn't include the A7 epitope and presumably after the bit coded for by the variant, therefore A7 cannot bind to TSHRV. Consequently, using these two antibodies could distinguish between the full length and the variant isoforms in order to determine whether there is a signalling competent TSHR in the skin (**figure 3.1**). These two antibodies can also distinguish between the A and B subunits generated by enzymatic cleavage of the holoreceptor.

3.2 Materials and Methods

3.2.1 Immunohistochemistry (IHC)

3.2.1.1 Tissues used in the project

Human thyroid tissue and normal skin tissue was purchased from a commercial source (AMS Biotechnology, UK). Some skin samples were from the Dermatology department, Cardiff University and were collected for research purposes with patient consent prior to the 2004 human tissue act. To avoid problems of antigen preservations, accessibility of antibodies encountered in paraffin or plastic-embedded material and for simple and rapid processing of the biopsies[181] frozen section techniques were employed.

Serial sections (5-8 µm) were obtained from the frozen tissue blocks using a Thermo Scientific Cryotome FSE cryostat. The sections were then mounted on SuperFrost® Plus glass slides (Menzel-Glaser GmbH, Braunschweig, Germany). The SuperFrost® is characterized by a process in which a permanent positive charge exists on standard microscope slides, which ensures firm electrostatic attraction of frozen tissue sections to the slide. These slides were left to air dry for 30 minutes. After drying, they were labelled and wrapped back to back in aluminium foil and then stored in the freezer at -80˚C until the time of staining.

3.2.1.2 TSHR antibodies used

Cryostat sections from human thyroid and human skin were analysed by immunohistochemistry using two different monoclonal TSHR antibodies .These antibodies are; A9 monoclonal antibody (Santa Cruz Biotechnology, Inc)[176] and A7 monoclonal

antibody (AbCam)[177]. The individual antibodies were selected on the basis of their recognition of specific epitopes in the TSHR protein where each antibody recognises certain peptide in the TSHR. A thyroid tissue was used as positive control (**table 3.1**).

Table 3.1: Summary of antibodies and immunostaining conditions used in this study

1º ab	Host	Corresponding aa	Source	Block	Diluent	All washes	Dilution & incubation period	2º ab	Tertiary
A9	Mouse monoclonal antibody	147-228 (ECD)	Santa Cruz Biotechnology, Inc	Hydrogen peroxide for 10minutes 5% normal sheep serum + 0.1% BSA in PBS-T for 30 minutes Avidin/Biotin blocking.	0.1% BSA in PBS-T	PBS-T	1:100 over night	1:200 Anti-mouse biotinylated (from sheep)	ABC Kit
A7	Mouse monoclonal antibody	402-415 last bit of (ECD)	AbCam	Hydrogen peroxide for 10minutes 5% normal sheep serum + 0.1% BSA in PBS-T for 30 minutes Avidin/Biotin blocking.	0.1% BSA in PBS-T	PBS-T	1:50 over night	1:200 Anti-mouse biotinylated (from sheep)	ABC Kit

3.2.1.3 The Buffer solution

Five litres stock of x10 PBS solution (phosphate buffered saline, pH 7.2) was prepared and stored in bottles and used as stock for x1PBS (**table 3.2**)

Table 3.2: Constituents for preparation of x10 Phosphate Buffered Saline solution

Constituents	**Amount (in grams) required for 1 Litre (L)**	**Amount (in grams) required for 5L**
Sodium chloride, NaCl	80	400
Disodium hydrogen phosphate (dodecahydrate), Na2HPO4.12H2O	35.8	179
Potassium dihydrogen phosphate (anhydrous), KH2PO4	2.4	12
Potassium chloride, KCl	2	10
Distilled water	To make up to 1L	To make up to 5L

X1 PBS with 0.05% Tween 20 (PBS-T) (Sigma-Aldrich, Dorset, UK) was used as the buffer solution which helps in washing steps to reduce non-specific binding (for washes and for preparing the diluents). The diluents (intended for dilution of the primary antibody, secondary antibody and the tertiary reagent, and also used as a negative control), was prepared by adding 0.25 g of BSA (bovine serum albumin) (Sigma-Aldrich, Dorset, UK) and/or 0.25 g of Marvel (non-fat milk protein) to 25 ml of the PBS-T. BSA and Marvel were added to prevent non-specific binding of the primary antibody, reducing the background by minimising non-specific interactions between the primary antibody and non-target cellular proteins.

3.2.1.4 IHC methods

Generally, the immunohistochemical methods are divided into direct and indirect methods. The direct method is a simple one-step staining procedure that involves direct interaction of the antigen with a specific labelled primary antibody (eg FITC conjugated, HRP conjugated)[182]. Whilst this method is quick to perform, since it utilises only one antibody, it is less sensitive giving little signal amplification. Indirect methods involve using a labelled secondary antibody (must be raised against an immunoglobulin of the same type and species as the primary antibody) or a secondary antibody and labelled tertiary compound, that binds to the unlabelled primary antibody-antigen complex. This indirect approach is more sensitive as it generates an amplified signal. To further amplify the signal, various three-step methods have been developed such as the peroxidase anti-peroxidase, alkaline phosphatase-anti-alkaline phosphatase and avidin-biotin based methods[182]. In this project the avidin-biotin based method has been employed (ABC method)[133] . In this method, the first layer is an unlabelled primary antibody, the second layer is a biotinylated secondary antibody and the third layer is either a complex of avidin-biotin peroxidase (ABC method) or an enzyme-streptavidin conjugate (Streptavidin method)

Slides were taken out of the freezer and allowed to reach room temperature, before removing the foil. Slides were labelled and fixed in acetone (Fisher Scientific, UK) for 15 minutes. The acetone-fixed slides were then air dried for 15 minutes to allow evaporation of excess acetone followed by three five-minute washes in PBS-T and than treated for 10-20 minutes with 3/% hydrogen peroxide (Fisher Scientific, UK). Each section on the slides were encircled with a water-repelling wax pen (Dako Pen, Glostrup, Denmark) and placed in a humidified chamber (a shallow plastic box with a moistened paper towel placed at the bottom). To reduce non-specific binding of the secondary antibody, the slides were incubated with 5% normal serum

(from the same species in which the secondary antibody was raised) for 30 minutes at room temperature. This was followed by three five-minute washes PBS/tween. To suppress endogenous biotin activity it is necessary to block it with avidin and then block the unoccupied biotin binding-sites of avidin with biotin. Therefore, an avidin/biotin blocking kit (Vector Laboratories, Burlingame, CA) was used. The slides were incubated with avidin for fifteen minutes followed by fifteen minutes incubation with biotin with brief rinses (x 3) in the buffer solution in between. The sections were incubated with an optimum dilution of the primary antibody **(table 3.1**) overnight at 4˚C. Slides incubated with diluent (without any primary antibody) were run in parallel as a negative control for each experiment. This was followed by three five-minute washes in the buffer solution.

The sections were then incubated with a relevant biotinylated secondary antibody for 30 minutes at room temprature, and then washed by PBS/tween three times five minutes each, followed by incubation with reagents of the avidin-biotinylated enzyme complex kit (Vectastain ABC kit, Vector Laboratories Inc.) for a further 30 minutes. The ABC reagent was prepared at least thirty minutes before being used by adding 1 drop of reagent A and 1 drop of reagent B to 2.5 ml of the diluent. The sections were then washed in the buffer solution three times and developed with (5mgs in 5ml of PBS) of horse radish peroxidase substrate solution (0.5 ml of 3, 3' Diaminobenzidine (DAB), 4.5 ml of PBS and 6 µl of H_2O_2) (Fisher Scientific UK) for 10 minutes at room temprature to produce colorimetric immunoprecipitates.

The sections were then rinsed in tap water and counterstained with haematoxylin (Sigma Aldrich, UK) for 5 minutes and washed again in tap water. Finally, all sections were dehydrated through a graded series of alcohol solutions (1 x 70%, 1 x 90%, and 3 x 100% industrial methylated spirit; Genta Medica, York, UK) for 5 minutes each, and cleared in

three changes of xylene (Genta Medica, York, UK) for 5 minutes each. The slides were then carefully mounted with a cover slip using DPX mounting medium (a mixture of distyrene, a plasticizer, and xylene; RA Lamb, East Sussex, UK) and then left to dry overnight.

3.2.1.5 Photography

The following day, the slides were observed under a Nikon optiphot microscope for detection of positive staining. Positive staining (or antibody binding) was visualised as brown staining. Digital images were captured with Axiocam camera system (Zeiss) and Axiovision software (Zeiss) under different magnifications using three objectives (x10, x20, and x40). Standardised settings were used on the microscope and image capturing software to allow accurate comparisons.

3.2.1.6 Optimization of the IHC protocol

The protocols used in these experiments were optimized until good positive staining was detected and all the non-specific staining and background were minimised. Additional blocking step was required to block endogenous peroxidise by treating the sections with hydrogen peroxide for variable duration (10-20 minutes) before the standard blocking step with 5% normal serum.

3.3 Results

The immunohistochemical analysis of the TSHR protein was performed using commercial monoclonal antibodies A9 and A7 that recognise specific peptides of TSHR (**figure 3.2**), thyroid tissue was analysed as positive control.

3.3.1 The A9 Antibody

The standard ABC method was utilized first then a protocol modification was required where the Avidin and Biotin blocking steps were replaced by an additional blocking method by using hydrogen peroxide[133]. Although, hydrogen peroxide blocks the endogenous peroxidise, it could have a negative effect on the architecture of the tissue (because of the effervescence); this might explain why some of the sections look a bit 'ragged. The sections where treated with hydrogen peroxide for variable duration (10-20 minutes) before blocking with 5% normal serum (**table 3.3**).

Table 3.3: Optimization conditions for A9 TSHR antibody

A9 primary Ab	Secondary Ab	Blocking method	Tissue	Comment
1:100 O/N	1:200 anti-mouse biotinylated	Endogenous peroxidase blocked for 20 minutes. 5% sheep serum in BSA in PBS-T for 30 minutes	Normal thyroid sections	Strong immunoreactivity. Strong background staining
1:200 O/N 1:500 O/N	1:200 anti-mouse biotinylated	Endogenous peroxidase blocked 20 minutes 5% sheep serum in BSA in PBS-T for 30 minutes	Normal thyroid sections	Good, positive immunoreactivity with 1:200 O/N
1:200 O/N	1:200 anti-mouse biotinylated	Endogenous peroxidase blocked 10 minutes 5% sheep serum in BSA in PBS-T for 30 minutes	Normal thyroid, Human skin sections	Good staining of thyroid, Positive staining of dermal fibroblasts in some skin sections but most showed no immunoreactivity.
1:100 O/N	1:200 anti-mouse biotinylated	Endogenous peroxidase blocked 10 minutes 5% sheep serum in BSA in PBS-T for 30 minutes	Normal thyroid, Human skin sections	Strong positive staining of thyroid. No epidermal staining. Positive dermal fibroblast & sweat gland staining. Borderline staining of sebaceous gland.

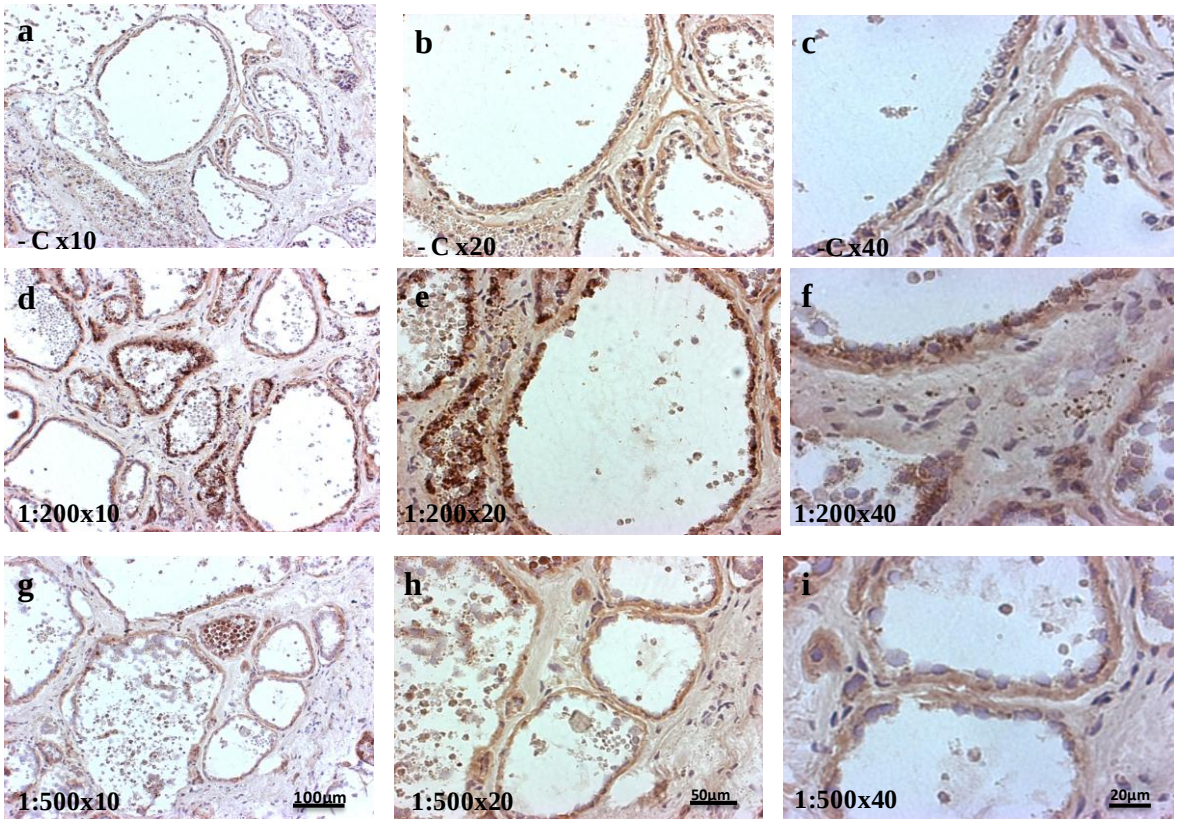

Figure 3.3: Immunostaining of TSHR in human thyroid using A9 monoclonal antibody during the process of optimization. Negative controls (panels a, b and c) are sections incubated with secondary antibody only. Panels d, e and f are thyroid follicles sections incubated with A9 antibody at 1:200 dilutions. (Panels g, h and i) are thyroid follicles sections incubated with A9 antibody at 1:500 dilution. Scale bar x10=100µm, x20=50 µm, x40=20 µm.

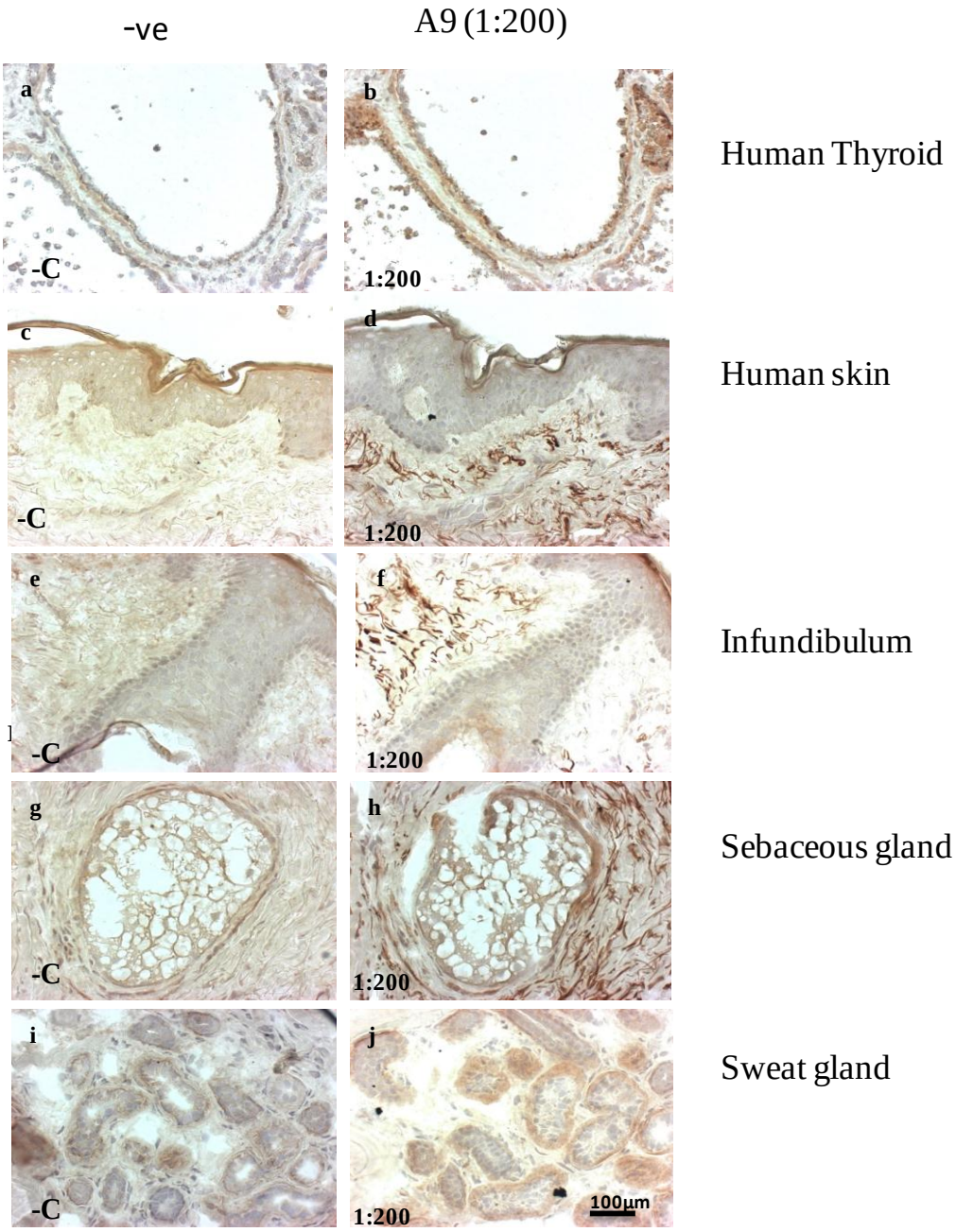

Figure 3.4: Immunostaining of TSHR in normal thyroid, normal skin and skin appendages using A9 monoclonal antibody at dilution of 1:200 during the process of optimization. Negative controls (panels a, c, e, g, i) are sections incubated with secondary antibody. Thyroid and skin section (panels b, d, f, h, j) are sections incubated overnight with A9 antibody at dilution of 1:200. Scale bar x10=100µm.

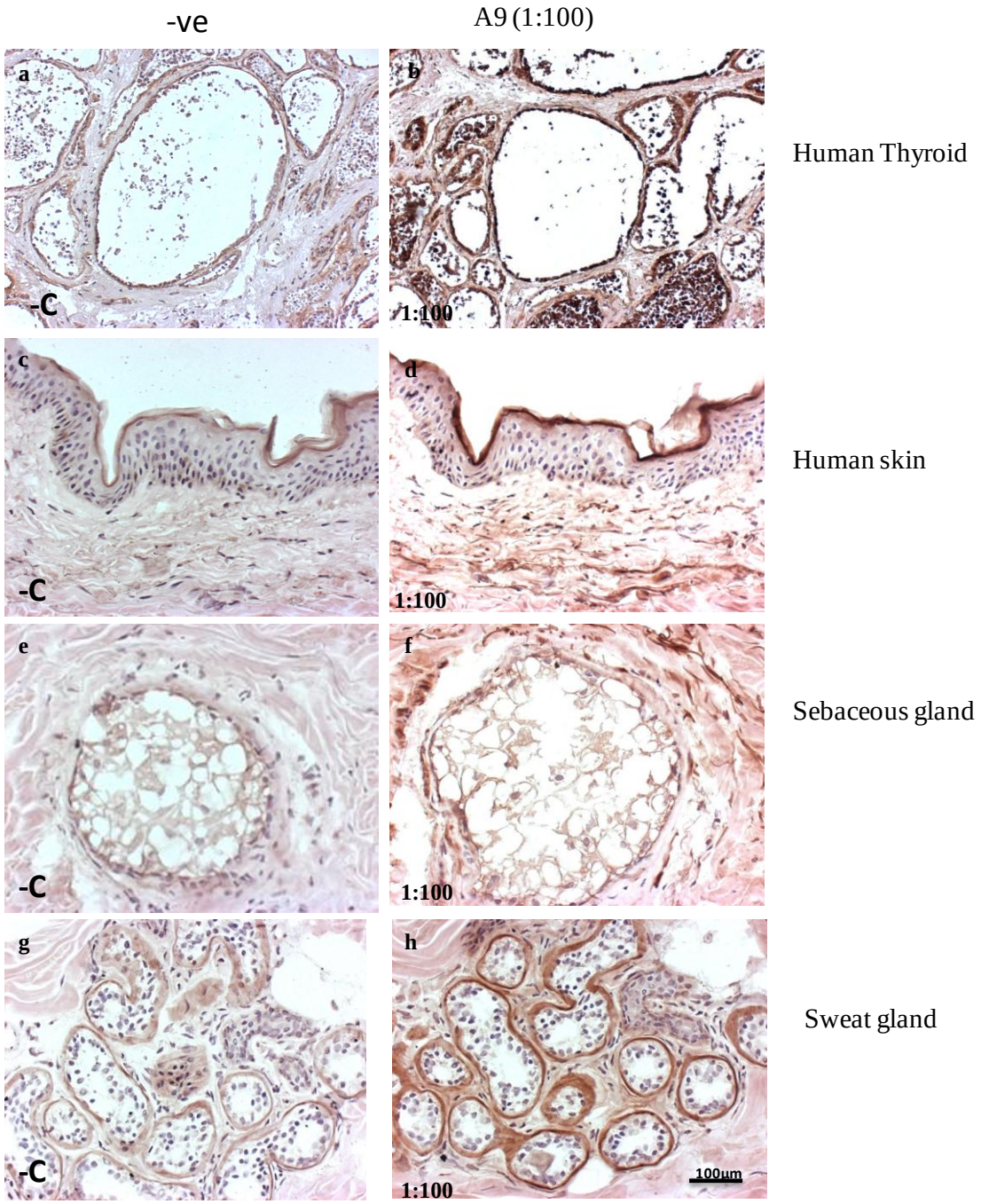

Figure 3.5: Immunostaining of TSHR in normal thyroid, normal human skin, sebaceous gland and sweat gland using A9 monoclonal antibody. Negative controls (panels a, c, e and g) are sections incubated with secondary antibody only. In contrast, thyroid and skin section (panels b, d, f, h) are sections incubated overnight with A9 antibody at dilution of 1:100. Scale bar x10=100µm.

As shown in figures 3.3 to figure 3.5, the A9 monoclonal TSHR antibody was optimized using two dilutions of the primary antibody. The TSHR A9 antibody at 1:100 dilution seems

to be the optimal dilution in the thyroid tissue. Positive TSHR immunoreactivity is shown on the basolateral surface of the thyroid follicles. A9 antibody at 1:200 dilution, the epidermis shows no immunoreactivity. However, the dermis shows positive fibroblast-like immunstaining, this staining is also obvious in the dermis surrounding the hair follicle and the sebaceous gland. Borderline staining is seen in the sebaceous glands and a borderline staining is shown in the periglandular myoepithelial cells of sweat gland. Similarly, at 1:100 dilution the A9 antibody showed no immunoreactivity of epidermis while the dermis shows positive fibroblast-like immunorstaining with borderline staining of sebaceous glands. Interestingly the periglandular myoepithelial cells surrounding the sweat gland showed prominent TSHR immunoreactivity.

3.3.2 The A7 antibody

As mentioned in A9 experiment, the standard ABC method was utilized[133], then the protocol was modified by replacing the Avidin and Biotin blocking steps with an additional blocking step to block endogenous peroxidise (**table 3.4**).

Table 3.4: Optimization conditions for A7 TSHR antibody

A7 Ab	Secondary Ab	Blocking Method	Tissue	Comment
1:50 O/N	1:200 anti-mouse biotinylated	Hydrogen peroxide for 10minutes 5% normal sheep serum + 0.1% BSA in PBS-T for 30 minutes	Normal thyroid, Human skin	Strong background (skin) Immunoreactivity in the thyroid, non specific staining of the epidermis, sebaceous glands and sweat glands.

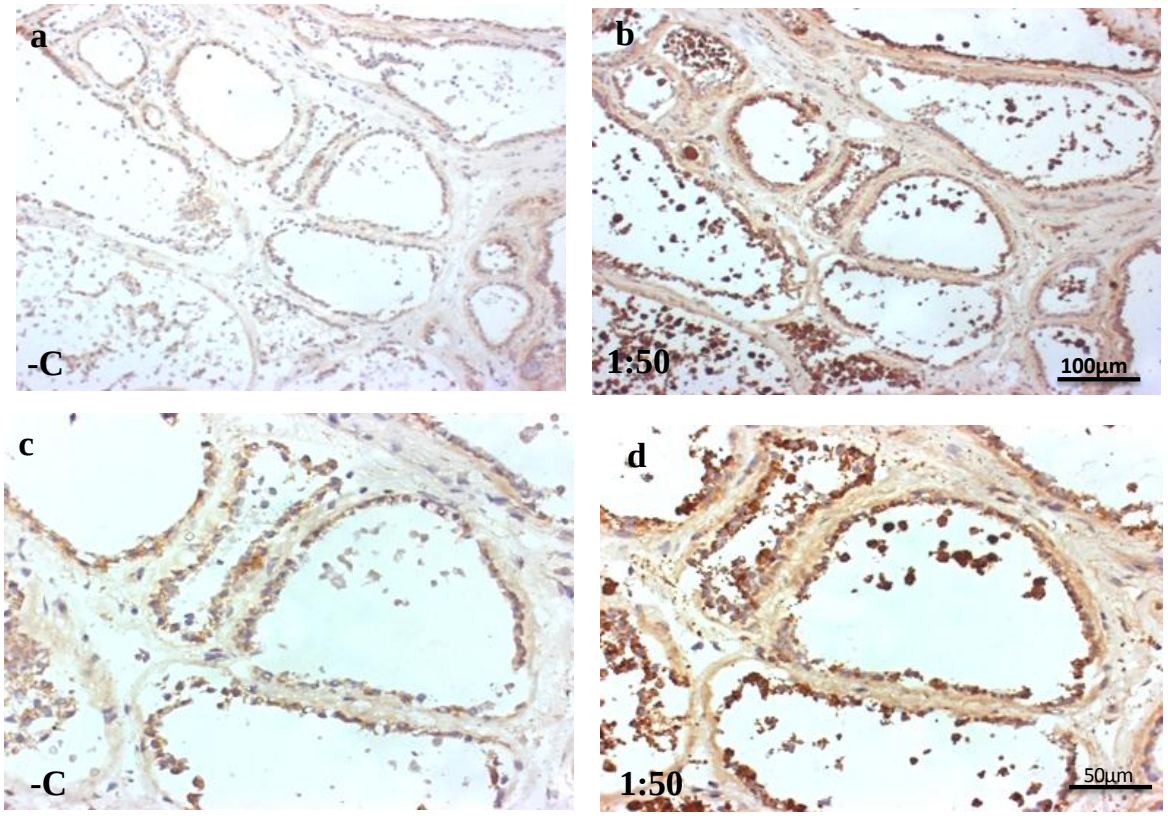

Figure 3.6: Immunostaining of TSHR in normal thyroid using A7 monoclonal antibody. Negative controls (panels a, c) are sections incubated with secondary antibody only. Panels b, d are thyroid follicles incubated with A7 antibody at dilution (1:50). Scale bar x10=100µm, x20=50 µm.

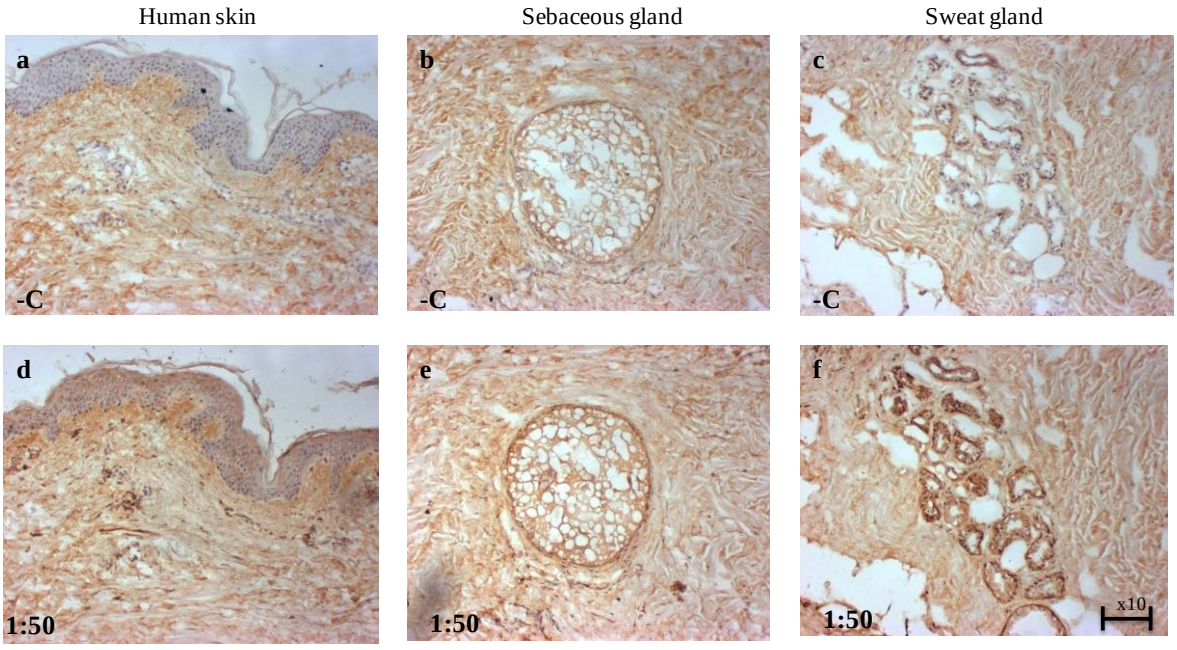

Figure 3.7: Immunostaining of TSHR in normal skin, sebaceous gland and sweat gland using A7 monoclonal antibody. Negative controls (panels a, b and c) are sections incubated with secondary antibody only and reveal non-specific background staining. In panels d and e, staining is present but mainly non-specific, apart from some regions of the dermis and sebaceous gland with borderline positive staining. Periglandular myoepithelial cells are positively stained (f). Scale bar x10=100µm.

As shown in figure 3.6 and figure 3.7, The A7 antibody dilution of 1:50 on normal thyroid sections (as a positive control), using an overnight incubation at 4ºC and with endogenous peroxidise blocking for 10 minutes was determined to be the best condition for clear positive thyroid staining. However, applying the same conditions on skin tissues reveals strong non-specific immune staining of skin, apart from some regions of the dermis and the outer rim of sebaceous gland with borderline positive staining. There was much less clear cut immuno-staining of TSHR expressing fibroblast with A7 antibody. Periglandular myoepithelial cells of sweat glands show positive staining.

3.4 Discussion

TSH operates by activating the TSHR expressed mainly on the thyroid epithelial cells[43,97]. However, several reports suggested that there are extra-thyroidal target cells for TSH and, therefore extra-thyroid TSHR expression including; adipose tissue[155], cultured human hair follicle keratinocyte, human dermal papilla fibroblast[133], human skin fibroblasts[132], and melanoma cell lines[53].

The immunolocalization of TSHR at protein level in human skin was investigated by using A9 and A7 monoclonal antibodies. The pattern of staining obtained with both antibodies, on thyroid tissues was similar; i.e. dense staining at the basolateral surface of the thyroid follicular cells, in keeping with the known localization of the TSHR in the thyroid gland. However, the immunohistological results on human skin showed non-convincing TSHR immunoreactivity in human epidermis with both antibodies. Interstingly, when A9 antibody was used, the dermis showed a positive spindle-like or fibroblast-like immunostaining most probably of dermal fibroblast and a similar staining is observed in the dermal tissue surrounding the sebaceous gland and the infundibulum. However, there was much less clear cut immunostaining of TSHR expressing fibroblast with A7 antibody. This suggests that the A9 antibody might be detecting the TSHRV isoform or might be detecting the full length TSHR. Further details will be discussed in the general discussion. Additionally, border line immunoreactivity is shown in the thin rim of cytoplasm surrounding the classic "honey comb" morphology of the sebaceous gland.

Furthermore, positive TSHR immunostaining was observed in periglandular myoepithelial cells of sweat glands in sections treated with both A7 and A9 monoclonal antibodies. Our results are in agreement with the results obtained by Rapoport and his team where they used

A9 monoclonal antibody to compare the expression of TSHR in frozen skin sections obtained from severe case of pretibial myxedems patient and from sections obtained from normal individual, they found a positive elongated fibroblast-like staining in the dermis, although perhaps less intense, in normal individuals similar to that of the pretibial myxedema patient[61]. In this context, it is worth mention that the positive elongated fibroblast-like staining in the dermis was not detected in all the skin sections used. This could be related to the type of skin used (healthy vs adjacent to diseased skin).

More recently, Cianfarani et al, 2010 studied the expression of TSHR at protein level by immunohistchemistry using A9 antibody and showed immunoreactivity of TSHR in human epidermis and sparse cells in the dermis. They also used an antibody against prolyl 4-hydroxylase, a fibroblast marker and proved that the cells in the dermis were fibroblasts[132]. Moreover, a previous study by Slominski et al.2002 described TSHR mRNA expression in epidermal, hair follicle HaCaT keratinocytes and melanocytes, also in dermal and hair follicle fibroblast and melanoma cell line[53].

The absence of TSHR immunoreactivity in human epidermis and the positive sweat glands immunostaining is in agreement with that of the work done recently by Eniko Bodo and her team[133] where they immunolocalized the TSHR in human scalp skin and hair follicle using BA8 monoclonal antibody, they reported the expression of TSHR in the mesenchymal cells of the pilosebaceous unit including the follicular dermal papilla (DP), the connective tissue sheath (CTS), and the arrector pili muscle and sebaceous gland whereas TSHR was not observed in interfollicular dermal fibrobalsts and keratinocyte in female scalp skin[133]. The conceivable reasons for the discrepancy between their finding and ours might be related to the lack of hair follicles in our sections (non scalp skin), different skin locations scalp vs non

scalp, terminal hair vs. villous hair and/ or reagents used (anti-TSHR antibodies) may give an explanation for such discrepant data.

In conclusion, our results are in agreement with others[61,132,133] showed TSHR expression in the skin and this might provide evidence to support the idea that TSHR signalling could be an alternative mechanisim of extrathyroidal manifestations of thyroid disease rather than disturbance in thyroid hormone levels. Furthermore, that the isolated fibroblast-like cells shown in this chapter might be the fibrocytes which will be further discussed later. If we had enough time we would have carried further experiment to confirm the fibroblast immunostaining in the demis by using antibody against proly 4-hydroxylase fibroblast marker antibody[132].

Chapter four

Characterization of thyrostimulin antibodies

4. Chapter four

4.1 Introduction

As mentioned in the general introduction, thyrostimulin is a noncovalent heterodimer composed of a unique beta subunit (β5) and a novel alpha subunit (α2) which is different from the common α subunit (α1 subunit) shared by the other members of the glycoprotein family[153]. Thyrostimulin has three N-linked glycosylation sites, two in the α2 subunit and one in the β5 subunit which are important for secretion and receptor activation[147]. The human glycoprotein hormone α2 (GPHα2) gene (accession no. AF403384) has an open reading frame that codes for a precursor of 129 –amino acids with a 23-amino acid signal peptide at the N-terminus (**figure 4.1**), and two N-linked glycosylation sites. The putative 106- amino acid mature protein has a calculated molecular mass of 11.68 kDa. Whereas, the glycosylated human glycoprotein hormone α2 protein has a calculated molecular mass 13 kDa[145].

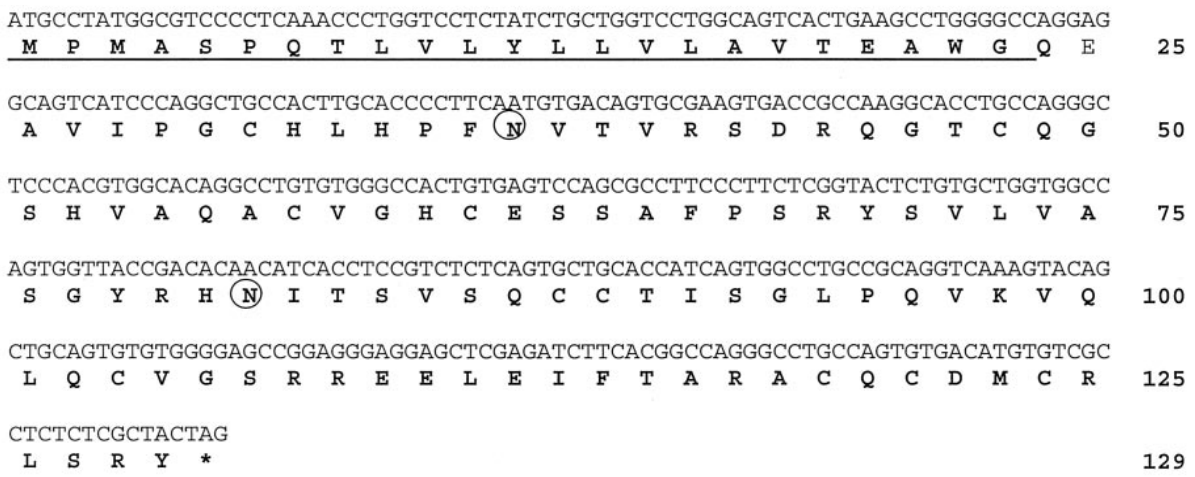

Figure 4.1 Nucleotide and deduced protein sequences of human GPHα2. Amino acid numbers are on the *right*, and the stop codon is marked with an *asterisk*. Putative N-linked glycosylation residues are *circled*. (Adapted from Hus et al, 2002[145])

The human glycoprotein β5 (GPHβ5) gene (accession no. AF403430) has an open reading frame that codes for a precursor of 130 amino acids with a 24-amino acid signal peptide at the N-terminus (**figure 4.2**), and a single N-linked glycosylation site. The unglycosylated human glycoprotein hormone β5 protein has a molecular mass of 11.74 kDa. Whereas, the glycosylated β5 protein is 16 kDa[145].

Figure 4.2 Nucleotide and deduced protein sequences of human GPHβ5. Amino acid numbers are on the *right*, and the stop codon is marked with an *asterisk*. The putative N-linlked glycosylation residue is circled (Adapted from Hus et al, 2002[145]).

4.1.1Aim of chapter four

To characterise new α2 and β5 thyrostimulin polyclonal antibodies using a fibroblast cell line transiently transfected with α2 or β5 expression vectors and then to study the expression and immunolocalisation of thyrostimulin subunits in human skin.

4.2 Materials & Methods

4.2.1 Thyrostimulin antibodies

Both α2 and β5 thyrostimulin antibodies are guinea pig polyclonal antibodies (Moravian Biotechnology, BRNO, Czech Republic) raised to specific peptides as shown in **figures 4.3** and **4.4** below.

MKLAFLFLGPMALLLLAGYGCV
LGASSGNLRTFVGCAVREFTFL
AKKPGCRGLRITTDACWGRCET
WQKPILEPPYIEAHHRVCTYNE
TKQVTVKLPNCAPGVDPFYTYP
VPSAVTAEPAPLATTECETI

Figure 4.3 Beta5 (β5) thyrostimulin antibody peptide.
The sequence of β5 thyrostimulin subunit, NCBI reference sequence (NP_660154.3) is shown with the peptide used as antigen in green.

MPMASPQTLVLYLLVLAVTEAW
GQEAVIPGCHLHPFNVTVRSDR
QGTCQGSHVAQACVGHCESSAF
PSRYSVLVASGYRHNITSVSQC
CTISGLKKVKVQLQCVGSRREE
LEIFTARACQCDM

Figure 4.4 Alpha2 (α2) thyrostimulin antibody peptide.
The sequence of α2 thyrostimulin subunit, NCBI reference sequence (BC093960) is shown with the peptide used as antigen in red.

4.2.2 Western blotting (Immunoblotting)

Western blotting (also called immunoblotting) is a method for detecting specific proteins in a given sample of tissue homogenate or extract. It uses gel electrophoresis to separate denatured proteins according to molecular weight. The proteins are then transferred to a

nitrocellulose membrane, where they are detected using antibodies specific to the target protein. The amount of protein can be examined and compared between samples. The term "blotting" refers to the transfer of biological samples from a gel to a membrane and their subsequent detection on the surface of the membrane.

4.2.2.1. Electroporation of HCA2

The tissue culture and electroporation were done by other colleagues in the Dermatology laboratory. HCA2 fibroblasts were transfected with α2 or β5 cDNA cloned into pcDNA3 by electroporation. Proteins were extracted from α2 and β5 transfected cells. Because thyrostimulin is secreted we assumed it would be in the cell condition medium therefore, the conditioned medium was also collected. Untransfected cell lysate and medium were used as negative controls. The GFP vector control contained cDNA for green fluorescent protein which was used as a positive control to prove successful transfection.

The HCA2 cells were transfected with pcDNA3 vector containing α2, β5 and the GFP control vector by electroporation using Amaxa® Cell line Necleofector® Kit V (Lonza). In summary, cells were trypsinized, and seeded, the day before transfection and grown on 6-well plates in serum containing medium (FCS) at a density such that they were 70-80% confluent on the day when they were transfected. Cells were grown in DMEM with 10 % heat inactivated fetal calf serum.

For transfection, the cells were trypsinised and the cell pellet was resuspended in 100µl electroporation solution (Nucleofector® Solution V (Lonza) at room temperature. The cell suspension (100µl) was combined with 1µg of vector (i.e.: pcDNA3 containing α2, or β5 and the GFP vector). The cell/ DNA suspension was transferred into a cuvette and then

electroporated on programme U012 optimised for HCA2 in the Amaxa nucleofector machine. Once the programme had finished, ~ 500 µl of pre-equilibrated culture medium was added to the electroporation cuvette and the cells were transferred into a 6-well plate (final volume 1.5 ml medium per well). The cells were incubated in humidified 37ºC/ 5% CO_2 incubator overnight. At 24 hours the cells were visualised using an inverted microscope (Nikon Eclipse TS100) to check for cell viability (~70-80%) and using a UV lamp (Nikon Intensilight C-HGFI) to check that at least 50% viable cells remaining were positive for GFP expression. The medium was changed to DMEM alone in wells prepared for the collection of conditioned medium or DMEM plus 10% FCS in wells for cell lysate preparation. After 24 hours the serum-free medium was harvested and replaced and then harvested again after another 24 hours. The medium was frozen for concentration later. The cell lysates were prepared 72 hours after electroporation.

4.2.2.1.1 Preparation of protein cell lysates from electroporated fibroblasts

The culture medium was removed; the cells washed gently three times with 2 ml chilled PBS, then 300 µl x2 sample buffer added (**table 4.1**). The surface of the well was rubbed vigorously with the plunger from a plastic syringe to aid cell lysis. To ensure complete homogenization of the cells and removal of cellular contaminants, the cell homogenate was boiled for 5 minutes at 95°C. The proteins were then transferred to a clean Eppendorf tube and used directly or frozen at -20°C until needed**.**

4.2.2.1.2 Preparation of proteins from Conditioned medium from transfected cells

The conditioned medium was thawed until it reached room temperature and then concentrated using Amicon Ultra-4 Centrifugal Filter columns, (Millipore, USA) by spinning in the centrifuge for 40 minutes at 4250 rpm. The flow-through was discarded and then an equal volume of x2 sample buffer was added (**table 4.1**) to the solution remaining in the tube and transferred to a clean Eppendorf tube and used directly or frozen at -20°C until needed.

Table 4.1: Constituents of x2 Sample buffer

Name	Amount
0.5 Tris PH6.8	1 ml
Glycerol	0.8 ml
10% SDS (Sodium Dodecyl Sulphate)	1.6 ml
IM DTT (Dithiothreitol)	0.08 ml
BPB(Bromophenol Blue) 0.05%(Sigma)	0.2 ml

4.2.2.2 Electrophoretic separation of the proteins

The initial step in a western blotting procedure is to separate the proteins using Sodium Dodecyl Sulfate polyacrylamide gel electrophoresis (SDS-PAGE), therefore, a running gel (also known as resolving or separating gel) has to be prepared first. The percentage of acrylamide to be used in the running gel depends on the size of the protein of interest, large proteins require a less concentrated gel and small proteins require a more concentrated gel.

The estimated molecular size of α2 and β5 subunits is 13 kDa and 16 kDa respectively, so the proteins were separated on 15 % polyacrylamide gel.

4.2.2.2.1 Gel preparation

The Sodium Dodecyl Sulfate Polyacrylamide gels (SDS-PAGE) were prepared from the reagents listed in (**tables 4.2, 4.3)** and loaded into two Novex disposable (8cm X 6cm) cassettes (Invitrogen, Paisley, UK) up to a level of about 2 cm below the top of the cassette. The running gel was then carefully layered with water to ensure a flat top surface. Whilst, waiting for the running gel to set, the solution for the stacking gel was prepared. Both stacking and running gels are parts of the SDS-gel. However, the stacking gel is usually 4% and it is the portion in which the wells are formed and the protein samples are loaded.

Table 4.2 Constituents of the running gel

Constituent	Running gel (15%)
1.5M Tris pH8.8	3.75ml
30% Acrylamide/bis- acrylamide gel solution (Sigma)	7.5ml
10% SDS	150µl
H_2O	3.6 ml
10% Ammonium per sulphate (sigma)*	75 µl
TEMED (N,N,N,N tetramethyl ethylene diamine) 99% sigma	7.5 µl

*Should be added just prior to pouring the gel into the cassette.

Table 4.3 Constituents of the stacking gel

Constituent	Stacking gel (4%)
0.5 Tris PH 6.8	1.25 ml
30% Acrylamide/bis- acrylamide gel solution (Sigma)	0.65 ml
10% SDS	50 µl
H_2O	3.05 ml
10% Ammonium per sulphate (sigma)*	50 µl
TEMED	10 µl

*Should be added just prior to pouring the gel into the cassette.

Once the running gel was set, the water from the top was drained off and the stacking gel was loaded on to the cassettes. A plastic comb was immediately inserted into the liquid stacking gel before it sets. Once set, the comb was carefully removed and the wells are rinsed with distilled water. The white strip at the lower end of the cassettes was removed and the cassettes were placed in the electrophoresis cell (XCell SureLock™ Mini-Cell Electrophoresis System, Invitrogen, Paisley, UK) with the wells facing inwards and locked in place.

Following this step, x1 running buffer prepared from the x10 stock running buffer (as described in **table 4.4**) was loaded into the wells. Low-range prestained SDS-PAGE molecular weight marker (about 5 µl) (Precision plus, Catalogue no. 161-0373, Bio-Rad Laboratories, Richmond, CA) was loaded into the assigned wells, and then (5 µl) samples of protein of interest (α2, β5, GFP transfected cell lysate, untreated cell lysate, conditioned medium of transfected cells, GFP conditioned medium) were also loaded in to the assigned wells. The chamber between the gels and the outer chamber of the apparatus were then filled

with the x1 running buffer. The electrophoresis apparatus was then connected to a power pack and run at a starting voltage of 150V and a constant current of 50 mA (25mA per gel) until the tracking dye reached the bottom of the gel. The cassettes were unlocked and removed from the apparatus, after which they were carefully dismantled by breaking the seal around them using the supplied Novex spatula. The stacking gel and the lower portion of the running gel were cut off.

Table 4.4 Composition of x10 running buffer

Constituent	Volume
Tris (Mw121.1)	30g
Glycine	144g
SDS (Sodium dodecyl sulphate)	10g
Distilled Water	To make up to 1L

The x1 running buffer was made from a readymade stock of x10 running buffer (1:10).

4.2.2.2.2 Transfer of proteins to the membrane

After the electrophoresis step, the proteins are transferred from the electrophoresis gel to Immobilon membrane. For this purpose, western blotting buffer was prepared using a stock x 25 blotting buffer (**table 4.5**).

Table 4.5 Composition of x25 blotting buffer

Constituent	Volume
Tris (Mw121.1)	18.2g
Glycine	90g
H2O	Up to 500ml

The 500 ml x1 blotting buffer was made by mixing 20ml x25 blotting buffer, 100ml methanol and 380 ml H2O.

Four pieces of filter paper and two pieces of polyvinylidene difluoride (PVDF) membrane (Immobilon-P Transfer Membrane, Watford, UK) were cut according to the dimensions of the gel (8 cm x 6 cm). The filter paper and the four pads were soaked in the western blotting buffer. Before soaking in the western blotting buffer, the hydrophobic membrane was made hydrophilic by immersing it in methanol for 10 seconds followed by two five minute washes in distilled water. The gel membrane sandwich for two gels was assembled on the cathode plate of the blotting apparatus in the following order: sponge pad, filter paper, gel, membrane, filter paper, sponge pad, filter paper, gel, membrane, filter paper and the remaining two pads (**figure 4.5**).

The other plate of the module was placed on top and closed. The assembled module (X Cell II Blot Module; Invitrogen, Paisley, UK) was then inserted into the tank of the blotting Apparatus **(figure 4.6)**. The inner blotting chamber was filled with 1x western blotting buffer and the outer chamber of the blotting apparatus was filled with distilled water for cooling during the electrophoresis. It was then run at 25 V constant voltage (around 100 mA starting current) for 2 hours.

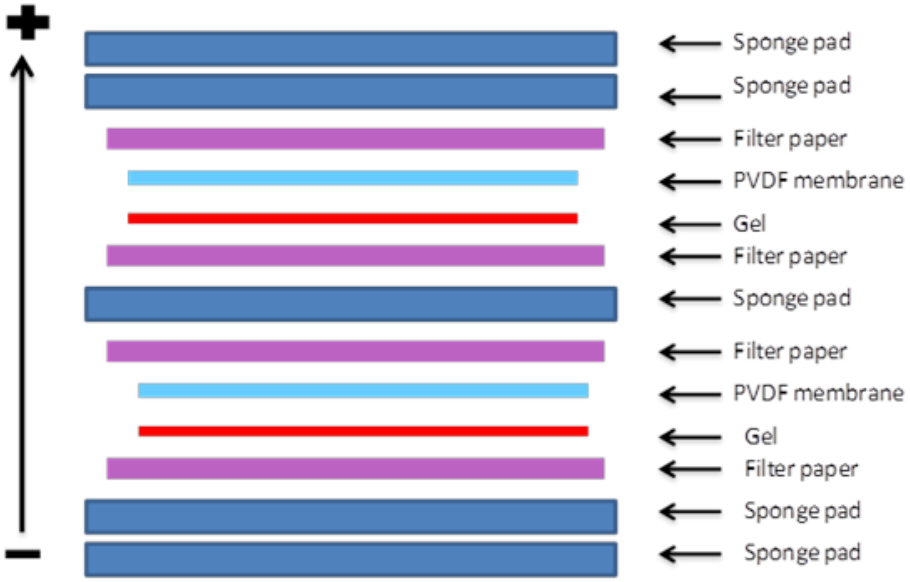

Figure 4.5 Illustration of a gel-membrane sandwich for two gels.

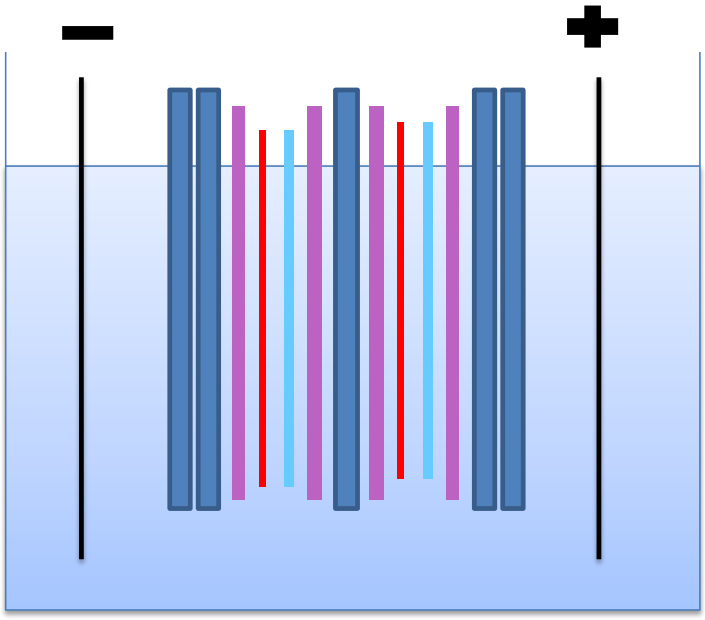

Figure 4.6 Illustration of Electroblotting Apparatus

4.2.2.2.3 Blocking and antibody incubation

After 2 hours, the membranes were carefully removed and placed in a Petri dish and washed once in PBS-T (**table 4.6**) for 5 minutes. All the washing, blocking, and primary and secondary antibody incubation steps were performed on an orbital shaker to ensure proper contact with the membrane.

Table 4.6 Constituents for preparation of PBS-T20

Constituents	Amount required to make up 500 ml
PBS (x10)	50 ml
Tween-20	0.5 ml
Distilled water	449.5 ml

The PVDF membrane used in western blotting has a high affinity for proteins. Therefore, after the transfer of the proteins from the gel, it is important to block the remaining surface of the membrane to prevent any nonspecific binding of the antibodies to the membrane surface in subsequent steps. Therefore, the membranes were then placed in blocking buffer (5 g of Marvel in 100 ml of PBS-T), protein side down for an hour.

Following this, the membranes were placed in primary (α2, β5) thyrostimulin antibodies diluted in 5% Marvel in PBS-T, overnight at 4° C on the rocker (**table 4.7**) The next day the membranes were washed in PBS-T (3 times for 5 minutes) to remove unbound reagents and reduce background. The membranes were placed in 10 ml of 1:500 dilution (diluted with 2% Marvel in PBS-T) of the anti-guinea pig secondary antibody (species corresponding to the primary anti body) conjugated to horse radish peroxidase (Dako UK Ltd, Ely, UK) for 30

minutes. This was followed by washes in 2% Marvel in PBS-T five times for two minutes each and, finally washed with PBS for one minute.

Table 4.7 α2 & β5 thyrostimulin antibodies protocol used for western blotting

Primary ab	Host	Source	Dilution	Blocking Buffer	Secondary labelled HRP ab	Gel %
β5	Guinea pig	Moravian Biotechnology, BRNO, Czech Republic	1:500 O/N	5% Marvel in PBS-T	Anti guinea pig 1:500	15%
			1:2000 O/N			
α2			1:500 O/N	5% Marvel in PBS-T	Anti guinea pig 1:500	15%
			1:2000 O/N			

4.2.2.3. Chemiluminescent detection of proteins.

To visualise the protein signals, an enhanced chemiluminescence (ECL) technique was employed, which has to be performed in a dark room. The membranes were placed on cling film with the protein side up and a 1:1 mixture of solution I (**table 4.8**) and solution II (**table 4.9**) were added to the membranes (approximately 2 ml per membrane) and it was left for 5 minutes.

Table 4.8 Constituents for preparation of solution I

Constituents	Amount required
Luminol (250 mM in dimethyl sulfoxide, DMSO)	1 ml
Coumaric acid (90 mM in DMSO)	0.44 ml
Tris (pH 8.5)	10 ml
Distilled water	To make up to 100 ml

Table 4.9 Constituents for preparation of solution II

Constituents	Amount required
30 % Hydrogen peroxide	64 µl
Tris (pH 8.5)	10 ml
Distilled water	To make up to 100 ml

Following this the excess solution was drained off and the membranes were placed protein side down on fresh cling film, wrapped up and placed in an X-ray cassette with the protein side facing upwards. The lights in the dark room were switched off and an X-ray film (Amersham Hyperfilm ECL, catalogue number: 28-9068-35; GE Healthcare UK Limited, Buckinghamshire, UK) of appropriate dimension was placed over the wrapped membranes in the cassette. The exposure time ranged from 30 seconds up to 5 minutes. The film was removed from the cassette and placed in the developer solution till clear bands appeared, following which it was briefly immersed in the stop solution (water) and then in the fixer for around 30 seconds. The films were washed in distilled water for 15 minutes and then allowed to dry. Once dried the size of the bands on the film were determined by comparing it with the prestained molecular weight marker.

4.2.2.4. Coomassie Blue staining

To visualize the proteins and to check for even loading of protein, the gels were stained for 30 minutes with 0.05g Coomassie brilliant blue R250 (Sigma) dissolved in 40ml methanol, 10ml acetic acid and 50ml water followed by destaining with a mixture of 50ml methanol, 75ml Acetic acid and 875ml H_2O for every 30 minutes until the background of the gel is clear.

4.2.2.5. Silver staining

Silver staining detects proteins after electrophoretic separation on polyacrylamide gels. Its main advantages are its high sensitivity (in the very low ng range) and can be achieved with simple and cheap laboratory equipment and chemicals. The main phases of silver staining are protein fixation followed by sensitization, then silver impregnation (infusion) and finally image development[183]. Several variants of silver staining protocols described in the literature which can be completed in a time range from 2 h to 1 day after the end of the electrophoretic separation. Once completed, the stain is stable for several weeks[183] . The silver staining was performed using PlusOne Silver Staining Kit, Protein (Code No.17- 1150-01, GE Healthcare Bio-Sciences AB, Sweden). The initial step is to prepare the reagent solutions described in (**table 4.10**) from the chemicals provided in PlusOne Silver Staining Kit which are; Ethanol, Glacial acetic acid and Glycerol (87%w/w) (1000ml). For each gel, 250ml solution is needed per gel. All steps should be performed with gentle shaking of the staining tray.

Table 4.10 Constituents of reagent solutions used in silver staining

Reagent name	Component and quantity
Fixing solution 30% Ethanol	Ethanol 75ml Glacial acetic acid 25ml Water up to 250ml
Sensitizing solution	Ethanol 75ml Sodium thiosulphate (15%w/v)10 ml Sodium acetate(17g) 1 packet Water up to 250ml ***1.25ml Glutaraldehyde (25%w/v)**
Silver solution	Silver nitrate solution(2.5% w/v) 25ml Water up to 250ml
Developing solution	Sodium carbonate (6.25g) 1 packet Water up to 250ml Sir vigorously to dissolve the Sodium carbonate ***0.2 ml formaldehyde (37%w/v)**
Stop solution	EDTA-Na_2.2H_2O(3.65g)) 1 packet Water up to 250ml
Washing solution	Water
Reserving solution	Ethanol 75ml Glycerol(87%w/w) Water up to 250ml

*** Glutaraldehyde and formaldehyde should be added immediately before use**

To fix the proteins, the gels are soaked in fixing solution for 60 minutes, the fixing solution was removed and sensitization solution was added with continuous shaking for 60 minutes. After removing the sensitization solution the gels are washed four times for 15 minutes each with distilled water. Then the gels were soaked in silver solution for 60 minutes with continuous shaking to ensure proper infusion of proteins with the silver stain. The silver solution removed and the gels washed four times in distilled water for one minute each

followed by adding the developing solution and continuous shaking for 4-6 minutes until the bands reach the desired intensity, then the gels were transferred to stopping solution for 60 minutes with shaking. The gels were transferred to preserving solution for 60 minutes. Finally, the gels were placed between two wet gel drying membranes (Sigma Aldrich. Dorset, UK) sheets and allowed to dry at room temperature overnight.

4.2.3. Immunohistochemistry of β5 thyrostimulin antibody

Despite different attempts, techniques used in western blotting experiment to detect the thyrostimulin α2 & β5 subunit proteins using thyrostimulin antibodies, results fail to show α2 subunit expression whereas only β5 subunit was detected. Therefore, IHC was utilized to explore whether β5 is expressed in the skin or not.

4.2.3.1 Tissues used

Human thyroid tissue and normal skin tissue was purchased from a commercial source (AMS Biotechnology, UK). Normal human skin was also collected from the Dermatology Department, Cardiff University. Frozen section techniques were employed as described in chapter three, section (**3.2.1.1).**

4.2.3.2 Antibody used

Only β5 polyclonal thyrostimulin antibody is used (as described above).

4.2.3.3 The protocol

Two protocols were tried 1) ABC method as in chapter 3 section (**3.2.1.4)**. 2) The streptavidin method as described below:

4.2.3.3.1The streptavidin method

Slides were taken out of the freezer and allowed to reach room temperature; foil was removed and the slides then labelled, fixed in acetone and air dried for 15 minutes each, followed by three five-minute washes in 1x PBS-T (**table 3.2**) with 0.05% Tween 20 buffer solution. To reduce non-specific binding, the slides were incubated with 5% goat normal serum in 1% BSA/PBS-T for 30 minutes at room temperature. After tapping off the excess, the slides were washed three times five-minute each in 1x PBS-T The sections were incubated with an optimum dilution of the β5 primary antibody overnight at 4˚C (**table 4.11**). Slides incubated with diluent without any primary antibody were run in parallel as a negative control. This was followed by three five-minute washes in the buffer solution.

The sections were then incubated with anti guinea pig biotinylated secondary antibody at a dilution of 1:400 (**table 4.11**) for 30 minutes, Followed by three five-minute washes in 1x PBS-T. The sections were then incubated with streptavidin (GE Healthcare, UK) at a dilution of (1:200) for a further 30 minutes. The sections were then washed in the buffer solution three times and developed with (5mgs in 5ml of PBS) horse radish peroxidase substrate solution (0.5 ml of 3, 3’ Diaminobenzidine (DAB), 4.5 ml of PBS and 6 µl of H_2O_2) (Fisher Scientific UK) for 10 minutes to produce colorimetric immunoprecipitates. The sections were then rinsed in tap water and counterstained with haematoxylin for 5 minutes and washed again in tap water. Finally, all sections were dehydrated through a graded series of alcohol solutions (1 x 70%, 1 x 90%, and 3 x 100% industrial methylated spirit; Genta Medica, York,

UK) for 5 minutes each, and cleared in three changes of xylene (Genta Medica, York, UK) for 5 minutes each. The slides were then carefully mounted with a cover slip using DPX mounting medium (a mixture of distyrene, a plasticizer, and xylene; RA Lamb, East Sussex, UK) and then left to dry overnight.

4.2.3.4 Optimization of β5 thyrostimulin antibody

The protocols used in these experiments were optimized until good positive staining was detected and all the non-specific staining and background were minimised.

4.2.3.5 Optimization of primary and secondary antibodies

Frozen sections of human skin were used to optimize β5 thyrostimulin primary antibody and anti guinea pig biotinylated secondary antibody. The Streptavidin method was used initially, and later on the standard ABC method was employed as described in chapter three, section (**3.2.1.4).** A summary of the protocols used during the optimization process is shown in (**table 4.11**).All sections were treated with diluent only without the primary antibody as a negative control. Another negative control experiment was carried out with the pre immune serum instead of the primary antibody. The pre-immune serum is basically the serum of the host animal before it was immunized with the peptide of interest.

Table 4.11 Summary of primary and secondary antibody optimization conditions

β5 primary ab	Secondary ab	Tissue	Blocking	Tertiary (Method)
1:200, 1:500, 1:1000 O/N	Anti guinea pig biotinylated 1:400 O/N	Normal skin	Endogenous peroxidase for 10 minutes 5% goat serum in PBS-T for 30 minutes	Streptavidin (1:200)
1:50 O/N	Anti guinea pig biotinylated 1:200 O/N	Normal skin	Endogenous peroxidase for 10 minutes 5% goat serum in BSA/Marvel in PBS-T for 30 minutes	ABC
none	Only anti guinea pig biotinylated secondary Ab is used (1:200, 1:400, 1:800 O/N	Normal skin	Endogenous peroxidase for 10 minutes 5% goat serum in BSA/Marvel in PB**S-** T for 30 minutes	ABC
1:500, 1:750, 1:1000 O/N	Anti guinea pig biotinylated 1: 400 O/N	Normal skin	Endogenous peroxidase for 10 minutes 5% goat serum in BSA/Marvel in PB**S-** T for 30 minutes	ABC

4.2.3.6 Testing the pre immune serum

In this protocol, frozen sections of human skin were used, immunoreactivity of skin sections treated with β5 thyrostimulin antibody were compared with immunoreactivity of skin sections treated with guinea pig pre-immune serum in the same conditions. The standard ABC method was used as described in chapter three, section (**3.2.1.4**), in addition to the use of hydrogen peroxide to block the endogenous peroxidase. The different dilutions of β5 antibody and the pre immune serum samples were prepared (**table 4.12**) using the same diluent (1% BSA/Marvel in PBS-T) at room temperature at the same time. Equal volumes of the β5 antibody and the pre immune serum were added to diluent. A summary of pre-immune serum protocol is shown in (**table 4.13**).

Table 4.12 Dilutions of β5 and pre immune serum

β5 antibody	Guinea pig pre immune serum
Blank (Diluent only)	Blank (Diluent only)
1:1000	1:1000
1:2000	1:2000
1:4000	1:4000

Table 4.13 Summary of pre-immune serum experiment protocol

Primary Ab	Secondary ab	Tissue	Blocking	Method
Anti β5 Ab 1:1000 1:2000 1:4000 O/N	Anti guinea pig biotinylated 1: 400	Normal skin sections	Endogenous peroxidase blocked for 10 minutes. 5% goat serum in BSA/Marvel in PBS-T for 30 minutes Avidin & Biotin for 15 minutes each	ABC Kit
Guinea pig β5 pre-immune serum 1:1000 1:2000 1:4000 O/N				

4.2.3.7 β5 Peptide neutralization

Peptide neutralization or immunizing peptide blocking is a technique used to determine if the immunoreactivity is specific. The initial step in this approach is to neutralize (incubate) the primary antibody with an excess of peptide that was used to raise the primary antibody. The antibody that is bound to the blocking peptide is no longer available to bind to the peptide epitope present in the protein in the cell. The neutralized antibody is then used side-by-side with the antibody alone, and the results are compared. By comparing the staining from the blocked antibody versus the antibody alone, the specific staining can be observed in the IHC sections. Staining recognized by the antibody will be absent in the tissue/cells probed with

neutralized antibody. In this project we compared the immunoreactivity of skin sections treated with β5 thyrostimulin antibody alone with sections treated with a mixture of β5 thyrostimulin antibody plus the β5-blocking peptide (the peptide that the β5 antibody was raised to) under the same conditions. All antibody and blocking peptide samples were prepared at room temperature with the same antibody diluent (1% BSA/Marvel in PBS-T) and then centrifuged for 15 minutes for at least two hours before the start of the experiment to allow interaction between the antibody and the peptide. After fixation and blocking steps, the antibody solutions were incubated with skin sections overnight at 4^{o}C. The standard ABC staining method was continued as described in chapter three, section (**3.2.1.4).** A summary of the β5 Peptide neutralization protocol is shown in (**table 4.14).**

Table 4.14: Summary **of β5 Peptide neutralization protocol.**

Primary ab	Diluent	Secondary Ab	Tissues	Blocking method & duration	Method
β5 1:1000 O/N	1% BSA/Marvel in PBS-T	Anti Guinea pig Ab (1: 400)	Normal skin sections	Endogenous peroxidase , 10 minutes 5% goat serum in BSA/Marvel in PBS-T, for 30 minutes. Avidin & Biotin, 15 minutes each	ABC Kit
β5 1:1000 + blocking Peptide 1:1000 O/N					

4.3 Results

4.3.1 Western blotting results

4.3.1.1 β5 thyrostimulin antibody

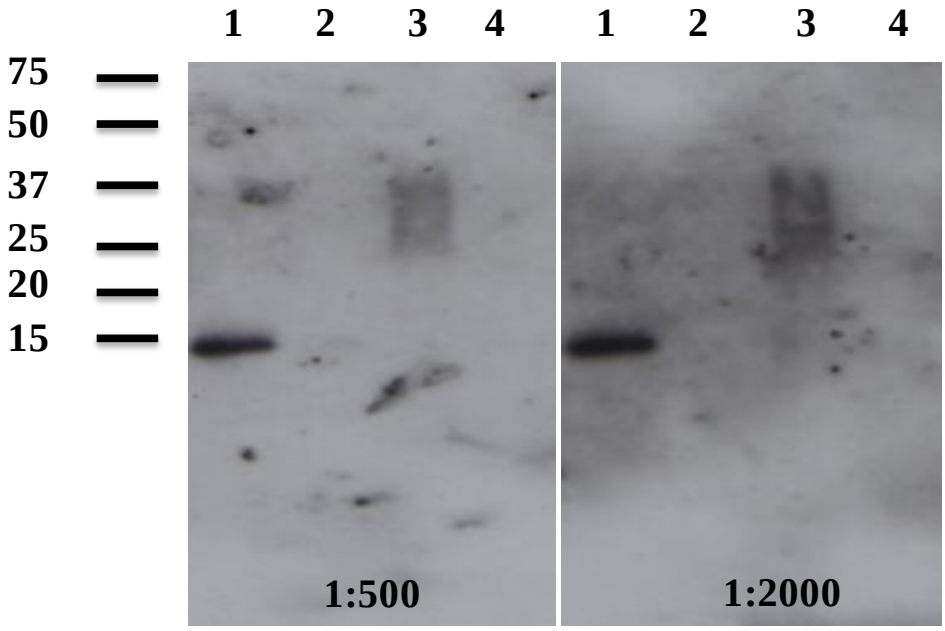

Figure 4.7 Western blot for detection of β5 subunit protein in cultured fibroblast transfected with β5 vector. Lane 1) β5 cell lysate, **Lane 2)** unelectroporated cell lysate (-ve control), **Lane 3)** conditioned medium from β5 transfected cells**, Lane 4)** conditioned medium from GFP transfected cells, Marker = Precision plus marker in kilo-Dalton (kDa).

As shown in figure 4.7, immunoblots of protein prepared from cells transiently transfected with β5 expression vector, using the β5 thyrostimulin antibody at dilutions of 1:500 & 1:2000 detected a band in the β5 cell lysate of approximately 15 kDa. There was no band detected in the un-transfected cell lysate. There is a smear like band in the β5 conditioned medium. However, no band detected in GFP conditioned medium.

4.3.1.2 α2 thyrostimulin antibody

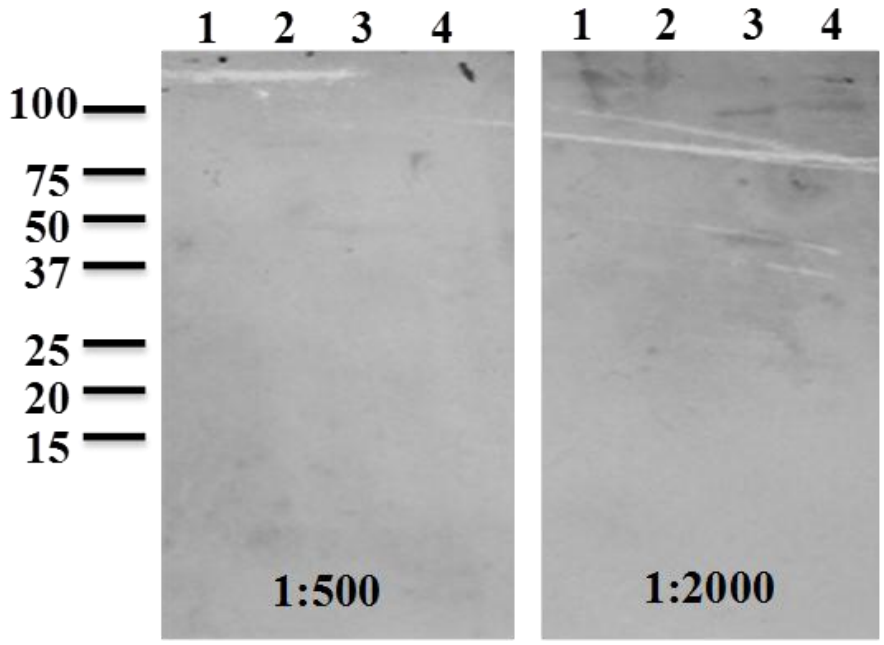

Figure 4.8 Western blot for detection of α2 subunit protein extract in cultured fibroblast transfected with α2 vector. Lane 1) α2 cell lysate, **lane 2)** unelectroporated cell lysate (-ve control), **lane 3)** α2 condition medium, **lane 4)** GFP condition medium, Marker = Precision plus marker in kilo Dalton (kDa).

As shown in figure 4.8 immunoblots of proteins prepared from cells transiently transfected with α2 expression vector using α2 thyrostimulin antibody at dilutions of 1:500 & 1:2000 showed no reactivity with the α2 subunit protein in the cell lysate or the conditioned medium. Two faint bands are visible in lanes 3, 4 at dilution of 1:2000 most probably due to non specific binding in the serum since they are in the control as well and are of a protein too large to be thyrostimulin.

4.3.1.3 Coomassie Brilliant Blue result

Coomassie staining of condition medium and cell lysate of α 2 and β5, GFP was applied.

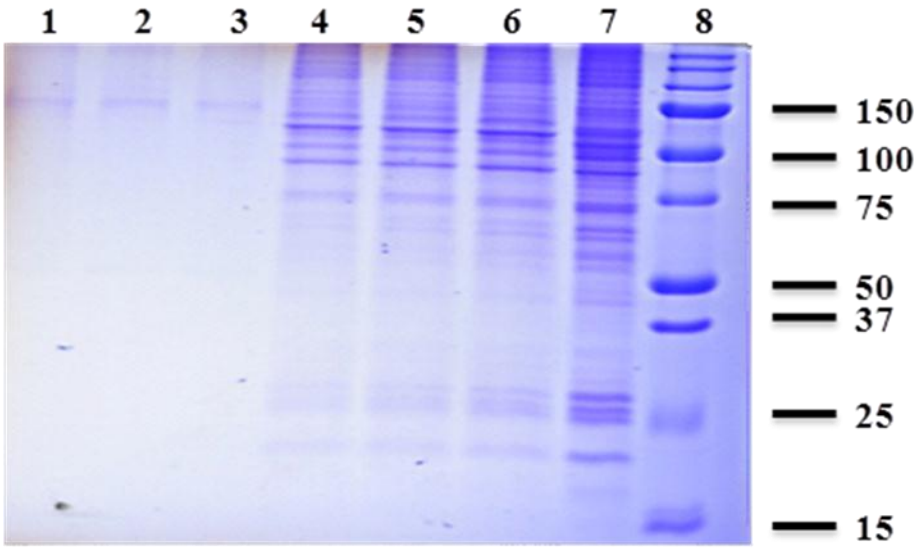

Figure 4.9 Coomassie Brilliant Blue staining of proteins from cell lysate and culture medium of HCA2 cell line transfected with α2, β5 and GFP vectors. Lane 1) α2 conditioned medium, **lane 2)** β5 condition medium, **lane 3)** GFP condition medium, **lane 4)** α2 cell lysate, **lane 5)** β5 cell lysate, **lane 6)** untreated cell lysate, **lane 7)** data used for a different experiment, **lane 8)** Precision Plus marker in kDa.

Coomassie Brilliant Blue staining of a 15% gel (**figure 4.9**) used to separate proteins extracted from cell lysate and culture medium of HCA2 fibroblast cell line transfected with α2, β5 and GFP. Lanes 1, 2 and 3 are difficult to comment on due to the fact that the proteins are below the detection level of Coomassie Brilliant Blue staining. Lanes 4, 5 and 6 looks similar and evenly loaded. Lane 7 is data used for different experiment.

4.3.1.4 Silver stain result

Despite concentration of the conditioned media the levels of proteins are mostly below the detection level for Coomassie Brilliant Blue (**figure 4.9**). Therefore, silver staining, a sensitive method to detect even low levels of protein expression, was undertaken.

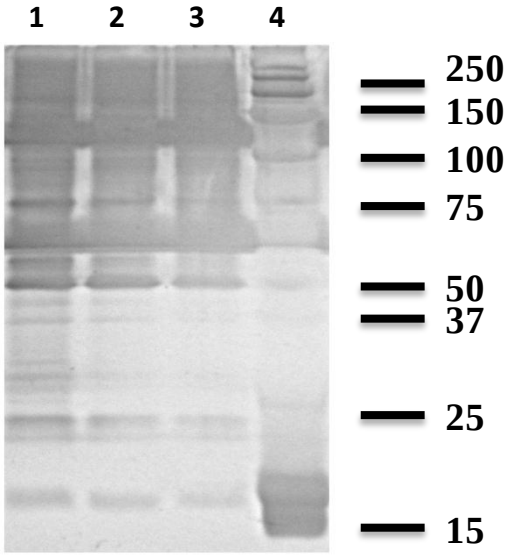

Figure 4.10 Silver staining of SDS-PAGE gel of concentrated conditioned media. Lane 1) HCA2 cells condition medium transfected with α2 expression vector, **lane 2)** HCA2 cells condition medium transfected with β5 expression vector, **lane 3)** HCA2 cells condition medium transfected with GFP vector and **lane 4)** precision plus marker in kilo Dalton (kDa).

As shown in Figure 4.10, proteins in the concentrated conditioned media from HCA2 cells transfected with α2 expression vector, β5 expression vector and GFP vector were investigated using silver staining of 15 % SDS-PAGE gel. Even using this sensitive method there were no obvious bands present in the condition medium of the α2, β5-transfected cells that were not present in the GFP transfected cells at the expected molecular weights. The α2 and β5 expression is probably too low to be detected even with silver stain.

4.3.2 IHC results

4.3.2.1 Optimization of β5 antibody using streptavidin method

The streptavidin method as a less direct method was carried out

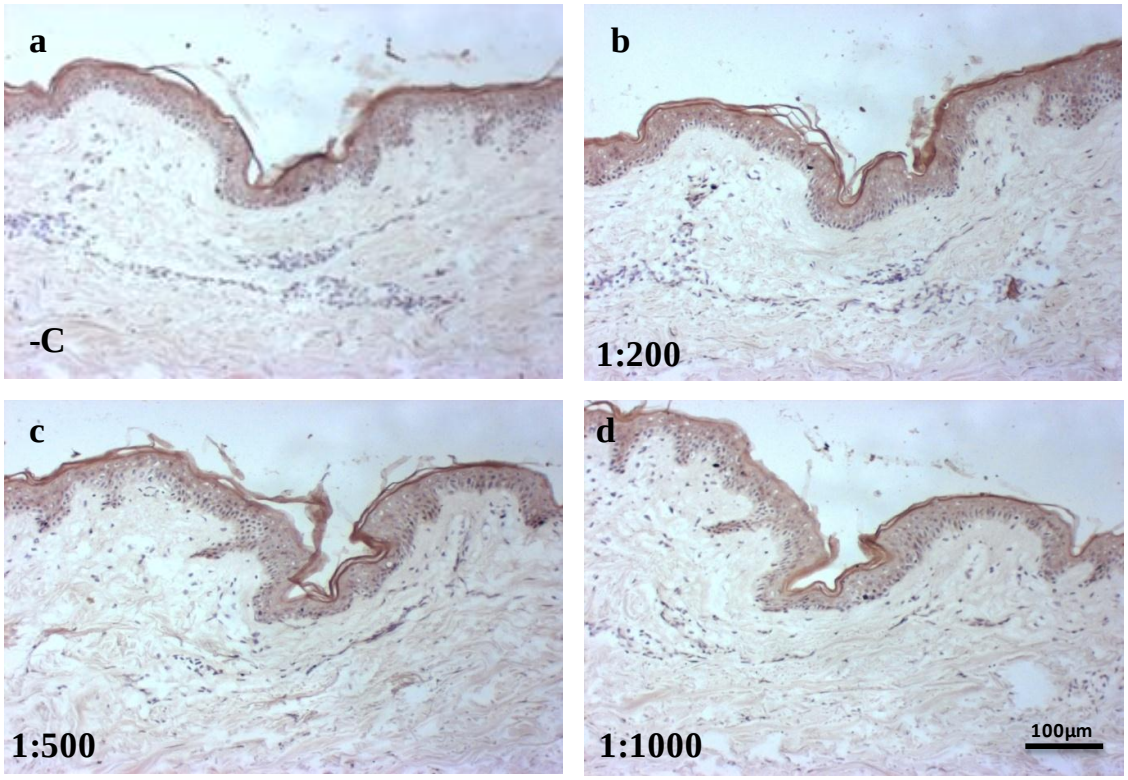

Figure 4.11 Optimization of the β5 polyclonal thyrostimulin using the streptavidin method. a) Negative control is section incubated with secondary antibody (1:400). Skin sections treated with different dilutions of β5 thyrostimulin antibody b) 1:200, c) 1:500 and d) 1:1000 respectively. Scale bar x10= 100µm.

As shown in figures 4.11, the immunostaining of thyrostimulin in human skin using β5 polyclonal thyrostimulin antibody using the streptavidin method, the negative control is skin section treated with no primary antibody and only secondary antibody (1:400) used, and was of similar pattern and intensity in the negative control (skin incubated with no primary antibody) and in sections treated with β5 antibody at a range of dilutions of 1:200, 1:500 and 1:1000. Therefore a more sensitive method was needed (such as ABC) but with more stringent blocking.

4.3.2.2 ABC method with higher concentration of primary and secondary antibodies

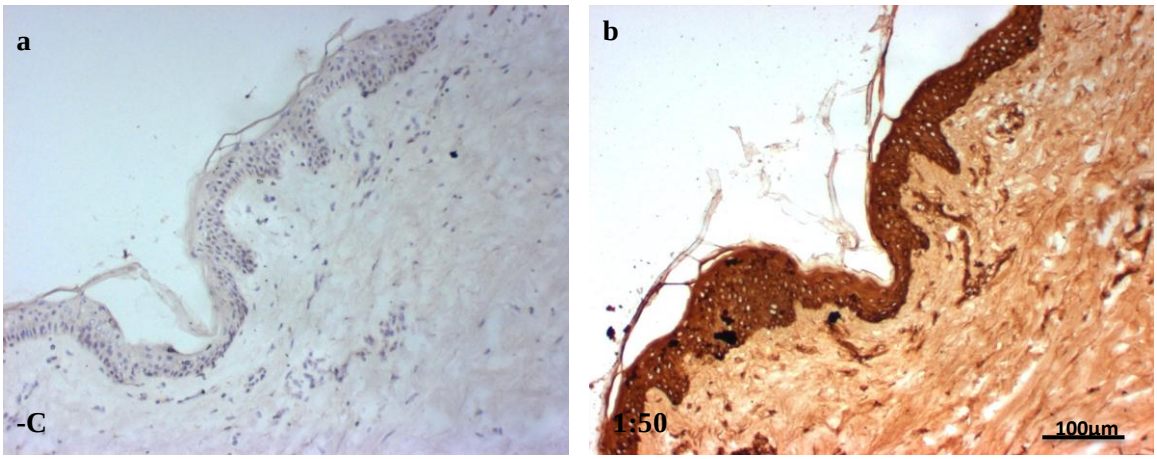

Figure 4.12 Optimization of the β5 polyclonal thyrostimulin using higher concentration of primary and secondary. a) Negative control is section incubated with secondary antibody (1:200). b) Skin section treated with 1:50 dilution of β5 thyrostimulin antibody. Scale bar x10= 100µm.

As shown in figures 4.12, images of immunostaining of thyrostimulin in human skin using β5 polyclonal thyrostimulin antibody during the process of optimization using ABC method. Negative control is skin section incubated with no primary antibody and reveals no staining. Because, the streptavidin method showed no immunoreactivity, skin section treated with higher concentration of primary β5 antibody (1:50) and a high concentration of the secondary antibody (1:200) using ABC method was carried out. Higher concentrations were used just to get a signal as a start point for the optimization process. At 1:50 dilution B5 antibody showed strong non-specific background signals, thus optimization of secondary antibody was required.

4.3.2.3 Optimization of secondary antibody

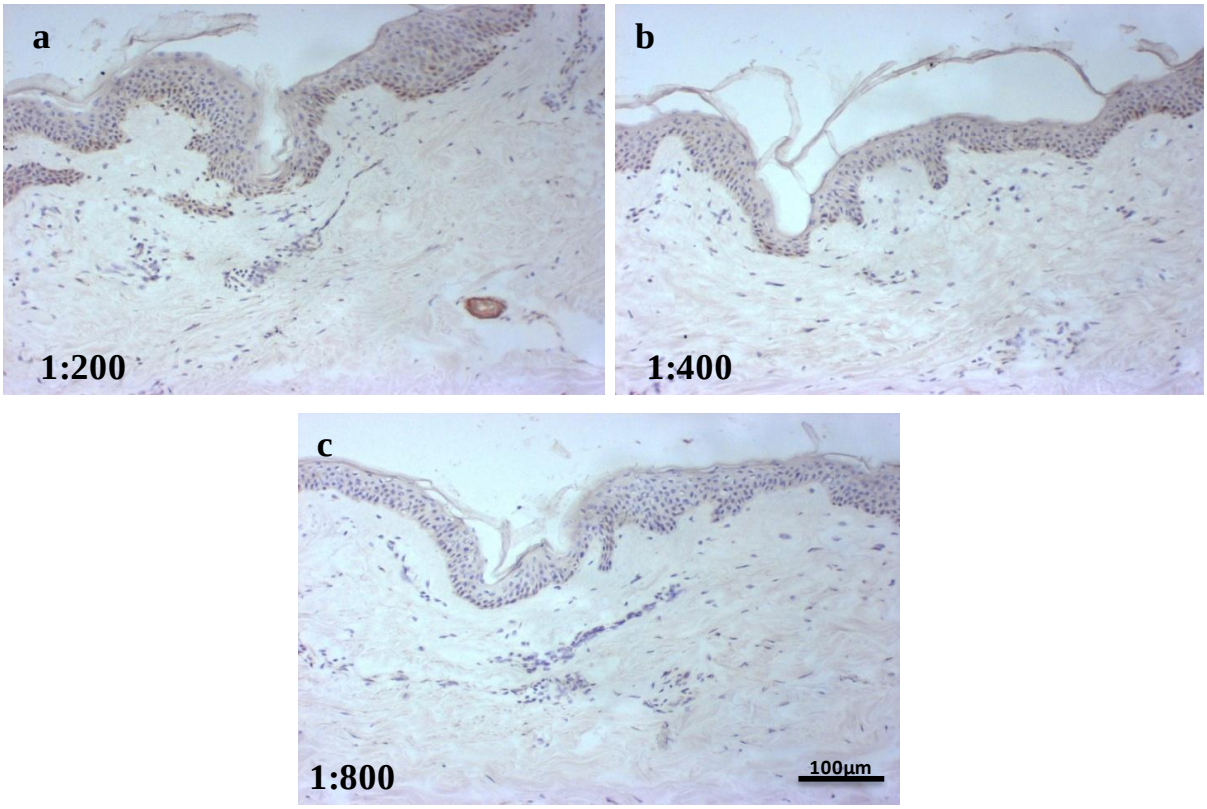

Figure 4.13: Optimization of the anti-guinea pig secondary antibody concentration. Sections incubated without primary antibody at dilutions of secondary of a) 1:200, b) 1:400, c) 1:800. Scale bar x10= 100µm.

As shown in figure 4.13, images of immunohistological staining during the process of secondary antibody optimization using the ABC method. In all sections no primary antibody was used (diluent only was used instead), the secondary antibody used at a range of dilutions (1:200, 1:400, 1:800) respectively. The anti guinea pig secondary at dilution of 1:400 seemed to be the highest concentration that revealed a clear background with no nonspecific staining in skin sections, so this dilution was used in the next experiments.

4.3.2.4 Optimization of β5 antibody using ABC method

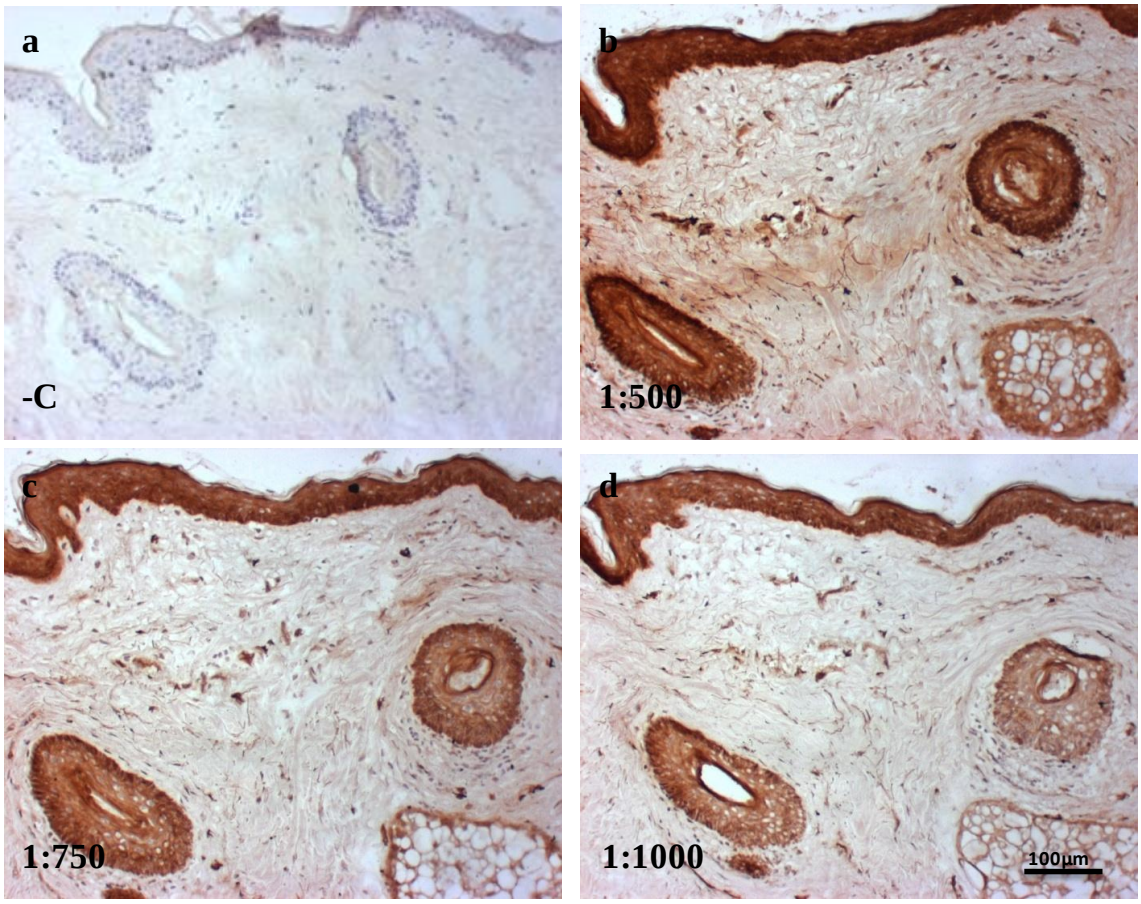

Figure 4.14: Optimization of β5 polyclonal thyrostimulin antibody using ABC method. Negative control (panel a) is section incubated with secondary antibody (1:400). In contrast, panels (b, c and d) are skin sections treated with different dilutions of β5 antibody (1:500, 1:750 and 1:1000) respectively. Scale bar x10= 100µm.

As shown in figures 4.14, Images of immunostaining of thyrostimulin in human skin using β5 polyclonal thyrostimulin antibody during the process of optimization using ABC method with extra blocking. Negative control section (blank) is incubated with no primary antibody (diluent used instead) and reveals no staining. Skin sections treated with β5 antibody at a range of dilutions of (1:500, 1:750 and 1:1000) showed strong staining and additional controls are required to confirm the specificity.

4.3.2.5 β5 pre-immune serum control

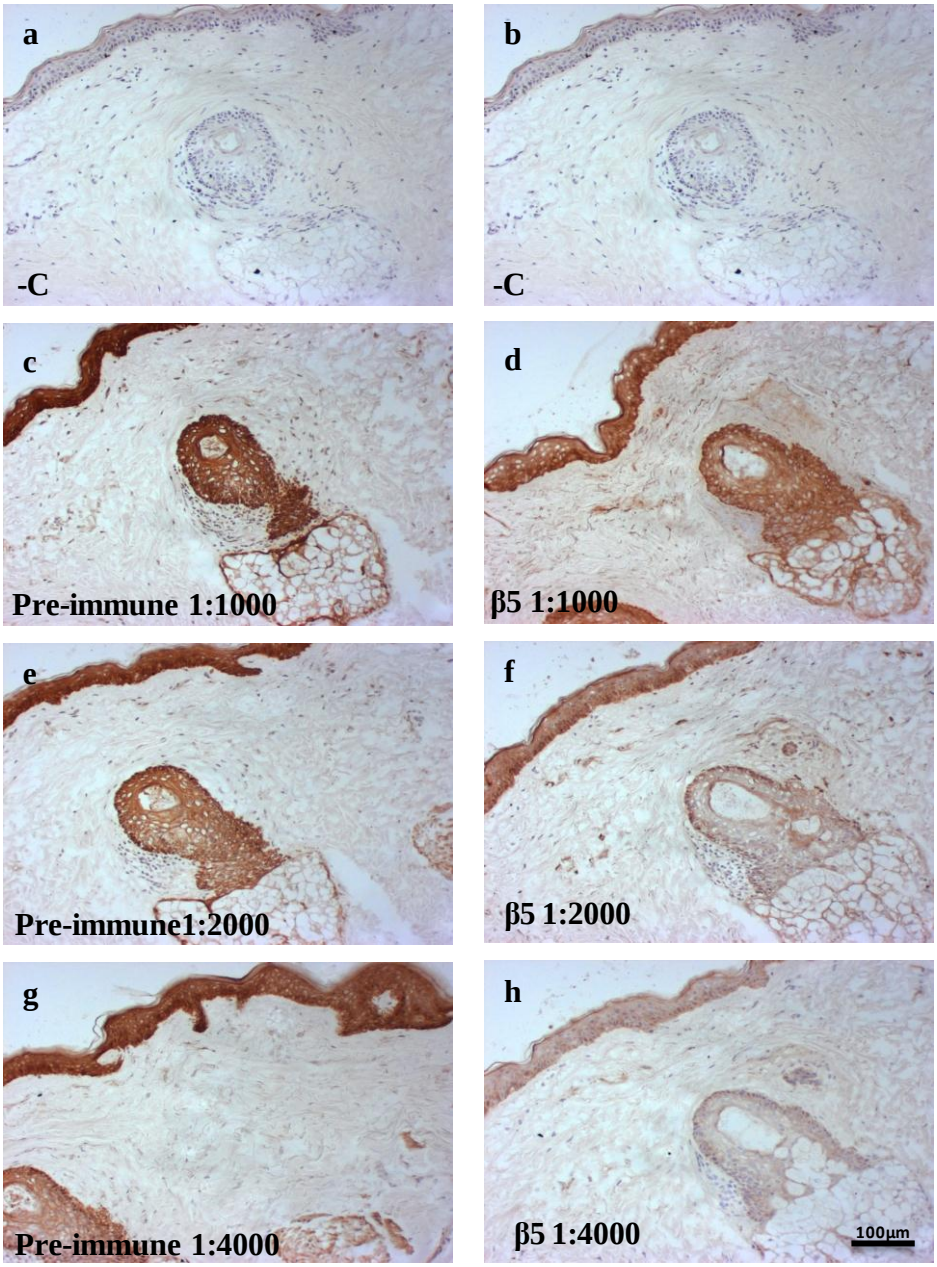

Figure 4.15: Immunostaining of thyrostimulin in human skin treated with β5 antibody compared to the pre-immune serum. Negative controls (panel a and b) are sections incubated with no primary antibody. Skin sections treated with β5 antibody (panels d, f and h), and human skin sections treated with pre-immune serum (panels c, e and g) (as negative control). β5 antibody and pre-immune serum used in a range of dilutions (1:1000, 1:2000, 1:4000). The two sets of sections were run in parallel to each other at the same time under the same conditions. Scale bar x10= 100µm.

Shown in figures 4.15, are images of immunostaining of thyrostimulin in serial sections of human skin treated with β5 antibody and human skin sections treated with pre-immune serum (as negative control) during the process of optimization of β5 polyclonal thyrostimulin antibody using a range of dilutions (1:1000,1:2000,1:4000). For comparison, the two sets of sections were analysed in the same time using the same dilutions and under the same conditions. Negative controls are section incubated with no primary antibody (diluent used instead) and reveal no staining. Unexpectedly, the pre-immune skin sections, in the tested dilutions, show strong nonspecific staining. Furthermore, the skin sections treated with β5 antibody under the same conditions show positive non-specific inconclusive staining. Therefore, an extra blocking method was added.

4.3.2.6 Blocking with β5 immunizing peptide

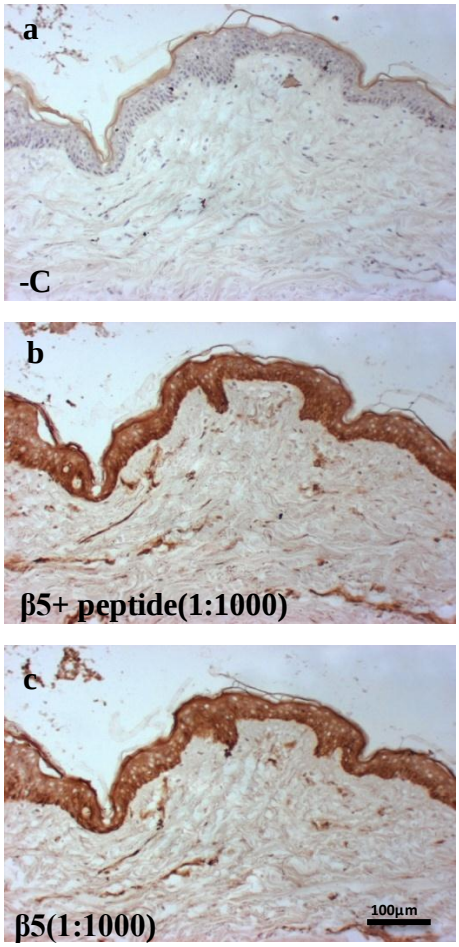

Figure 4.16: β5 antibody characterisation using the neutralization peptide technique. Skin section treated with no primary antibody (panel a) (as negative control), β5+ peptide (panel b) (as additional negative control), β5 antibody (panel c). The sections were prepared at the same time under the same conditions with the same dilution (1:1000). Scale bar x10= 100µm.

The pattern of immunostaining obtained with β5 polyclonal thyrostimulin antibody, on serial sections of human skin during the process of characterisation using peptide neutralization is shown in **figure 4.16**. Three skin sections were used: the first skin section incubated with no primary antibody used as a negative control and reveals no staining. The second skin section incubated with β5 plus the peptide (as an additional negative control) and the third skin section treated with β5 antibody. The sections were prepared at the same time under the same

conditions with the same dilution (1:1000). The last two sections show positive strong nonspecific immunoreactivity. **Table 4.15** summarizes the optimization conditions for β5 Thyrostimulin antibody.

Table 4.15 Summary of optimization conditions of β5 thyrostimulin antibody.

β5 primary ab	Secondary ab	Tissue	Blocking	Tertiary (Method)	Comment
Streptavidin method, optimising the primary antibody					
1:200, 1:500, 1:1000 O/N	Anti guinea pig biotinylated 1:400	Normal skin	Endogenous peroxidase for 10 minutes, 5% goat serum in PBS-T	Streptavidin 1:200	No signal obtained More sensitive method required More stringent blocking
ABC method with higher concentration of primary and secondary					
1:50 O/N	Anti guinea pig biotinylated 1:200	Normal skin	Endogenous peroxidase for 10 minutes, 5% goat serum in BSA/Marvel in PBS-T	ABC	Too strong signal
ABC method, optimisation of secondary antibody					
none	Anti guinea pig biotinylated 1:200, 1:400, 1:800 O/N	Normal skin	Endogenous peroxidase for 10 minutes, 5% goat serum in BSA/Marvel in PBS-T	ABC	1:400 seems to be the optimal dilution for secondary antibody
ABC method, optimising the primary antibody					
1:500, 1:750, 1:1000 O/N	Anti guinea pig biotinylated 1:400	Normal skin	Endogenous peroxidase blocked 10 minutes, 5% Goat serum in BSA/Marvel in PBS-T	ABC	Strong background
β5 pre-immune serum control					
1:1000, 1:2000 1:4000 O/N	Anti guinea pig biotinylated 1:400	Normal skin	Endogenous peroxidase blocked 10 minutes, 5% Goat serum in BSA/Marvel in PBS-T	ABC	Pre immune show stronger signal than β5 antibody
Blocking with β5 immunizing peptide					
1:1000 O/N	Anti guinea pig biotinylated 1:400	Normal skin	Endogenous peroxidase blocked10 minutes, 5% Goat serum in BSA/Marvel in PBS-T	ABC	Positive strong nonspecific immunoreactivity.

4.3 Discussion

In this study α2 and β5 thyrostimulin polyclonal antibodies were characterised. The β5 polyclonal antibody detected the β5 thyrostimulin subunit in the HCA2 fibroblast cell line transfected with β5 expression vector at the expected molecular weight. However, α2 thyrostimulin polyclonal antibody failed to recognize the α2 subunit in the same cell line transfected with α2 expression vector under the same conditions. Therefore, for the purpose of the study the analysis only focuses on the β5 thyrostimulin subunit. The western blotting result for β5 thyrostimulin antibody shows a positive band at the expected molecular weight and the fact that there was no band detected in the cell lysate of untransfected cells is another important result as it confirms that the detected band can only be due to the expression of protein derived by β5 expression vector therefore it to indicates specificity of this result.

Using the GFP expression vector suggests that plasmid has gone into the cells. However, that does not necessarily mean the transfection was successful and it is no guarantee that α2 and β5 proteins will be expressed. For β5, it seems that there is enough protein in the transfected cells and the β5 antibody was able to bind to it. To confirm if the α2 was transfected or not, it would be ideal to detect the transcript by RT-PCR, but this was not possible since this was a transient transfection and that would be contaminated with the expression vector.

The inability of the α2 thyrostimulin antibody to detect the α2 subunit protein in cell lysates or conditioned medium of the α2 transfected cells may be due to the fact that the antibody was used at a dilution of 1:500 or 1:2000; this may be too dilute, since the manufacturer's dot blot obtained a signal using concentrations of 1:100 and 1:400. Hence, a higher concentration of antibody could have been tried.

The western blotting analysis using β5 thyrostimulin antibody showed a smear like band in the conditioned medium of the cells transfected with β5 expression vector; this suggests that the detected band could be the glycosylated heterodimer of α2 and β5 thyrostimulin. To confirm that we could have tried α2 thyrostimulin antibody at a lower dilution, to see if it can detect any protein. Another experiment we could have used is to treat the sample with a de-glycosylation enzyme (for example; N-glycosidase F[144]) and run it alongside the glycosylated protein and compare the results.

The other possible explanation is that the β5 antibody could be detecting lots of β5 subunits binding together, and the reducing agent in the sample buffer was not enough. This possibility could be investigated further by adding more reducing agent or by trying a different reducing agent such as β-mercaptoethanol.

The investigations were not able to detect the β5 subunit protein in conditioned medium of the transfected cells for the following possible reasons; the β5 subunit protein was below the detection level even by using the silver stain as a sensitive method for detection of low level proteins. The other possible reason is that during the preparations for the culture medium the fetal calf serum was taken out from the cells and was replaced with DMEM medium instead which lacks the nutrients and we could have starved the cells to the level that they were unable to synthesis the protein. However, this possibility seems unlikely since that will take longer than 24 hours to starve the cells.

Because of the technical challenges and the lack of good positive control our investigations focused only on β5 thyrostimulin antibody. Because of the constraint of time we were not able to explore these possibilities since we already have positive results for β5 cell lysate.

Following the positive western blotting result with β5 antibody, the immunohistological analysis was conducted to investigate the expression of thyrostimulin β5 subunit at the level in human skin using this β5 thyrostimulin polyclonal antibody. During this process, I faced several technical challenges to achieve clear visible specific staining. Therefore, multiple blocking methods were carried out. None of the methods and techniques applied show positive clear immunoreactivity of β5 antibody in skin sections and we were unable to show any positive results in the skin.

Because, the thyrostimulin α2 subunit is expressed in human pituitary[144], tissue extract from human pituitary could be used as a positive control to test if the α2 antibody is functional. If it worked, the α2 antibody could be used for immunohistochemistry using human pituitary. Because of the technical challenges and the lack of good positive controls it was not possible to continue any further in investigating the α2 thyrostimulin antibody.

The unexpected positive signal stronger than the β5 antibody obtained with the pre immune serum could be explained by the fact that the pre immune serum was provided in small volume and probably evaporated over a period of time and just concentrated any antibodies that were there prior to immunisation with the β 5 peptide. The large number of antibodies in the pre immune serum would potentially mask any β5 immunoreactivity.

The results indicate that β5 antibody is clearly a good antibody. However, it cannot be used in its current form for immunohistochemistry and needs to be cleaned. If we had enough time we could have affinity purified the β5 antibody. In its un-purified form the β5 antibody could be used for cell culture expression studies by western blotting.

Chapter Five

General discussion

5. Chapter five

5.1 General discussion

The main aims of this work were to investigate the presence of functional TSHR in the skin and to investigate the expression of α2 and β5 subunits of thyrostimulin in the skin as a potential alternative ligand responsible for TSHR activation.

The full length TSHR transcript was demonstrated by reverse transcription-PCR techniques in human skin and mouse skin but not in cultured cells including HaCaT, HCA2 fibroblast, 3T3L1 pre-adipocyte and 3T3 cell lines. Although the TSHR transcript was expressed in human skin, the immunohistochemistry results failed to demonstrate the TSHR protein in the epidermis. The opposite was true for the TSHR expression in fibroblast. The RT-PCR of cultured fibroblasts did not show the TSHR transcript however, the immunohistochemistry showed TSHR protein expression in cells that are most probably fibroblasts. The reason for the diverse results could be explained by the following reasons; the culture fibroblasts are at an unnaturally high density and, in a monolayer culture instead of being in a 3D matrix of extracellular proteins so might show different expression patterns. Alternatively, the skin samples used in these IHC experiments were obtained from the Dermatology Department, they may be skin adjacent to a lesion and therefore might not entirely normal.

The immunohistochemical data presented in this thesis demonstrated TSHR positive fibroblast-like immunostaining most probably of TSHR expressing dermal fibroblasts and a similar staining is observed in the dermal tissue surrounding the sebaceous gland and hair follicle. These results are in agreement with previous reports which demonstrated TSHR expression in dermal fibroblast[132], cultured fibroblast[53] and from patient with pretibial

myxedema[61]. According to the immunohistochemistry results presented here , it is intriguing to ask whether the TSHR expression is present in the normal resident skin cells (keratinocytes, sweat gland, hair follicle or the dermal cells) or is the TSHR expressed in some other cells that is brought in to the skin in response to injury, inflammation or, autoimmune reaction. Douglas et al, 2010, revealed that the TSHR is expressed in the $CD34^+$ fibrocytes which are wandering stem cells and they showed evidence of the presence of these cells in cultured peripheral blood mononuclear cells (PBMC) in patient with Graves's disease. Furthermore, they demonstrated that these cells express TSHR at a level similar to the levels found on thyroid epithelium. They showed evidence of $CD34^+$ TSHR+ fibrocytes infiltrating orbital tissues in situ[184]. These findings may suggest the potential link of CD34+ TSHR+ fibrocyte infiltration and their potential participation in the pathogenesis of the Graves' disease[184]. In addition, our results and others may provide evidence to support the suggestion that the dermal fibroblasts may present the autoantigen against which TSHR autoantibodies are generated[53,61,126,133,185,43,132,184,186].

The chapter three results demonstrated positive immunostaining of the TSHR expressing fibroblast with A9 antibody. However, there was much less clear cut immunostaining with A7 antibody. It is of interest to mention that both Rapoport et al, 2000[61] and Cianfarani et al, 2010[132] have used A9 antibody which recognises the 147-228 residues of TSHR ECD to show the TSHR expression in dermal fibroblast, In addition, Bell et al, 2000[187] used "anti-TSHR (352-366) antibody" which recognises the ECD of the TSHR. Collectively, that could suggest that the TSHRV only is expressed in these fibroblast like cells rather than the full length TSHR, these results are further supported by a study by Paschke R and colleagues in 1994 who reported that the TSHR variant transcript is expressed in skin fibroblast[141]. In this context, it is important to mention that the A7 antibody is able to detect the epitope very close

to the membrane spanning region and it might be difficult for antibodies to have access to an epitope which is within the membrane spanning region as it really could be on the inside of the cell. Although it should be noted that the A7 epitope is predicted to be just outside the cell in the part of the membrane spanning region which forms the disulphide bonds with the extracellular domain of the TSHR, which in turn could prevent the antibody binding by a process known as steric hindrance.

In addition, positive TSHR immunostaining was demonstrated in periglandular myoepithelial cells of sweat glands in human skin. This is in agreement with the report from Bodo et al, 2009, who showed TSHR expression in the myoepithelial sweat gland[133]. It is well known that patients with hyperthyroid status, whether due to TSHR binding to its natural ligand, TSH, or because of pathological autoimmune antibodies in Graves' disease, experience excessive sweating (hyperhydrosis). There is no specific treatment for excessive sweating in Graves' disease. This raises the question, is the excessive sweating due to increase in the overall metabolic rate or is it due to TSHR signalling (activation) in the skin which might explain the hyperhydrosis in autoimmune Graves' disease. It is obvious that skin involvement in thyroid disease is very site specific and there are still many questions to be answered: Is there aberrant TSHR expression in all skin sites or is there something special about certain skin sites, which may explain why only particular areas are involved in Graves' disease. Is there an elevated level of TSHR in these sites and, if so what triggers the increase in expression. It would be interesting to investigate and compare the skin from different sites in the body for the expression of TSHR.

The RT-PCR data in chapter two showed highest levels of TSHR gene expression associated with early anagen, reducing to low levels in late anagen when the hair follicles have achieved

their full length and reducing still further in telogen when adipogenesis is quiescent. These results are in agreement with several other studies where TSHR transcript and protein are shown to be expressed in scalp hair follicle and hair follicle mesenchymal compartment[131,133,165,188].

The TSHR variant was only demonstrated in mouse skin and at different stages of the hair cycle but not in human skin or cultured cells (chapter two). This suggests that the TSHRV transcript expression could be involved in the hair cycle as the human skin samples used (non scalp skin) had few or no hair follicles compared with the dense pelage of mouse skin.

Although TSHR expression was not observed in undifferentiated 3T3L1, RT-PCR of cells during adipogenesis showed TSHR transcript on day 7 when adipogenesis is clearly apparent in these cells. The TSHRV expression occurs earlier at day 3 and persists until day 10, longer than TSHR. Previous studies have also shown an increase in TSHR during 3T3L1 cell differentiation[155,189,190]. This may offer a potential alternative explanation for elevated TSHR in the mouse anagen stage; that it may be associated with adipogenesis. Other reports which support this interpretation include elevated TSHR expression in 3T3L1 differentiation, rat preadipocytes and orbital fibroblasts undergoing adipogenesis [189,191,192,193].

With the generally elevated levels of TSHR and of TSHRV seen during 3T3L1 differentiation there is clearly a need to investigate whether the relative levels of these two isoforms significantly controls the level of signalling through the TSHR. The synchronised hair cycle in mouse could explain why the levels of TSHRV are higher in mouse than human since the adipose tissue will need to be more dynamic.

These experiments have shown that TSHR expression is increased (transcript and protein levels) during lineage specific differentiation (adipogenesis), one would ask does this mean that TSH is important for helping cells going through differentiation decide which kind of differentiation route they want to follow or is it just an artefact of the fact that they are about to go through differentiation, because many other kinds of receptors are upregulated as well. Studies have suggested that TSHR is functional during adipogenesis[80,155,187], but being functional in biochemical sense does not mean functional in biological sense for controlling cell differentiation. The presence of functional TSHR in preadipocytes raises the possibility of a novel role for TSHR signalling in cell differentiation but further analysis is required to investigate whether TSHR is functional in differentiating cells or not.

Generally, patients with hyperthyroidism have TSHR activation and high levels of thyroid hormones, whereas, hypothyroid patients have TSHR activation and low levels of thyroid hormone levels. These two factors may contribute to the differences in the skin changes in each case. The TSHR expression shown here together with the findings of other studies[53,132,133], suggest that the circulating TSHR auto-antibodies may participate together with the abnormal levels of thyroid hormones towards the skin and hair changes associated with Graves' disease and this might suggest that some forms of this disease may be due to a direct autoimmune response towards cutaneous TSHR and increased signalling through the TSHR has to be considered as an intriguing possibility. TSHR expression in the hair follicle could be a direct target of the autoantibody and could explain the alopecia areata in patients with Graves's disease[133]. The pretibial myxedema in Graves' hyperthyroidism and a more generalised myxedema in Hashimoto's hypo-thyroidism[62,65,81], could also be partly due to direct effect of the autoimmune antibodies towards the TSHR in the dermal fibroblast and preadipocytes[61]. Pretibial myxedema is a relatively rare event and only occurs in some

patients with thyroid disease. Considering the elevation of TSHR in 3T3L1 differentiation, certain conditions such as wound healing may be required to elevate TSHR to critical levels in dermal fibroblasts to cause autoimmune driven disease. Furthermore, TSHR signalling could also explain some of the other skin symptoms associated with thyroid disorders for instance, the epidermal melanocyte could explain the pigmentation in Graves' disease as an intercellular mediator, and it might also explain vitiligo as TSHR could turn melanocyte to a target for the autoimmune antibodies[53].

Studies demonstrated thyrostimulin expression in skin and, in vivo and in vitro data showed that this new hormone is capable of forming a dimer and may compete with TSH for TSHR[144,153]. The higher affinity of thyrostimulin to TSHR[144] suggests the potential role for thyrostimulin as an alternative ligand rather than TSH in the normal functioning of TSHR signalling in the skin. In this study, the α2 & β5 thyrostimulin subunits transcripts were readily expressed in human and α2 subunit in mouse skin, cultured HaCaT, HCA2 fibroblast cell lines and in some mouse tissues.

Since the data in chapter two confirms the expression of thyrostimulin in α2 subunit mouse skin, it would be interesting to study whether the thyrostimulin is expressed during the mouse hair cycle and to investigate if the level of expression varies in relation to 3T3L1 differentiation which would support the suggestion of thyrostimulin might be the alternative ligand of TSHR signalling and illustrates the need for good thyrostimulin antibody. The β5 antibody we produced is able to detect exogenous β5 in transfected fibroblasts and may be able to bind the endogenous subunit (if present). The RT-PCR data shown in chapter two confirms the expression of α2 thyrostimulin transcript in the skin. This underlines the need for α2 antibody to investigate the site of α2 expression in the skin.

The current modalities for treatment of Graves' disease are anti-thyroid medications, radioactive iodine, or surgery, each treatment has shown to be effective and well tolerated by the patients[194]. However, there is a significant rate of relapse especially with anti-thyroid medications and radioactive iodine[195]. Recently, Neumann et al, 2011 suggested a small molecule antagonist which inhibits Graves' disease antibody activation of the TSH Receptor[171,196]. If these antagonists were administered to those patients with hyper active autoimmune thyroid, the autoantibody would no longer bind to TSHR either in thyroid or in the extra thyroidal locations, such as orbital and dermal fibroblasts, sweat gland and hair follicle. It would not only make the patients euthyroid but would also improve the clinical outcome of the other extrathyroidal symptoms which are sometimes difficult to treat and may also improve the quality of life of those patients.

5.2 Recommendation and future work

There are two important issues that need to be investigated in more detail. Firstly, the full length TSHR and the TSHR variant have completely opposite roles and the balance between these two isoforms is very important. When TSH, stimulating antibodies or thyrostimulin bind to the signalling competent full length TSHR receptor this will have an effect on the cell. However, when TSH, stimulating antibodies or the thyrostimulin bind the TSHR variant, as the TSHR variant is not attached to the cell there will be no signal and therefore its activation will have no effect on the cell. Thus, the balance between the two could be very important for how much TSHR activation happens even in the cell type where there is a lot of full length receptor such as the thyroid gland itself, and to our knowledge this area has not been explored before. It would be interesting to investigate and compare balance between these two isoform and probably the way to do that is to use the q-PCR method for full length TSHR and TSHR variant expression in well characterized cells like thyroid follicular cells or the 3T3L1 as a starting point.

Secondly, the results in this work suggested that the TSHR and the TSHRV are expressed in mouse hair cycle and it would be interesting to investigate the gene expression of these two isoforms in more depth. Probably by studying the gene expression in different stages of hair cycle in TSHR knockout mouse and the hair cycle in mice model with mutated TSHR known as (hyt/hyt) mouse.

References

1 Wolf, k. *et al. Fitzpatrick's Dermatology in General Medicine*. seventh edn, Vol. 1 57-67 (McGraw-Hill, 2008).

2 Eckert, R. L. Structure, function, and differentiation of the keratinocyte. *Physiol Rev* **69**, 1316-1346 (1989).

3 Burns, T., Breathnach, S., Cox, N. & Griffiths, C. *Rook's Textbook of Dermatology*. 8th edn, Vol. 4 66.3-66.15 (Blackwell Publishing Ltd, 2010).

4 Candi, E., Schmidt, R. & Melino, G. The cornified envelope: a model of cell death in the skin. *Nat Rev Mol Cell Biol* **6**, 328-340,(2005).

5 Champion, R., Burton, J. & Breathnach, S. M. *Textbook of Dermatology* sixth ed edn, (Blackwell Science Ltd 1998).

6 Holthofer, B., Windoffer, R., Troyanovsky, S. & Leube, R. E. Structure and function of desmosomes. *Int Rev Cytol* **264**, 65-163,(2007).

7 Green, K. J. & Simpson, C. L. Desmosomes: new perspectives on a classic. *J Invest Dermatol* **127**, 2499-2515,(2007).

8 Mehrel, T. *et al.* Identification of a major keratinocyte cell envelope protein, loricrin. *Cell* **61**, 1103-1112 (1990).

9 Landmann, L. Epidermal permeability barrier: transformation of lamellar granule-disks into intercellular sheets by a membrane-fusion process, a freeze-fracture study. *J Invest Dermatol* **87**, 202-209 (1986).

10 Freinkel, R. K. & Traczyk, T. N. Lipid composition and acid hydrolase content of lamellar granules of fetal rat epidermis. *J Invest Dermatol* **85**, 295-298 (1985).

11 Downing, D. T. *et al.* Skin lipids: an update. *J Invest Dermatol* **88**, 2s-6s (1987).

12 Proksch, E., Brandner, J. M. & Jensen, J. M. The skin: an indispensable barrier. *Exp Dermatol* **17**, 1063-1072 (2008).

13 Fine, J. D. Structure and antigenicity of the skin basement membrane zone. *J Cutan Pathol* **18**, 401-409 (1991).

14 Christiano, A. M. & Uitto, J. Molecular complexity of the cutaneous basement membrane zone. *Experimental Dermatology* **5**, 1-11 (1996).

15 Reilkoff, R. A., Bucala, R. & Herzog, E. L. Fibrocytes: emerging effector cells in chronic inflammation. *Nat Rev Immunol* **11**, 427-435 (2011).

16 Downie, M. M., Guy, R. & Kealey, T. Advances in sebaceous gland research: potential new approaches to acne management. *Int J Cosmet Sci* **26**, 291-311,(2004).

17 Sato, K., Kang, W. H., Saga, K. & Sato, K. T. Biology of sweat glands and their disorders. II. Disorders of sweat gland function. *J Am Acad Dermatol* **20**, 713-726 (1989).

18 Saga, K. Structure and function of human sweat glands studied with histochemistry and cytochemistry. *Prog Histochem Cytochem* **37**, 323-386 (2002).

19 Schmidt-Ullrich, R. & Paus, R. Molecular principles of hair follicle induction and morphogenesis. *Bioessays* **27**, 247-261 (2005).

20 Fuchs, E. Scratching the surface of skin development. *Nature* **445**, 834-842 (2007).

21 Fuchs, E. Skin stem cells: rising to the surface. *J Cell Biol* **180**, 273-284 (2008).

22 Fuchs, E. & Horsley, V. More than one way to skin. *Genes Dev* **22**, 976-985 (2008).

23 Costarelis G & VA, B. *Biology of Hair Follicles*. (2008).

24 Schneider, M. R., Schmidt-Ullrich, R. & Paus, R. The hair follicle as a dynamic miniorgan. *Curr Biol* **19**, R132-142,(2009).

25 Ito, M. Biologic roles of the innermost cell layer of the outer root sheath in human anagen hair follicle: further electron microscopic study. *Arch Dermatol Res* **281**, 254-259 (1989).

26 Zaias. *The nail in health and disease* 2nd edn, (CT Appleton & Lange, 1990).
27 Cohen, P. R. The lunula. *J Am Acad Dermatol* **34**, 943-953; quiz 954-946 (1996).
28 De Berker, D. *et al.* Keratin expression in the normal nail unit: markers of regional differentiation. *Br J Dermatol* **142**, 89-96 (2000).
29 Muller-Rover, S. *et al.* A comprehensive guide for the accurate classification of murine hair follicles in distinct hair cycle stages. *J Invest Dermatol* **117**, 3-15, (2001).
30 Sanders, D. A., Philpott, M. P., Nicolle, F. V. & Kealey, T. The isolation and maintenance of the human pilosebaceous unit. *Br J Dermatol* **131**, 166-176 (1994).
31 Porter, R. M. Mouse models for human hair loss disorders. *J Anat* **202**, 125-131 (2003).
32 Price, V. H. Treatment of hair loss. *N Engl J Med* **341**, 964-973,(1999).
33 Mounsey, A. L. & Reed, S. W. Diagnosing and treating hair loss. *Am Fam Physician* **80**, 356-362 (2009).
34 McDonagh, A. J. & Messenger, A. G. The pathogenesis of alopecia areata. *Dermatol Clin* **14**, 661-670 (1996).
35 Gilhar, A., Paus, R. & Kalish, R. Lymphoctes Neuropeptides, and Genes involved in Alopecia Areata. *J Clin Invest* **111**, 2019 (2007).
36 Harrison, S. & Sinclair, R. Telogen effluvium. *Clin Exp Dermatol* **27**, 389-385 (2002).
37 Hoyes, A. D. & Kershaw, D. R. Anatomy and development of the thyroid gland. *Ear Nose Throat J* **64**, 318-333 (1985).
38 Stone, J. A. & Figueroa, R. E. Embryology and anatomy of the neck. *Neuroimaging Clin N Am* **10**, 55-73, viii (2000).
39 CC, C. *Thyroid anatomy*. 8th ed edn, (Lippincott Williams &Wilkins, 2000).
40 Lang, D., Powell, S. K., Plummer, R. S., Young, K. P. & Ruggeri, B. A. PAX genes: roles in development, pathophysiology, and cancer. *Biochem Pharmacol* **73**, 1-14, (2007).
41 Guazzi, S. *et al.* Thyroid nuclear factor 1 (TTF-1) contains a homeodomain and displays a novel DNA binding specificity. *EMBO J* **9**, 3631-3639 (1990).
42 Civitareale, D., Lonigro, R., Sinclair, A. J. & Di Lauro, R. A thyroid-specific nuclear protein essential for tissue-specific expression of the thyroglobulin promoter. *EMBO J* **8**, 2537-2542 (1989).
43 Braverman, L., E & Utiger, R., D. *Werner & Ingbar's the Thyroid; A Fundamental and Clinical Text*. 9th edn, (LIPPINCOTT WILLIAM & WILKINS, 2005).
44 Carrasco, N. Iodide transport in the thyroid gland. *Biochim Biophys Acta* **1154**, 65-82, (1993).
45 Davies, T., Marians, R. & Latif, R. The TSH receptor reveals itself. *J Clin Invest* **110**, 161-164,(2002).
46 Lechan RM & AN, H. *Thyrotropin releasing hormone (TRH)*. 510 (Elsevier Science, 2003).
47 Park, S. M. & Chatterjee, V. K. Genetics of congenital hypothyroidism. *J Med Genet* **42**, 379-389, (2005).
48 Larsen, P. R. The pituitary-thyroid regulatory system. *Adv Exp Med Biol* **261**, 11-26 (1989).
49 Braverman & Utiger, R. D. *Werner & Ingbar's the thyroid: a fundemantal and clinical text*. 9th edn, (Lippincott Williams &Wilkins, 2005).
50 Burman, K. D. & McKinley-Grant, L. Dermatologic aspects of thyroid disease. *Clin Dermatol* **24**, 247-255,(2006).
51 Jabbour, S. A. Cutaneous manifestations of endocrine disorders: a guide for dermatologists. *Am J Clin Dermatol* **4**, 315-331 (2003).

52 Thiboutot, D. M. Clinical review 74: Dermatological manifestations of endocrine disorders. *J Clin Endocrinol Metab* **80**, 3082-3087 (1995).
53 Slominski, A. *et al.* Expression of hypothalamic-pituitary-thyroid axis related genes in the human skin. *J Invest Dermatol* **119**, 1449-1455 (2002).
54 Paschke, R., Van Sande, J., Parma, J. & Vassart, G. The TSH receptor and thyroid diseases. *Baillieres Clin Endocrinol Metab* **10**, 9-27 (1996).
55 Paschke, R. & Ludgate, M. The thyrotropin receptor in thyroid diseases. *N Engl J Med* **337**, 1675-1681 (1997).
56 Heymann, W. R. Cutaneous manifestations of thyroid disease. *J Am Acad Dermatol* **26**, 885-902 (1992).
57 Mullin, G. E. & Eastern, J. S. Cutaneous consequences of accelerated thyroid function. *Cutis* **37**, 109-114 (1986).
58 Niepomniszcze, H. & Amad, R. H. Skin disorders and thyroid diseases. *J Endocrinol Invest* **24**, 628-638 (2001).
59 Kohar, Y. M. & Tan, K. C. Preradial myxedema: a case report. *Ann Acad Med Singapore* **25**, 281-282 (1996).
60 Wortsman, J., Dietrich, J., Traycoff, R. B. & Stone, S. Preradial myxedema in thyroid disease. *Arch Dermatol* **117**, 635-638 (1981).
61 Rapoport, B., Alsabeh, R., Aftergood, D. & McLachlan, S. M. Elephantiasic pretibial myxedema: insight into and a hypothesis regarding the pathogenesis of the extrathyroidal manifestations of Graves' disease. *Thyroid* **10**, 685-692,(2000).
62 Fatourechi, V., Pajouhi, M. & Fransway, A. F. Dermopathy of Graves disease (pretibial myxedema). Review of 150 cases. *Medicine (Baltimore)* **73**, 1-7 (1994).
63 Safer, J. D. Thyroid hormone action on skin. *Dermatoendocrinol* **3**, 211-215,(2011).
64 Schwartz, K. M., Fatourechi, V., Ahmed, D. D. & Pond, G. R. Dermopathy of Graves' disease (pretibial myxedema): long-term outcome. *J Clin Endocrinol Metab* **87**, 438-446 (2002).
65 Kriss, J. P. Pathogenesis and treatment of pretibial myxedema. *Endocrinol Metab Clin North Am* **16**, 409-415 (1987).
66 Kriss, J. P., Pleshakov, V., Rosenblum, A. & Sharp, G. Therapy with occlusive dressings of pretibial myxedema with fluocinolone acetonide. *J Clin Endocrinol Metab* **27**, 595-604 (1967).
67 Koshiyama, H., Mori, S., Fujiwara, K., Hayakawa, K. & Koh, T. Successful treatment of hypothyroid Graves' disease with a combination of levothyroxine replacement, intravenous high-dose steroid and irradiation to the orbit. *Intern Med* **32**, 421-423 (1993).
68 Holt, P. J. & Marks, R. The epidermal response to change in thyroid status. *J Invest Dermatol* **68**, 299-301 (1977).
69 Safer, J. D., Fraser, L. M., Ray, S. & Holick, M. F. Topical triiodothyronine stimulates epidermal proliferation, dermal thickening, and hair growth in mice and rats. *Thyroid* **11**, 717-724 (2001).
70 Holt, P. J. In vitro responses of the epidermis to triiodothyronine. *J Invest Dermatol* **71**, 202-204 (1978).
71 Safer, J. D. *et al.* Thyroid hormone action on skin: diverging effects of topical versus intraperitoneal administration. *Thyroid* **13**, 159-165,(2003).
72 Isseroff, R. R., Chun, K. T. & Rosenberg, R. M. Triiodothyronine alters the cornification of cultured human keratinocytes. *Br J Dermatol* **120**, 503-510 (1989).
73 Rosenberg, R. M., Isseroff, R. R., Ziboh, V. A. & Huntley, A. C. Abnormal lipogenesis in thyroid hormone-deficient epidermis. *J Invest Dermatol* **86**, 244-248 (1986).

74 Hanley, K., Jiang, Y., Katagiri, C., Feingold, K. R. & Williams, M. L. Epidermal steroid sulfatase and cholesterol sulfotransferase are regulated during late gestation in the fetal rat. *J Invest Dermatol* **108**, 871-875 (1997a).
75 Ohtsuki, M., Tomic-Canic, M., Freedberg, I. M. & Blumenberg, M. Regulation of epidermal keratin expression by retinoic acid and thyroid hormone. *J Dermatol* **19**, 774-780 (1992).
76 Ramot Y, P. R., Tiede S, Zlotogorski A. Endocrine controls of keratin expression. *Bioessays*, 31(34):389-399,(2009).
77 Safer, J. D., Crawford, T. M. & Holick, M. F. A role for thyroid hormone in wound healing through keratin gene expression. *Endocrinology* **145**, 2357-2361 (2004).
78 Tomic, M. *et al.* Nuclear receptors for retinoic acid and thyroid hormone regulate transcription of keratin genes. *Cell Regul* **1**, 965-973 (1990).
79 Parving, H. H. *et al.* Mechanisms of edema formation in myxedema--increased protein extravasation and relatively slow lymphatic drainage. *N Engl J Med* **301**, 460-465, (1979).
80 Zhang, L. *et al.* Thyrotropin receptor activation increases hyaluronan production in preadipocyte fibroblasts: contributory role in hyaluronan accumulation in thyroid dysfunction. *J Biol Chem* **284**, 26447-26455 (2009).
81 Smith, T. J., Bahn, R. S. & Gorman, C. A. Connective tissue, glycosaminoglycans, and diseases of the thyroid. *Endocr Rev* **10**, 366-391 (1989).
82 Ahsan, M. K., Urano, Y., Kato, S., Oura, H. & Arase, S. Immunohistochemical localization of thyroid hormone nuclear receptors in human hair follicles and in vitro effect of L-triiodothyronine on cultured cells of hair follicles and skin. *J Med Invest* **44**, 179-184 (1998).
83 Smith, T. J., Murata, Y., Horwitz, A. L., Philipson, L. & Refetoff, S. Regulation of glycosaminoglycan synthesis by thyroid hormone in vitro. *J Clin Invest* **70**, 1066-1073 (1982).
84 Murata, Y., Ceccarelli, P., Refetoff, S., Horwitz, A. L. & Matsui, N. Thyroid hormone inhibits fibronectin synthesis by cultured human skin fibroblasts. *J Clin Endocrinol Metab* **64**, 334-339 (1987).
85 Faergemann, J. *et al.* Dose-response effects of tri-iodothyroacetic acid (Triac) and other thyroid hormone analogues on glucocorticoid-induced skin atrophy in the haired mouse. *Acta Derm Venereol* **82**, 179-183 (2002).
86 Safer, J. D., Crawford, T. M. & Holick, M. F. Topical thyroid hormone accelerates wound healing in mice. *Endocrinology* **146**, 4425-4430,(2005).
87 Lindenbaum, E. S. *et al.* Stimulated healing of recalcitrant wounds by topical application of enriched cell culture medium: a clinical report. *Plast Reconstr Surg* **108**, 104-113 (2001).
88 Hale, P. A. & Ebling, F. J. The effect of a single epilation on successive hair eruptions in normal and hormone-treated rats. *J Exp Zool* **207**, 49-71,(1979).
89 Schell, H., Kiesewetter, F., Seidel, C. & von Hintzenstern, J. Cell cycle kinetics of human anagen scalp hair bulbs in thyroid disorders determined by DNA flow cytometry. *Dermatologica* **182**, 23-26 (1991).
90 Lindenbaum, E. S. *et al.* Pilot study of a novel treatment for androgenetic alopecia using enriched cell culture medium: clinical trials. *Dermatol Online J* **9**, 4 (2003).
91 Mullin, G. E. & Eastern, J. S. Cutaneous signs of thyroid disease. *Am Fam Physician* **34**, 93-98 (1986).
92 Kasumagic-Halilovic, E. Thyroid autoimmunity in patients with alopecia areata. *Acta Dermatovenerol Croat* **16**, 123-125 (2008).

93 Means, M. A. & Dobson, R. L. Cytological changes in the sweat gland in hypothyroidism. *JAMA* **186**, 113-115 (1963).
94 Robertshaw, D. Hyperhidrosis and the sympatho-adrenal system. *Med Hypotheses* **5**, 317-322 (1979).
95 Gitter, D. G. & Sato, K. Localized hyperhidrosis in pretibial myxedema. *J Am Acad Dermatol* **23**, 250-254 (1990).
96 Pierce, J. G. & Parsons, T. F. Glycoprotein hormones: structure and function. *Annu Rev Biochem* **50**, 465-495,(1981).
97 Larsen, K., Melmed, S. & Polonsky, K. *Tyhroid. In: Williams Textbook of Endocrinology*. 10th edn, 331-490 (Saunders, 2003).
98 Lapthorn, A. J. *et al.* Crystal structure of human chorionic gonadotropin. *Nature* **369**, 455-461, (1994).
99 Grossmann, M., Weintraub, B. D. & Szkudlinski, M. W. Novel insights into the molecular mechanisms of human thyrotropin action: structural, physiological, and therapeutic implications for the glycoprotein hormone family. *Endocr Rev* **18**, 476-501 (1997).
100 Szkudlinski, M. W., Fremont, V., Ronin, C. & Weintraub, B. D. Thyroid-stimulating hormone and thyroid-stimulating hormone receptor structure-function relationships. *Physiol Rev* **82**, 473-502,(2002).
101 Thotakura, N. R. & Blithe, D. L. Glycoprotein hormones: glycobiology of gonadotrophins, thyrotrophin and free alpha subunit. *Glycobiology* **5**, 3-10 (1995).
102 Baenziger, J. U. Protein-specific glycosyltransferases: how and why they do it! *FASEB J* **8**, 1019-1025 (1994).
103 Ruddock, L. W. & Molinari, M. N-glycan processing in ER quality control. *J Cell Sci* **119**, 4373-4380,(2006).
104 Fairlie, W. D., Stanton, P. G. & Hearn, M. T. The disulphide bond structure of thyroid-stimulating hormone beta-subunit. *Biochem J* **314 (Pt 2)**, 449-455 (1996).
105 Shupnik, M. A., Ridgway, E. C. & Chin, W. W. Molecular biology of thyrotropin. *Endocr Rev* **10**, 459-475 (1989).
106 Wondisford, F. E., Magner JA & Weintraub, B. D. *Thyrotropin. In Bravermann LE, Utiger RD (eds) Werner and Ingbar' The Thyroid.*, pp 190-207 (Lippincott-Reaven, 1996).
107 Kawakami, A. *et al.* Thyroid-stimulating hormone inhibits Fas antigen-mediated apoptosis of human thyrocytes in vitro. *Endocrinology* **137**, 3163-3169 (1996).
108 Parmentier, M. *et al.* Molecular cloning of the thyrotropin receptor. *Science* **246**, 1620-1622 (1989).
109 Rapoport, B., Chazenbalk, G. D., Jaume, J. C. & McLachlan, S. M. The thyrotropin (TSH) receptor: interaction with TSH and autoantibodies. *Endocr Rev* **19**, 673-716 (1998).
110 Libert, F., Lefort, A. & Gerard, C. Cloning,sequencing and expression of the human thyrotropin receptor(TSH) receptor: evidance for binding of autoantibodies. *Biochemical and Biophysical Research Communications* **165**, 1250-1255 (1989).
111 Vassart, G. & Dumont, J. E. The thyrotropin receptor and the regulation of thyrocyte function and growth. *Endocr Rev* **13**, 596-611 (1992).
112 Rees Smith, B. & Furmaniak, J. Structural analysis of the TSH receptor. *Horm Metab Res Suppl* **23**, 28-32 (1990).
113 Tanaka, K., Chazenbalk, G. D., McLachlan, S. M. & Rapoport, B. Subunit structure of thyrotropin receptors expressed on the cell surface. *J Biol Chem* **274**, 33979-33984 (1999).

114 Rapoport, B. & McLachlan, S. M. The thyrotropin receptor in Graves' disease. *Thyroid* **17**, 911-922,(2007).
115 de Bernard, S. *et al.* Sequential cleavage and excision of a segment of the thyrotropin receptor ectodomain. *J Biol Chem* **274**, 101-107 (1999).
116 Misrahi, M. & Milgrom, E. Cleavage and shedding of the TSH receptor. *Eur J Endocrinol* **137**, 599-602 (1997).
117 Chazenbalk, G. D., Nagayama, Y., Kaufman, K. D. & Rapoport, B. The functional expression of recombinant human thyrotropin receptors in nonthyroidal eukaryotic cells provides evidence that homologous desensitization to thyrotropin stimulation requires a cell-specific factor. *Endocrinology* **127**, 1240-1244 (1990).
118 Smits, G. *et al.* Glycoprotein hormone receptors: determinants in leucine-rich repeats responsible for ligand specificity. *EMBO J* **22**, 2692-2703,(2003).
119 Loosfelt, H. *et al.* Two-subunit structure of the human thyrotropin receptor. *Proc Natl Acad Sci U S A* **89**, 3765-3769 (1992).
120 Gross, B., Misrahi, M., Sar, S. & Milgrom, E. Composite structure of the human thyrotropin receptor gene. *Biochem Biophys Res Commun* **177**, 679-687, (1991).
121 Couet, J. *et al.* Cell surface protein disulfide-isomerase is involved in the shedding of human thyrotropin receptor ectodomain. *Biochemistry* **35**, 14800-14805,(1996).
122 Graves, P. N., Vlase, H., Bobovnikova, Y. & Davies, T. F. Multimeric complex formation by the thyrotropin receptor in solubilized thyroid membranes. *Endocrinology* **137**, 3915-3920 (1996).
123 Kosugi, S., Sugawa, H. & Mori, T. Epitope analysis of the thyrotropin receptor, 1997. *Mol Cell Endocrinol* **128**, 11-18 (1997).
124 Damante, G. & Di Lauro, R. Thyroid-specific gene expression. *Biochim Biophys Acta* **1218**, 255-266 (1994).
125 Ellerhorst, J. A. *et al.* Human melanoma cells express functional receptors for thyroid-stimulating hormone. *Endocr Relat Cancer* **13**, 1269-1277, (2006).
126 Leonhardt, J. M. & Heymann, W. R. Thyroid disease and the skin. *Dermatol Clin* **20**, 473-481, vii (2002).
127 Hanley, K., Rassner, U., Elias, P. M., Williams, M. L. & Feingold, K. R. Epidermal barrier ontogenesis: maturation in serum-free media and acceleration by glucocorticoids and thyroid hormone but not selected growth factors. *J Invest Dermatol* **106**, 404-411 (1996).
128 Tomic-Canic, M., Day, D., Samuels, H. H., Freedberg, I. M. & Blumenberg, M. Novel regulation of keratin gene expression by thyroid hormone and retinoid receptors. *J Biol Chem* **271**, 1416-1423 (1996).
129 Komuves, L. G. *et al.* Ligands and activators of nuclear hormone receptors regulate epidermal differentiation during fetal rat skin development. *J Invest Dermatol* **111**, 429-433,(1998).
130 Slominski, A. & Wortsman, J. Neuroendocrinology of the skin. *Endocr Rev* **21**, 457-487 (2000).
131 Radoja, N. *et al.* Thyroid hormones and gamma interferon specifically increase K15 keratin gene transcription. *Mol Cell Biol* **24**, 3168-3179 (2004).
132 Cianfarani, F. *et al.* TSH receptor and thyroid-specific gene expression in human skin. *J Invest Dermatol* **130**, 93-101, (2010).
133 Bodo, E. *et al.* Human female hair follicles are a direct, nonclassical target for thyroid-stimulating hormone. *J Invest Dermatol* **129**, 1126-1139, (2009).
134 Graves, P. N., Tomer, Y. & Davies, T. F. Cloning and sequencing of a 1.3 KB variant of human thyrotropin receptor mRNA lacking the transmembrane domain. *Biochem Biophys Res Commun* **187**, 1135-1143,(1992).

135 Loosfelt, H. *et al.* Cloning and sequencing of porcine LH-hCG receptor cDNA: variants lacking transmembrane domain. *Science* **245**, 525-528 (1989).
136 Koo, Y. B., Ji, I. & Ji, T. H. Characterization of different sizes of rat luteinizing hormone/chorionic gonadotropin receptor messenger ribonucleic acids. *Endocrinology* **134**, 19-26 (1994).
137 Gromoll, J., Gudermann, T. & Nieschlag, E. Molecular cloning of a truncated isoform of the human follicle stimulating hormone receptor. *Biochem Biophys Res Commun* **188**, 1077-1083 (1992).
138 O'Shaughnessy, P. J. & Dudley, K. Discrete splicing alternatives in mRNA encoding the extracellular domain of the testis FSH receptor in the normal and hypogonadal (hpg) mouse. *J Mol Endocrinol* **10**, 363-366 (1993).
139 Libert, F. *et al.* Molecular cloning of a dog thyrotropin (TSH) receptor variant. *Mol Cell Endocrinol* **68**, R15-17 (1990).
140 Grommen, S. V. *et al.* Molecular cloning, tissue distribution, and ontogenic thyroidal expression of the chicken thyrotropin receptor. *Endocrinology* **147**, 3943-3951, (2006).
141 Paschke, R. *et al.* Presence of Nonfunctional Thyrotropin Receptor Variant Transcripts in Retroocular and Other Tissues. *J Clin Endocrinol Metab* **79**, 1234-1238 (1994).
142 Sokka, T., Hamalainen, T. & Huhtaniemi, L. Functional LH receptor appears in the neonatal rat ovary after changes in the alternative splicing pattern of the LH receptor mRNA. *Endocrinology* **130**, 1738-1740 (1992).
143 LaPolt, P. S., Tilly, J. L., Aihara, T., Nishimori, K. & Hsueh, A. J. Gonadotropin-induced up- and down-regulation of ovarian follicle-stimulating hormone (FSH) receptor gene expression in immature rats: effects of pregnant mare's serum gonadotropin, human chorionic gonadotropin, and recombinant FSH. *Endocrinology* **130**, 1289-1295 (1992).
144 Nakabayashi, K. *et al.* Thyrostimulin, a heterodimer of two new human glycoprotein hormone subunits, activates the thyroid-stimulating hormone receptor. *J Clin Invest* **109**, 1445-1452, (2002).
145 Hsu, S. Y., Nakabayashi, K. & Bhalla, A. Evolution of glycoprotein hormone subunit genes in bilateral metazoa: identification of two novel human glycoprotein hormone subunit family genes, GPA2 and GPB5. *Mol Endocrinol.* **16**, 1538-1551 (2002).
146 Nagasaki, H. *et al.* Differential expression of the thyrostimulin subunits, glycoprotein alpha2 and beta5 in the rat pituitary. *J Mol Endocrinol.* **37**, 39-50 (2006).
147 Okajima, Y. *et al.* Biochemical roles of the oligosaccharide chains in thyrostimulin, a heterodimeric hormone of glycoprotein hormone subunits alpha 2 (GPA2) and beta 5 (GPB5). *Regul Pept* **148**, 62-67,(2008).
148 Vitt, U. A., Hsu, S. Y. & Hsueh, A. J. Evolution and classification of cystine knot-containing hormones and related extracellular signaling molecules. *Mol Endocrinol* **15**, 681-694 (2001).
149 McDonald, N. Q. & Hendrickson, W. A. A structural superfamily of growth factors containing a cystine knot motif. *Cell* **73**, 421-424, (1993).
150 Matzuk, M. M. & Boime, I. The role of the asparagine-linked oligosaccharides of the alpha subunit in the secretion and assembly of human chorionic gonadotrophin. *J Cell Biol* **106**, 1049-1059 (1988).
151 Grossmann, M. *et al.* Expression of human thyrotropin in cell lines with different glycosylation patterns combined with mutagenesis of specific glycosylation sites. Characterization of a novel role for the oligosaccharides in the in vitro and in vivo bioactivity. *J Biol Chem* **270**, 29378-29385 (1995).

152 Li, C. *et al.* Distribution of thyrostimulin in the rat: an immunohistochemical study. *Endocr Regul* **38**, 131-142 (2004).
153 Okada, S. L. *et al.* A glycoprotein hormone expressed in corticotrophs exhibits unique binding properties on thyroid-stimulating hormone receptor. *Mol Endocrinol* **20**, 414-425, (2006).
154 Duprez, L. *et al.* TSH Receptor Mutations and Thyroid Disease. *Trends Endocrinol Metab* **9**, 133-140,(1998).
155 Haraguchi, K. *et al.* Functional expression of thyrotropin receptor in differentiated 3T3-L1 cells: a possible model cell line of extrathyroidal expression of thyrotropin receptor. *Biochem Biophys Res Commun* **223**, 193-198, (1996).
156 Misrahi, M. *et al.* Cloning, sequencing and expression of human TSH receptor. *Biochem Biophys Res Commun* **166**, 394-403, doi:0006-291X(90)91958-U [pii] (1990).
157 Grommen, S. V. *et al.* Identification of unique thyrotropin receptor (TSHR) splice variants in the chicken: the chicken TSHR gene revisited. *Gen Comp Endocrinol* **156**, 460-463,(2008).
158 Guttmacher, A. E. & Collins, F. S. Genomic medicine--a primer. *N Engl J Med* **347**, 1512-1520 (2002).
159 Davies, T. F., Ando, T., Lin, R. Y., Tomer, Y. & Latif, R. Thyrotropin receptor-associated diseases: from adenomata to Graves disease. *J Clin Invest* **115**, 1972-1983, (2005).
160 Van Sande, J. *et al.* Somatic and germline mutations of the TSH receptor gene in thyroid diseases. *J Clin Endocrinol Metab* **80**, 2577-2585 (1995).
161 Brokken, L. J., Bakker, O., Wiersinga, W. M. & Prummel, M. F. Functional thyrotropin receptor expression in the pituitary folliculo-stellate cell line TtT/GF. *Exp Clin Endocrinol Diabetes* **113**, 13-20, (2005).
162 Sun, S. C. *et al.* Thyrostimulin, but not thyroid-stimulating hormone (TSH), acts as a paracrine regulator to activate the TSH receptor in mammalian ovary. *J Biol Chem* **285**, 3758-3765, (2010).
163 Boukamp, P. *et al.* Normal keratinization in a spontaneously immortalized aneuploid human keratinocyte cell line. *J Cell Biol* **106**, 761-771 (1988).
164 Wyllie, F. S. *et al.* Telomerase prevents the accelerated cell ageing of Werner syndrome fibroblasts. *Nat Genet* **24**, 16-17, (2000).
165 Zhang, L. *et al.* Biological effects of thyrotropin receptor activation on human orbital preadipocytes. *Invest Ophthalmol Vis Sci* **47**, 5197-5203 (2006).
166 Todaro, G. J. & Green, H. Quantitative studies of the growth of mouse embryo cells in culture and their development into established lines. *J Cell Biol* **17**, 299-313 (1963).
167 Pillai, S., Bikle, D. D., Mancianti, M. L., Cline, P. & Hincenbergs, M. Calcium regulation of growth and differentiation of normal human keratinocytes: modulation of differentiation competence by stages of growth and extracellular calcium. *J Cell Physiol* **143**, 294-302 (1990).
168 Festa, E. *et al.* Adipocyte lineage cells contribute to the skin stem cell niche to drive hair cycling. *Cell* **146**, 761-771 (2011).
169 Pattwell, D. M., Lynaugh, K. J., Watson, R. E. & Paus, R. HaCaT keratinocytes express functional receptors for thyroid-stimulating hormone. *J Dermatol Sci* **59**, 52-55 (2010).
170 Poumay, Y. & Pittelkow, M. R. Cell density and culture factors regulate keratinocyte commitment to differentiation and expression of suprabasal K1/K10 keratins. *J Invest Dermatol* **104**, 271-276 (1995).

171 Schoop, V. M., Mirancea, N. & Fusenig, N. E. Epidermal organization and differentiation of HaCaT keratinocytes in organotypic coculture with human dermal fibroblasts. *J Invest Dermatol* **112**, 343-353 (1999).
172 Stark, H. J., Baur, M., Breitkreutz, D., Mirancea, N. & Fusenig, N. E. Organotypic keratinocyte cocultures in defined medium with regular epidermal morphogenesis and differentiation. *J Invest Dermatol* **112**, 681-691 (1999).
173 UK Guidelines for the Use of Thyroid Function Tests (2006).
174 Agretti, P. *et al.* Real-time PCR provides evidence for thyrotropin receptor mRNA expression in orbital as well as in extraorbital tissues. *Eur J Endocrinol* **147**, 733-739 (2002).
175 Wu, S. L. *et al.* Cloning and sequencing of complete thyrotropin receptor transcripts in pretibial fibroblast culture cells. *J Endocrinol Invest* **19**, 365-370 (1996).
176 Kosugi, S. *et al.* Substitutions of different regions of the third cytoplasmic loop of the thyrotropin (TSH) receptor have selective effects on constitutive, TSH-, and TSH receptor autoantibody-stimulated phosphoinositide and 3',5'-cyclic adenosine monophosphate signal generation. *Mol Endocrinol* **7**, 1009-1020 (1993).
177 Morgenthaler, N. G. *et al.* Direct binding of thyrotropin receptor autoantibody to in vitro translated thyrotropin receptor: a comparison to radioreceptor assay and thyroid stimulating bioassay. *Thyroid* **9**, 466-475 (1999).
178 Daumerie, C., Ludgate, M., Costagliola, S. & Many, M. C. Evidence for thyrotropin receptor immunoreactivity in pretibial connective tissue from patients with thyroid-associated dermopathy. *Eur J Endocrinol* **146**, 35-38, doi:14635 [pii] (2002).
179 Sequeira, M., Jasani, B., Fuhrer, D., Wheeler, M. & Ludgate, M. Demonstration of reduced in vivo surface expression of activating mutant thyrotrophin receptors in thyroid sections. *Eur J Endocrinol* **146**, 163-171, doi:146163 [pii] (2002).
180 Costagliola, S., Rodien, P., Many, M. C., Ludgate, M. & Vassart, G. Genetic immunization against the human thyrotropin receptor causes thyroiditis and allows production of monoclonal antibodies recognizing the native receptor. *J Immunol* **160**, 1458-1465 (1998).
181 Boenisch, T. *Handbook of Immunohistochemistry*. 3rd edn, (DAKO Corporation, 2001).
182 Kroese, F. Immunohistochemical detection of tissue and cellular antigens. *Encyclopedia of Life Sciences:John Wiley & Sons, Ltd*, 1-9 (2001).
183 Lelong C, C. M., Luche S, Rabilloud T. Silver staining of proteins in 2DE gels. *Methods Mol Biol* **519**, 339-350. (2009).
184 Douglas, R. S. *et al.* Increased generation of fibrocytes in thyroid-associated ophthalmopathy. *J Clin Endocrinol Metab* **95**, 430-438, (2010).
185 Kohn, L. D. *et al.* Graves' disease: a host defense mechanism gone awry. *Int Rev Immunol* **19**, 633-664 (2000).
186 Rose NR & IR, M. *Thyroid disease*. 467-83 (Elsevier Academic Press, 2006).
187 Bell, A. *et al.* Functional TSH receptor in human abdominal preadipocytes and orbital fibroblasts. *Am J Physiol Cell Physiol* **279**, C335-340 (2000).
188 Billoni, N. *et al.* Thyroid hormone receptor beta1 is expressed in the human hair follicle. *Br J Dermatol* **142**, 645-652, doi:bjd3408 [pii] (2000).
189 Haraguchi, K., Shimura, H., Lin, L., Endo, T. & Onaya, T. Differentiation of rat preadipocytes is accompanied by expression of thyrotropin receptors. *Endocrinology* **137**, 3200-3205 (1996a).
190 Lu, S. *et al.* Role of extrathyroidal TSHR expression in adipocyte differentiation and its association with obesity. *Lipids Health Dis* **11**, 17,(2012).

191 Agretti, P. *et al.* Evidence for protein and mRNA TSHr expression in fibroblasts from patients with thyroid-associated ophthalmopathy (TAO) after adipocytic differentiation. *Eur J Endocrinol* **152**, 777-784,(2005).
192 Bahn, R. S. Thyrotropin receptor expression in orbital adipose/connective tissues from patients with thyroid-associated ophthalmopathy. *Thyroid* **12**, 193-195, (2002).
193 Starkey, K. J. *et al.* Adipose thyrotrophin receptor expression is elevated in Graves' and thyroid eye diseases ex vivo and indicates adipogenesis in progress in vivo. *J Mol Endocrinol* **30**, 369-380 (2003).
194 Brent, G. A. Clinical practice. Graves' disease. *N Engl J Med* **358**, 2594-2605,(2008).
195 Torring, O. *et al.* Graves' hyperthyroidism: treatment with antithyroid drugs, surgery, or radioiodine--a prospective, randomized study. Thyroid Study Group. *J Clin Endocrinol Metab* **81**, 2986-2993 (1996).
196 Neumann, S. *et al.* A new small-molecule antagonist inhibits Graves' disease antibody activation of the TSH receptor. *J Clin Endocrinol Metab* **96**, 548-554, (2011).

Appendix

Full length human thyroid stimulating hormone receptor (TSHR), transcript variant 1, mRNA sequence showing position of primers used in different studies including this study:

NCBI Reference Sequence: **NM_000369.2**, Chr14:81421869-81612646

```
     CCTCCTCCAC AGTGGTGAGG TCACAGCCCC TTGGAGCCCT CCCTCTTCCC  50
ACCCCTCCCG CTCCCGGGTC TCCTTTGGCC TGGGGTAACC CGAGGTGCAG  100
AGCTGAGAAT GAGGCGATTT CGGAGGATGG AGAAATAGCC CCGAGTCCCG  150
TGGAAAATGA GGCCGGCGGA CTTGCTGCAG CTGGTGCTGC TGCTCGACCT  200
GCCCAGGGAC CTGGGCGGAA TGGGGTGTTC GTCTCCACCC TGCGAGTGCC  250
ATCAGGAGGA GGACTTCAGA GTCACCTGCA AGGATATTCA ACGCATCCCC  300
AGCTTACCGC CCAGTACGCA GACTCTGAAG CTTATTGAGA CTCACCTGAG  350
AACTATTCCA AGTCATGCAT TTTCTAATCT GCCCAATATT TCCAGAATCT  400
ACGTATCTAT AGATGTGACT CTGCAGCAGC TGGAATCACA CTCCTTCTAC  450
AATTTGAGTA AAGTGACTCA CATAGAAATT CGGAATACCA GGAACTTAAC  500
TTACATAGAC CCTGATGCCC TCAAAGAGCT CCCCCTCCTA AAGTTCCTTG  550
GCATTTTCAA CACTGGACTT AAAATGTTCC CTGACCTGAC CAAAGTTTAT  600
TCCACTGATA TATTCTTTAT ACTTGAAATT ACAGACAACC CTTACATGAC  650
GTCAATCCCT GTGAATGCTT TTCAGGGACT ATGCAATGAA ACCTTGACAC  700
TGAAGCTGTA CAACAATGGC TTTACTTCAG TCCAAGGATA TGCTTTCAAT  750
GGGACAAAGC TGGATGCTGT TTACCTAAAC AAGAATAAAT ACCTGACAGT  800
TATTGACAAA GATGCATTTG GAGGAGTATA CAGTGGACCA AGCTTGCTGG  850
ACGTGTCTCA AACCAGTGTC ACTGCCCTTC CATCCAAAGG CCTGGAGCAC  900
CTGAAGGAAC TGATAGCAAG AAACACCTGG ACTCTTAAGA AACTTCCACT  950
TTCCTTGAGT TTCCTTCACC TCACACGGGC TGACCTTTCT TACCCAAGCC 1000
ACTGCTGTGC TTTTAAGAAT CAGAAGAAAA TCAGAGGAAT CCTTGAGTCC 1050
TTGATGTGTA ATGAGAGCAG TATGCAGAGC TTGCGCCAGA GAAAATCTGT 1100
GAATGCCTTG AATAGCCCCC TCCACCAGGA ATATGAAGAG AATCTGGGTG 1150
ACAGCATTGT TGGGTACAAG GAAAAGTCCA AGTTCCAGGA TACTCATAAC 1200
AACGCTCATT ATTACGTCTT CTTTGAAGAA CAAGAGGATG AGATCATTGG 1250
TTTTGGCCAG GAGCTCAAAA ACCCCCAGGA AGAGACTCTA CAAGCTTTTG 1300
ACAGCCATTA TGACTACACC ATATGTGGGG ACAGTGAAGA CATGGTGTGT 1350
ACCCCCAAGT CCGATGAGTT CAACCCGTGT GAAGACATAA TGGGCTACAA 1400
GTTCCTGAGA ATTGTGGTGT GGTTCGTTAG TCTGCTGGCT CTCCTGGGCA 1450
ATGTCTTTGT CCTGCTTATT CTCCTCACCA GCCACTACAA ACTGAACGTC 1500
CCCCGCTTTC TCATGTGCAA CCTGGCCTTT GCGGATTTCT GCATGGGGAT 1550
GTACCTGCTC CTCATCGCCT CTGTAGACCT CTACACTCAC TCTGAGTACT 1600
ACAACCATGC CATCGACTGG CAGACAGGCC CTGGGTGCAA CACGGCTGGT 1650
TTCTTCACTG TCTTTGCAAG CGAGTTATCG GTGTATACGC TGACGGTCAT 1700
CACCCTGGAG CGCTGGTATG CCATCACCTT CGCCATGCGC CTGGACCGGA 1750
AGATCCGCCT CAGGCACGCA TGTGCCATCA TGGTTGGGGG CTGGGTTTGC 1800
TGCTTCCTTC TCGCCCTGCT TCCTTTGGTG GGAATAAGTA GCTATGCCAA 1850
AGTCAGTATC TGCCTGCCCA TGGACACCGA GACCCCTCTT GCTCTGGCAT 1900
ATATTGTTTT TGTTCTGACG CTCAACATAG TTGCCTTCGT CATCGTCTGC 1950
TGCTGTTATG TGAAGATCTA CATCACAGTC CGAAATCCGC AGTACAACCC 2000
AGGGGACAAA GATACCAAAA TTGCCAAGAG GATGGCTGTG TTGATCTTCA 2050
CCGACTTCAT ATGCATGGCC CCAATCTCAT TCTATGCTCT GTCAGCAATT 2100
CTGAACAAGC CTCTCATCAC TGTTAGCAAC TCCAAAATCT TGCTGGTACT 2150
CTTCTATCCA CTTAACTCCT GTGCCAATCC ATTCCTCTAT GCTATTTTCA 2200
CCAAGGCCTT CCAGAGGGAT GTGTTCATCC TACTCAGCAA GTTTGGCATC 2250
TGTAAACGCC AGGCTCAGGC ATACCGGGGG CAGAGGGTTC CTCCAAAGAA 2300
CAGCACTGAT ATTCAGGTTC AAAAGGTTAC CCACGAGATG AGGCAGGGTC 2350
```

```
TCCACAACAT GGAAGATGTC TATGAACTGA TTGAAAACTC CCATCTAACC  2400
CCAAAGAAGC AAGGCCAAAT CTCAGAAGAG TATATGCAAA CGGTTTTGTA  2450
AGTTAACACT ACACTACTCA CAATGGTAGG GGAACTTACA AAATAATAGT  2500
TTCTTGAATA TGCATTCCAA TCCCATGACA CCCCCAACAC ATAGCTGCCC  2550
TCACTCTTGT GCAGGCGATG TTTCAATGTT TCATGGGGCA AGAGTTTATC  2600
TCTGGAGAGT GATTAGTATT AACCTAATCA TTGCCCCCAA GAAGGAAGTT  2650
AGGCTACCAG CATATTTGAA TGCCAGGTGA AATCAAAATA ATCTACACTA  2700
TCTAGAAGAC TTTCTTGATG CCAAGTCCAG AGATGTCATT GTGTAGGATG  2750
TTCAGTAAAT ATTAACTGAG CTATGTCAAT ATAGAGCTTC TCAGTTTTGT  2800
ATAACATTTC ATACTAAAGA TTCAGCAAAT GGAAAATGCT ATTAATTTGG  2850
TTGGTGACCA CAAGATAAAA TCAGTCCCAC GTTGGCTCAG TTCAACTAGA  2900
TGTTCCCTGA TACAAAGAGA ACTTGATTTC CTTAAAACTG AAAAGCCAAA  2950
CACAGCTAGC TGTCATACAA GAAACAGCTA TTATGAGACA TGAAGGAGGG  3000
TAAGAATTAG CTTTAAGTTT TGTTTTGCTT TGTTTTGTTT TTTAACTCAA  3050
CCTATTAATC ATCTCTTCAC AAGAATCCAC CTGATGTGAC CAAGCTATTA  3100
TGTGTTGCCT GGAAAAACTG GCAAGATTTC AGCTTATGTG GCCTAGCAAA  3150
CTAAGAATTG CTCTTCTTGG CCAGCCTCAT AGCATAAAAG ATGTGAACTC  3200
TAGGAAGTCT TTCTGAGTAG CAATAAGTGG GAATTATGGG CAGAGCACAC  3250
TCAATCCCCT GTTGATTAAT AAAACAGGCT GGACACTAAT TAACTATGGG  3300
ACTTAAATCT GTAGAAATGA AGGAGTCCAA TAGCTTCTTC CAATTTTAAA  3350
ACTCTAGTAC ATCCCTTTCC CTCAAATATA TATTTCTAAG ATAAAGAGAA  3400
AGAAGAGCAC TAAGTAAGTA GAATCTGTTT TTCCTATTTT GTAGGGCTGC  3450
TGACTCCTAG TCCTTGAAGC CTAGACACAT GACCCAGGAA ATTTTTCCTT  3500
TGTTTCACTT TTGATTATGA TGTCTGAGCC AAAAATTCAA TTAAGTAAAC  3550
ATACTCGCCT GGATCTGAAT CATTCATTTA ATTACTAGAT CTACCCAGCT  3600
GTTATATCAG GCCAAAAACA GATTCGTGTT TATATAAAAG AGTAAACGAT  3650
GGTTGCAAAT TTTGGCTATT TAGAGTTGCT ACTTCACTAT GAAGAGTCAC  3700
TTCAAAACAC TTCGCTTGTC TTTAGGGATG ATTTTTGCCA TTTCCAGTCC  3750
ACGGTATGAT ACTAAAGCTG TCAAGAGAGG TTTCTTCTTT TCTGAAACTG  3800
CCAGCTCTTT CCAGCCCTGT TGATCACTGG ACATAAAGCT TCTTTTCCCC  3850
AATAATTCTT CTTTACTTAA AATAGTCAGG ATCTTTATCT ACAGATGTAC  3900
TCTCCAGGTT ACCTGTGATG ATAGCCCCCT AATGTCCTGC TAGAAAAGTC  3950
TCCAAGCAGA GATGACATTA CTTCTGAATG CTCATAAACC ACACCATGAA  4000
ATAAAAGCTC TTTGTTGTTT TAAGATTGTG AAGTGTCGTT AATGGGTCCC  4050
CACAGATGGT CCCTGCTGGA CTCACCTGGA ATCTCTCCAC AGCCATACCC  4100
ACTCATCACT ATCATTGAGA CCTGCACATC TTAATAGAAA TATTATAAAC  4150
ATCGAAAATC ATGACTTACC TAGAAGTTCG CTTGTAACTA ATGAAATTAA  4200
ACAAATGTGT TGCCTTTTGT CATGTGTTTC TCTCCTGTGA CATTTCAAAA  4250
TATCACATCT TGATAAATAA TGTGTTTCAT CTTGAATAGC TGAACTAATT  4300
GCTTTGGAAA CAGAGTCCTA GAAAAGTGAC TTCAACAGAA TTGTTACTAA  4350
AATTTGCACT CACAACATGA AATAAATTTT CTTCCTATGG AATAATCGTG  4400
    Aaaaaaaaaa
```

Figures 7.1 Human TSHR sequence gene showing the position of primers used in different syudies. The primers used in a various reports to amplify hTSHR were colour coded, Solminski et al,2002[53] (first pair of primers), Solminski et al,2002[53] (nested primers) , Bodo et al, 2009[133] , Cianfarani et al,2010 [132] , primers used in this stud

Human thyroid stimulating hormone receptor variant (TSHRV), transcript variant 2, mRNA sequence showing position of primers used in study:

NCBI Reference Sequence: **NM_001018036.2,** Chr14:81421869-81575286

```
CCTCCTCCAC AGTGGTGAGG TCACAGCCCC TTGGAGCCCT CCCTCTTCCC  50
ACCCCTCCCG CTCCCGGGTC TCCTTTGGCC TGGGGTAACC CGAGGTGCAG  100
AGCTGAGAAT GAGGCGATTT CGGAGGATGG AGAAATAGCC CCGAGTCCCG  150
TGGAAAATGA GGCCGGCGGA CTTGCTGCAG CTGGTGCTGC TGCTCGACCT  200
GCCCAGGGAC CTGGGCGGAA TGGGGTGTTC GTCTCCACCC TGCGAGTGCC  250
ATCAGGAGGA GGACTTCAGA GTCACCTGCA AGGATATTCA ACGCATCCCC  300
AGCTTACCGC CCAGTACGCA GACTCTGAAG CTTATTGAGA CTCACCTGAG  350
AACTATTCCA AGTCATGCAT TTTCTAATCT GCCCAATATT TCCAGAATCT  400
ACGTATCTAT AGATGTGACT CTGCAGCAGC TGGAATCACA CTCCTTCTAC  450
AATTTGAGTA AAGTGACTCA CATAGAAATT CGGAATACCA GGAACTTAAC  500
TTACATAGAC CCTGATGCCC TCAAAGAGCT CCCCCTCCTA AAGTTCCTTG  550
GCATTTTCAA CACTGGACTT AAAATGTTCC CTGACCTGAC CAAAGTTTAT  600
TCCACTGATA TATTCTTTAT ACTTGAAATT ACAGACAACC CTTACATGAC  650
GTCAATCCCT GTGAATGCTT TTCAGGGACT ATGCAATGAA ACCTTGACAC  700
TGAAGCTGTA CAACAATGGC TTTACTTCAG TCCAAGGATA TGCTTTCAAT  750
GGGACAAAGC TGGATGCTGT TTACCTAAAC AAGAATAAAT ACCTGACAGT  800
TATTGACAAA GATGCATTTG GAGGAGTATA CAGTGGACCA AGCTTGCTGC  850
TACCTCTTGG AAGAAAGTCC TTGTCCTTTG AGACTCAGAA GGCCCCACGC  900
TCCAGTATGC CATCATGATG CCTGCTAAGG CAGCCACCTT GGTGTACATG  950
CTCACAGAGG CTCTGTTCAT GGAGCAGCTG CTGTTTGAAA AATTTTGAAA  1000
TGCAAGATCC ACAACTAGAT GGAAGGCACT CTAGTCTTTG CAGAAAAAAA  1050
TGTACCTGAA TGTACATTGC ACAATGCCTG GCACAAAGAA GGAAGAATAT  1100
AAATGATAGT TCGACTCGTC TGTGGAAGAA CTTACAATCA TGGGGAAAGA  1150
TGGAATAAAA ACATTTTTTA AACAGCATGa aaa
```

Figure 7.2: Human TSHR variant 2 sequence. TSHRV spans exons1-8 plus 22 amino acids in the beginning of exon 9, sparing the transmembrane part of full length TSHR. Red is untranslated region (intron), blue is transulated region (exons). Yellow highlight represents the primers used in this project, forward primer is in exons 4/5 and reverse primer is in the unique sequence in intron between exons 8/9 of 1.3 variant form.